Martin Tengg

Methyltransferases for Novel Biocatalytic C-C Bond Formation

DISSERTATION

Zur Erlangung des akademischen Grades eines
Doktors der Naturwissenschaften

an der Technischen Universität Graz

Durchgeführt am Institut für Molekulare Biotechnologie
c/o ACIB GmbH

unter der Betreuung von
Univ.-Prof. Dipl.-Ing. Dr.techn. Helmut Schwab

2011

Mein besonderer Dank gilt

meiner Familie, allen voran meinen Eltern, die mich während meiner gesamten Studienzeit unterstützt, und mir immer einen Platz zur Erholung und Regeneration geboten haben;
Christian dafür, dass er immer für mich Zeit hatte wenn ich ihn brauchte;
Veronika für die schöne Zeit und ihr Verständnis;

Harald Stecher für die produktive und lockerer Zusammenarbeit, die gemeinsamen Konferenzbesuche, und die lustigen Abende nach getaner Arbeit;

Mandana Gruber für die erfolgreiche Projektleitung, ihre Begeisterung, Motivation, ihr Verständnis und die Anerkennung meiner Arbeit;

Peter Remler dafür, dass er jederzeit mit Rat und Tat zur Seite stand, mir alle Freiheiten ließ, und für ein angenehmes Arbeitsklima sorgte;

meinen KollegInnen am ACIB und IMBT, vorallem vom vierten Stock, für ihre Hilfsbereitschaft und die gute Zusammenarbeit;

Professor Helumt Schwab für die Betreuung der Dissertation, die inspirierenden Diskussionen, und das Ermöglichen und Unterstützen meiner wissenschaftlichen Entwicklung;

dem ACIB und der TU Graz für die Finanzierung dieser Arbeit.

Abstract

Biocatalysis has gained growing attention during the last decades in the field of applied life sciences. A major task of biocatalysis, the C-C bond formation has been described for several enzyme classes, but so far lacked the biocatalytic synthesis of alkylated aromatic compounds.

Methylation, a common reaction in all living cells is catalyzed by methyltransferases. Among these cofactor dependent enzymes, S-adenosyl-L-methionine is the most important methyl donor. A small group of S-adenosyl-L-methionine dependent methyltransferases catalyzes the transfer of the methyl moiety to the carbon atom.

This study shows that S-adenosyl-L-methionine dependent C-methyltransferases were able to catalyze the alkylation of aromatic molecules. An enzymatic equivalent to the classical Friedel-Crafts alkylation is described. A set of methyltransferases was investigated towards their ability to methylate their natural substrates and related ones. Not only methylation was observed, but also the regioselective monoalkylation of diverse substrates with the use of synthetic S-adenosyl-L-methionine analogues as cofactors.

Characterization of the methyltransferase NovO gave insights into the enzyme mechanism and organization of the protein. The preference towards coumarin derivatives and S-adenosyl-L-methionine, the striking performance concerning methylation of naphthalene derivatives and accelerated transfer of allyl groups to coumarin derivatives are important findings for a prospective application in biocatalysis. The alkyl group transfer depends on an active site histidine, which is essential for active deprotonation of the attacked substrate carbon atom.

The selective alkylation of aromatic compounds under mild reaction conditions can be performed for the synthesis of fine chemicals as well as bioactive intermediates and products.

Kurzfassung

In den letzten Jahrzehnten hat die Biokatalyse im Bereich der angewandten Biowissenschaften zunehmend an Bedeutung gewonnen. Die Knüpfung von C-C Bindungen, eine wichtige Aufgabe der Biokatalyse, wurde bereits für einige Enzymklassen beschrieben. Die biokatalytische Synthese von alkylierten aromatischen Verbindungen konnte jedoch noch nicht bewerkstelligt werden.

Die Methylierung, welche eine zentrale Rolle im Metabolismus aller Lebewesen darstellt, wird von Methyltransferasen katalysiert. Für diese, von Cofaktoren abhängigen Enzyme, ist S-Adenosyl-L-Methionin der am häufigsten verwendete Methyldonor. Eine kleine Gruppe dieser S-Adenosyl-L-Methionin abhängigen Methyltransferasen katalysiert die Bindung der Methylgruppe auf Kohlenstoffatome diverser Substrate.

In dieser Arbeit werden S-Adenosyl-L-Methionin abhängige C-Methyltransferasen beschrieben, welche die Alkylierung von aromatischen Molekülen katalysieren können. Damit ist eine äquivalente Reaktion der klassischen Friedel-Crafts Alkylierung mittels Enzymen möglich. Es wurde eine Reihe von Methyltransferasen, nach ihren Fähigkeiten zur Methylierung ihrer natürlichen und der damit verwandten Substrate, untersucht. Neben der natürlichen Methylierung konnte auch regioselektive Monoalkylierung von verschiedenen Substraten beobachtet werden. Dazu wurden synthetische Analoga von S-Adenosyl-L-Methionin verwendet.

Im Speziellen wurde die Methyltransferase NovO untersucht. Ihre Charakterisierung erlaubte Einblicke in den Enzymmechanismus und den Aufbau des Proteins. Es konnte gezeigt werden, daß das Enzym bevorzugt Coumarinderivate methyliert, aber auch zur effektiven Methylierung von Naphthalinen befähigt ist. Außerdem wurde ein beschleunigter Transfer von Allylgruppen beobachtet. Diese enzymatischen Reaktionen stellen die Grundlage für eine zukünftige Anwendung in der Biokatalyse dar. Zur Übertragung der Alkylgruppen ist ein Histidin im aktiven Zentrum des Enzyms

verantwortlich, welches die Deprotonierung zur Aktivierung des Substratkohlenstoffes bewerkstelligt.

Somit kann eine selektive Alkylierung von aromatischen Verbindungen unter milden Reaktionsbedingungen durchgeführt werden, welche für die Synthese von Feinchemikalien aber auch von bio-aktiven Zwischen- und Endprodukten dienen kann.

Contents

1 Introduction

1.1 Biotechnology and Biocatalysis

Biotechnology has a long history in human life. The oldest known reference which describes the use of microorganisms and therein enzymes for the production of wine goes back to circa 2100 B.C. in the ancient Babylon. Chemical products can be found in every day life, most frequently as food, fine chemicals or as pharmaceuticals. In order to meet the expectations of customers, the production of pure compounds is compulsory. For this purpose chemical synthesis was the method of choice since decades. A challenging task is to make a production process ecologically neutral and at the same time cost saving, but not loosing productivity in terms of purity and yield. Despite synthetic approaches, nature offers possibilities to achieve this goal.

In the last years biocatalysis became a strong alternative in this field. Lots of research has been done to find enzymes, which are capable to catalyze desired reactions. The advantages of biocatalysis are undeniable:

- highly efficient
- environmentally benign
- mild reaction conditions
- chemo-, regio-, and stereoselective

1.2 Friedel-Crafts alkylation

C-C bond formation is a major task in the field of biocatalysis. For example aldolases, trans-ketolases, and hydroxynitril lyases have been investigated thoroughly and some found their way to industrial application [1],[2]. A special type of C-C bond formation is the alkylation of aromatic compounds. This reaction is well know in organic chemistry as the Friedel-Crafts alkylation (Figure 1), which has been invented in 1887 by Charles Friedel and James Mason Crafts [3]. The transformation of alkyl groups is catalyzed

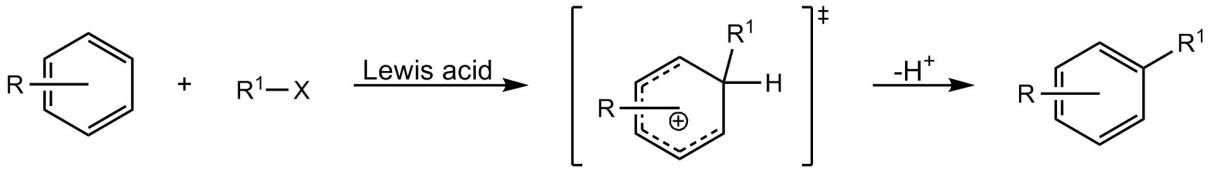

Figure 1: Mechanism of the Friedel-Crafts alkylation. The alkyl group R^1 is transferred to the aromatic structure by Lewis acids catalysis.

by Lewis acids such as $AlCl_3$, $FeCl_3$, BF_3, $SnCl_4$, $GaCl_3$, or HF [4]. Recent advantages in the chemical Friedel-Crafts alkylation have been reviewed by Rüping and Nachtsheim [5]. Next to harsh conditions, such as elevated temperatures and strong Lewis acids, also over-alkylation and low regioselectivity, are major drawbacks. Therefore an enzymatic equivalent to this reaction would be highly desirable. In nature alkylation occurs via the transfer of a methyl group onto various substrates. These reactions are carried out by methyltransferases EC [2.1.1], which are ubiquitous for every life form. In order to perform an enzymatic equivalent to the Friedel-Crafts alkylation, an enzyme that is capable to transfer an alkyl group to an aromatic substrate has to be isolated and adapted.

1.3 Enzymes

Nature has evolved special proteins for catalysis of various reactions. Similar to chemical catalysis enzymes promote product formation by lowering the activation energy of transition state formation.

Enzymes are proteins, and therefore they are composed of a variation of 20 amino acids. Concerning stereo configuration only L-amino acids are incorporated into protein sequences during ribosomal or non-ribosomal peptide synthesis. Amino acids of D-configuration are found in peptide antibiotics and in bacterial cell wall as part of the murein sacculus.

Enzymes can be specialists for a certain reaction of a certain substrate to form a certain product within a defined environment. In other cases the enzyme can be promiscuous towards substrates which will result in a set of products, and need not be surrounded by a special environment. If we want to work with enzymes we need to know about the requirement that is needed for an functional enzyme.

In general enzymes are ordered in six classes:

- EC 1 Oxidoreductases
- EC 2 Transferases
- EC 3 Hydrolases
- EC 4 Lyases
- EC 5 Isomerases
- EC 6 Ligases

1.4 Enzyme engineering - design of catalysts

The application of an enzyme for a biocatalytic reaction or even industrial purposes is a challenging task [6]. Nature evolved enzymes as perfect catalysts for a certain reaction in a certain environment under certain conditions (pH, temperature, salt concentration). If an enzyme should be used for a specific reaction outside its natural environment it faces several problems including stability and activity. The enzyme has to be provided with optimal reaction conditions. This includes the supply of substrate and at the same time avoidance of product inhibition.

There are two possibilities to meet the expectations of a wanted reaction. First, screening of microorganism which might contain an enzyme of interest. Second, engineering of an existing enzyme for improved functionality. The first option has been used successfully for several enzymes, but is covered with huge limitations concerning the problem of uncultureable organisms. We have to be aware of the fact that less than 1 % of all microorganism can be cultivated under laboratory conditions [6]. In addition isolation of enzymes from its hosts can be a challenging task, because in most cases only small amounts of an enzyme are produced in a certain phase of cell metabolism. Therefore this methodology is of limited success. The second methodology requires knowledge about the enzyme on the molecular level, meaning DNA sequence information, in order to perform recombinant DNA technologies. These include random mutagensis, rational design, and

a combination of both methods. These molecular techniques have been used thoroughly and could lead to the improvement of nearly every protein feature: pH stability, thermo stability, solvent stability, catalytic efficiency, enantioselectivity, substrate specificity, and even the introduction of new activities into protein scaffolds [7],[8].

Recent activities on α/β-hydrolase fold enzymes showed the improvement of members of this huge protein class towards solvent tolerance, enantioselectivity, substrate specificity, thermo stability, and activity [9]. One method, which led to an improved enantioselectivity of PEE, an esterase of *Pseudomonas fluorescens*, was the construction of so called 'smart libraries'. In this case a multiple sequence alignment of structurally similar enzymes was analyzed using 3DM software [10] (http://www.bioprodict.nl). This software allows the determination of the appearance frequency of certain amino acids within a superfamily of structurally related enzymes. Amino acids that appear frequently are believed to lead to a correctly folded and functional enzyme, and are therefore used in the setup of a mutant library. In the described case four positions within the active site were saturated simultaneously [11].

Several examples state the importance of enzyme engineering in the development of a green chemistry for the production of active pharmaceutical ingredients [12].

1.5 Methyltransferases

As the name implies methyltransferases belong to the second enzyme class the transferases. They are wide spread enzymes in nature. For example 2 % of all proteins of *E. coli* are methyltransferases [13]. The transfer of a methyl group is an essential step in lots of reactions occurring in every living cell. For example DNA and RNA methylation is a critical point in terms of gene expression and protection against degradation. All methyltransferases share the need for a cofactor to perform their action. For the first time Cantoni *et al.*, 1975 [14] described that S-adenosyl-L-methionine (common abbreviations are SAM and AdoMet) is the methyl donor for these reactions. Throughout his thesis SAM is used as abbreviation. It has to be mentioned that at this time only methylation of small molecules was known. Later it became clear that also DNA, RNA, proteins, lipids and carbohydrates are subject to methylation. Despite other methyl donors, SAM

is by far the most frequently used cofactor for methylation reactions. Over the years lots of investigations have been made to clarify structures and functions of SAM dependent methyltransferases and many of them have been described so far [15]. The methylation reaction occurs via a direct S_N2 mechanism with inversion of configuration at the reacting carbon atom [16]. This rearrangement involves a transient hybridization change from sp^3 to sp^2 and back to sp^3 (Figure 2). For activation of the substrate, a nucleophile has to be generated by abstraction of a proton, which can be achieved actively by an acidic amino acid inside the active center of the protein (the majority), or passively under deprotonating conditions (e.g. O-methylation of carboxyl groups, N-methylation of nucleosides) [17]. Classification of methyltransferases can be made either according to the substrate

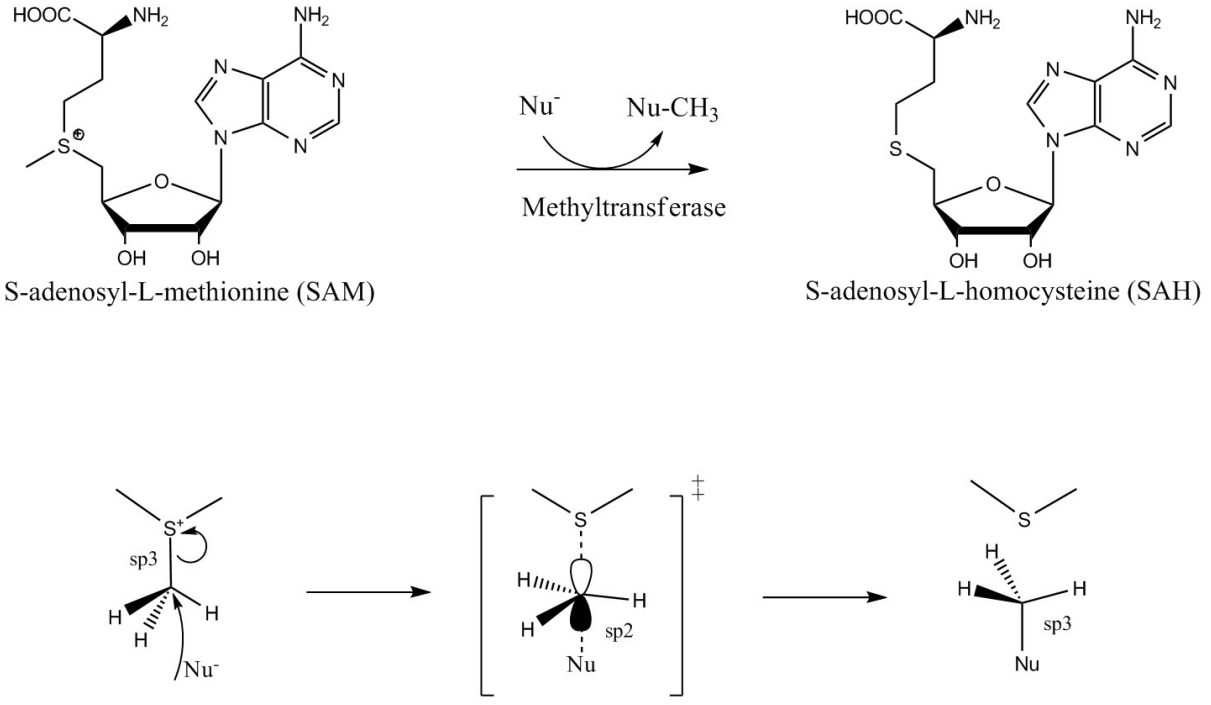

Figure 2: Reaction mechanism of SAM dependent methyltransferases. The attacking nucleophile and the methyl group are involved in a single transition state formation, which includes a transient hybridization change from sp^3 to sp^2 and back with inversion of configuration at the reacting carbon.

or to the atom they methylate.

1.5.1 DNA methyltransferases

In prokaryotes the methylation of DNA can be due to different functions. First, methylation is needed for gene expression, replication, and DNA repair. Dam and Dcm methyltransferases of *E. coli* are well studied examples of this type [18]. Second, methylation of a certain sequence that at the same time represents a recognition site of an endonuclease. This mechanism is known as a restriction - modification (R/M) system. One of the best studied enzyme of this type is M.HhaI of *Haemophilus haemolyticus* which methylates the C5 position of cytosine in the sequence GCGC [19]. Investigations of this enzyme also unraveled the mechanism of how the enzyme can get access to a single nucleotide within a DNA double helix [20]. Members of the third group are encoded by bacteriophages and are involved in survival of foreign DNA within a host [21]. Prokaryotic methyltransferases modify exocyclic amino groups of either adenine or cytosine. Cytosine can be methylated at the C5 or N4 position, and adenine at the N6 position. Certain bacterial DNA methyltransferases (e.g. M.HhaI) were able to accept modified cofactors like Allyl-SAH and transfer the respective alkyl group to the nucleobase substrate [22]. Moreover the same enzyme could be used to add aliphatic aldehyldes to DNA yielding hydroxyalkyl cytosine [23].

Methylation of eukaryotic DNA is restricted to the modification of the C5 position of cytosine. It has been described that this modification plays a central role in gene expression and regulation and therefore can be understood as an epigenetic tool for phenotypic development [24]. Defense against prokaryotic pathogens is another function of eukaryotic methyltransferases [25]. Dnmt1 represents the best understood enzyme of this type, which has been cloned and characterized from different species including mouse and human [26]. Enzymatically these proteins are remarkable concerning their low turnover number of 2-6 h^{-1}, which is about ten-fold decreased compared to bacterial DNA methyltransferases [27],[28]. In addition also demethylation occurs in eukaryotes by the action of methyltransferases. Active demethylation is thought to play a major role in the methylation pattern of developing cells and thereby regulate gene expression [29]. Despite the potential to methylate other nucleobases than cytosines, mammals are able to produce 5-hydroxymethylcytosine with the help of TET enzymes from methylcytosine [30]. As already mentioned before, the formation of 5-hydroxymethylcytosine was also observed for

the bacterial enzyme M.HhaI by incorporation of exogenous aliphatic aldehydes [23],[31]. Together with unmethylated (C) and methylated (mC) cytosine, hydroxymethylcytosine (hmC) is involved in gene regulation and therefore cellular development of higher eukaryotes.

The described examples explain the importance of the methylation state of DNA in both prokaryotic and eukaryotic organisms, and their different functionalities.

1.5.2 RNA methyltransferases

RNA molecules exhibit a variety of nucleoside modifications, and methylation is the most common one. Methylation can occur in all RNAs including tRNA, rRNA, mRNA, and snRNA (small nuclear RNA). Most RNA methylations are found in tRNAs. This methylation was found at varied nucleotides at their carbon, nitrogen, oxygen, or sulfur atoms. Investigations showed that tRNA methylations are involved in maintenance of translational efficiency and fidelity, regulation of cell cycle transitions, and tRNA–protein interaction [32]. Concerning functionality, it was shown that methylation of bases flanking the anticodon or within the anticodon are effecting the proper base pairing for codon recognition [33].

Methyltransferases that modify rRNA play critical roles in the assembly, maturation, and regulation of the protein synthetic machinery [34],[35]. It was also reported that rRNA methylation is involved in the development of antibacterial resistance [36]. Concerning the position of methylation these enzymes can methylate either the base or the ribose.

Eukaryotic mRNA undergoes post-transcriptional modifications including the methylation of certain nucleosides. Methylation of mRNA can happen at the 5'-cap structure or at internal positions. A well studied enzyme for cap-methylation is the N7mG methyltransferase which is specific for methylation of the guanosine in the terminal 5'-dinucleoside triphosphate in capped RNA. The N7mG cap structure is reported to enhance mRNA translation in *Xenopus* oocytes and is independent from polyadenylation at the 3' termini [37]. For methylation of internal nucleosides N6mA methyltransferase is the most frequent enzyme, resulting in about 50 % of all methylated nucleosides in higher eukaryotes [38].

1.5.3 Protein methyltransferases

The most common modification of proteins is phosphorylation via the transfer of a γ-phosphate from ATP to an amino acid side chain of a protein. Despite the high energetic costs of a methyltransfer reaction compared to phosphorylation, some requirements can only be met by methylation. The methylation of arginine via protein arginine-N-methyltransferase (PRMT) is important for transcriptional regulation and RNA splicing [39],[40]. Protein L-isoaspartyl methyltransferase (PIMT; EC 2.1.1.77) has been shown to be important for lifespan in flies [41].

1.5.4 Small molecule methyltransferases

Methylation of small molecules is an important reaction in the generation or degradation of bioactive compounds. Several bacterial species produce secondary metabolites that consist of methylated compounds, meaning that their biosynthesis depends on the action of methyltransferases. Some of these enzymes will be analyzed in detail in Section 1.8. Methylation of small molecules is also important in mammals where they are involved in bulk metabolic transformations by e.g. glycine-N-methyltransferase (GNMT) (Section 1.5.6), or the inactivation of drugs by e.g. catechol-O-methyltransferase (COMT) (Section 1.5.5).

1.5.5 Oxygen-methyltransferases

Oxygen methylation occurs via transfer of the methyl group to a hydroxyl group of phenols and riboses, or to carboxyl groups. The best studied enzyme of this class is catechol-O-methyltransferase (COMT), which attaches a methyl group on the phenolic compound catechol [42]. Enzymatically oxygen needs to be activated to generate enough nucleophilicity for the transfer of the methyl group [17]. COMT has been shown to depend on Mg^{2+} ions, which replace the proton from the hydroxyl group to generate a nucleophilic phenolate [42]. The already mentioned protein L-isoaspartate methyltransferase transfers the methyl group to the carboxyl of L-isoaspartate. Oxygen methylation is also of

great importance for the decoration of antibiotics. The penultimate step in the formation of novobiocin is arranged by methylation of the 4-OH group of the L-noviose moiety [43]. Also the biosynthesis of the antibiotics safracin and saframycin involve the action of O-methyltransferases [44],[45].

1.5.6 Nitrogen-methyltransferases

Methylation of nitrogen is catalyzed by DNA methyltransferases (e.g. M.TaqI, M.EcoRI) [46], which transfer the methyl group to the N6 position of adenine within the respective endonuclease recognition site. M.PvuII is able to methylate the N4 position of both cytosine and adenine [47],[48]. In the mentioned cases, the methylation reaction can take place easily, because of the high nucleophilicity of the exocyclic nitrogen. There is now need for an active deprotonation, due to physiological conditions, which keep the attacked nitrogen deprotonated [17]. In contrast, nitrogen methylation of proteins and small molecules follows a different mechanism. For example arginine-N-methyltransferase (PRMT) and glycine-N-methyltransferase (GNMT) depend on acidic residues for deprotonation of the attacked substrate nitrogen atom [49],[50].

1.5.7 Sulfur-methyltransferases

Sulfur methylation plays a central role in the SAM metabolism (Figure 3) resulting in the formation of methionine. There are two enzymes capable of transforming homocycteine into methionine. Methionine synthase transfers the methyl group from methyltetrahydrofolate (MTHF) to homocycteine (Hcy) and leaving methionine (Met) and tetrahydrofolate (THF). This reaction commonly occurs in some bacteria and mammals (Figure 3). Higher plants and mammals use S-methyl-L-methionine (SMM) or betaine as methyl donor for the same reaction catalyzed by homocysteine S-methyltransferase (HMT) (Figure 5, 6). SMM formation depends on a S-methylation of methionine via the cofactor SAM. This reaction of higher plants is catalyzed by S-adenosylmethionine:methionine S-methyltransferase (EC 2.1.1.12, MMT) [51]. The thiol methyltransferase (TMT) of *Brassica oleracea* (wild cabbage) is also capable of performing a different type of reaction, namely the methylation of thiols like HS^-, SCN^-, $C_6H_5S^-$ and even I^- [52]. Coiner *et al.*, 2006 [53] showed that

a TMT of *Catharanthus roseus* (Madagascar periwinkle), which shows > 50 % sequence identity with the O-methyltransferase COMT, exhibits S-methyltransferase activity on thiols with a preference for benzene and furfuryl thiol.

1.5.8 Carbon-methyltransferases

Compared to oxygen and nitrogen methylation, the methyl transfer to carbon atoms spends more energy for the generation of an intermediate carbanion [17]. However C-C bond formation is a common event in natural systems, and is also of great interest for organic synthesis. Prominent members of this type of enzymes are methyltransferases that bind a methyl group to the C5-position of cytosine nucleobases (e.g. M.HhaI) [20]. Mechanistically the neighboring carbon atom of cytosine has to be deprotonated by an active site cysteine, resulting in sufficient electron density at the attacking carbon, to facilitate the reaction [17]. But the C-methylation is not restricted to aromatic compounds, also aliphatic substrates such as sterol derivatives are being methylated. A well studied example provide sterol-C24 methyltransferases (SMT) of plants and fungi [54].

1.6 Cofactor dependence of methyltransferases

Methyltransfer reactions always depend on a cofactor, which will donate a methyl group that can be transferred to an activated substrate. SAM is by far the most widely used methyl donor of all investigated methyltransfer reactions [15]. Nevertheless several systems exist that use an alternative methyl donor. This includes S-methyl-L-methionine (SMM), betaine, methyltetrahydrofolate (MTHF), methylcobalamin (MeCbl), dimethylthetin, and trimethylsulfonium (Me3S).

Concerning biocatalysis cofactor-dependent enzymes are challenging, unless the needed cofactor can be regenerated easily or produced cheaply, because otherwise a application for commercial use will be unpromising.

1.6.1 S-adenosyl-L-methionine

In all existing systems in nature S-adenosyl-L-methionine is the second most widely used cofactor besides ATP [14]. The methyl group is transferred to various substrates with a more favorable enthalpy (≈ -70 kJ/mol) compared to other methyl donors. For comparison SAM is about 1000 times more reactive than methyltetrahydrofolate (MTHF) [14]. The chemical advantage of SAM for methyltransfer reactions is due to the charged sulfur atom which binds the methyl group. The sulfur atom destabilizes the SAM molecule and thereby leads to a very reactive methyl group. The SAM-dependent methyltransferases have been investigated thoroughly in the last two decades, leading to structure determination of > 100 proteins. As methylation of DNA is an essential modification for gene regulation and cellular metabolism, it is not surprising that the first SAM-dependent methyltransferase to be crystallized was the C5-cytosine methyltransferase M.HhaI back in 1993 [19].

Chemically SAM consists of a methionine part, which is presenting the methyl group, and of a covalently linked adenosine part. SAM metabolism involves several enzymes and cofactors, and depends on the organism (Figure 3). For example in mammals the SAM cycle is linked to spermine production [55]. In higher plants the SAM cycle interacts with the one of SMM, which itself is a cofactor of S-methyltransferases [56] (Figure 5). The bacterial metabolism reflects the core element of both cycles and involves an alternative route in the conversion of S-adenosyl-L-homocysteine (SAH) to homocysteine (Hcy) in two steps [57]. First, cleavage of SAH to S-D-ribosyl-L-homocysteine (SRH) and adenine by SAH nucleosidase (EC 3.2.2.9). Second, conversion of SRH to Hcy and 4,5-dihydroxy-2,3-pentanedione [58]. Concerning methylation of homocycteine, some bacteria and mammals use methylcobalamin, which derives from coenzyme B_{12}, instead of the commonly used methyltetrahydrofolate (MTHF). .

Besides the general S_N2 reaction mechanism SAM radical methylation has been reported for difficult chemical reactions. Sofia *et al.*, 2001 [59] used a bioinformatic approach for the identification of SAM dependent enzymes, which use a radical reaction mechanism. The listed enzymes share a conserved CxxxCxxC motif, and facilitate a broad range of enzymatic reactions. The methyl transfer reaction is coordinated by an iron-sulfur cluster

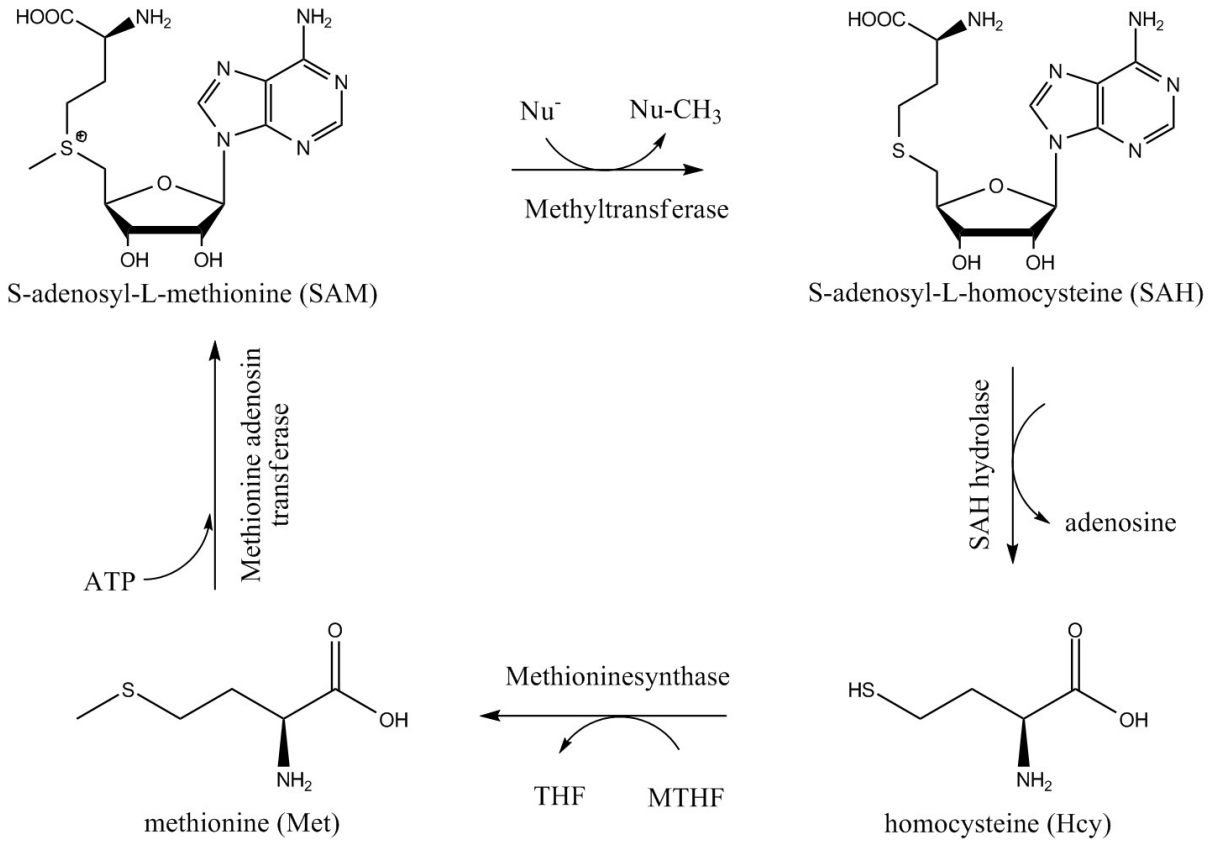

Figure 3: The core of the S-adenosyl-L-methionine cycle. The SAM-dependent methyltransferase transfers the methyl group of SAM to various substrate nucleophiles leaving S-adenosyl-L-homocysteine (SAH), which is hydrolyzed by SAH hydrolase to adenosine and homocysteine (Hcy). Methylation of Hcy is achieved by methionine synthase with the use of methyltetrahydrofolate (MTHF) in the formation of methionine. Finally SAM is regenerated by the methionine adenosine transferase that attaches the adenosine part to methionine under ATP hydrolysis

and the conserved cysteine residues, which generate a free radical by reductive cleavage of SAM. Methyltransferases using this reaction mechanism have been reported for the biosynthesis of the antibiotics clorobiocin, coumermycin A_1 and thiostrepton [60-62].

1.6.2 Analogues of S-adenosyl-L-methionine

Due to the fact that SAM-dependent methyltransferases are involved in lots of cellular processes, they and their substrates are recognized as potential targets for analytics, intermediates, or pharmaceuticals. In case of the SAM-dependent methyltransferases, which have strong binding affinities to their cofactor, a selective modification of the cofactor would lead to a promising target.

In 1980 SAM analogues, which showed inhibitory effects on methyltransferases were reported for the first time [63]. This promoted the research for the establishment of effective SAM analogous. Pignot *et al.*, 2000 [64] investigated several synthetic cofactors, which were based on the SAM structure, towards their binding affinities to the DNA-methyltransferase M.HhaI. This study gave insights into the molecular interactions between cofactor and protein. On the contrary, the natural SAM-analogue sinefungin did also serve for the investigations of protein-ligand interactions. Sinefungin, also known as adenosyl-ornithine, is an antimicrobial agent from *Streptomyces griseolus*, which inhibits methyltransferases by blockage of the cofactor binding site [65]. The analysis of sinefungin in comparison to SAM and SAH led to the identification of relevant binding positions of the cofactor. It was shown that both the methionine and the adenosine part of SAM interact via hydrogen- and van der Waals bonds with amino acids located in the binding pocket of the protein [66].

Later N-adenosylaziridine was invented for sequence specific labeling of DNA by incorporation of an aziridine cofactor linked to a fluorophore with the use of the DNA-methyltransferase M.TaqI [67] (Figure 4). This study revealed two striking facts. First, the transfer of more than just the methyl group, but the whole cofactor on the DNA substrate was achieved. Second, the amino acid part of the cofactor, which is replaced by an aziridine group, is not needed for cofactor recognition. A similar SAM modification was achieved by the synthesis of an N-mustard compound, which is related to the aziridine

cofactor described above, but also contains the methionine part of the natural cofactor SAM (Figure 4). It was shown that this N-mustard, which undergoes transformation to aziridine under biological conditions, can be utilized for alkylation of DNA (Figure 4). The DNA-methyltransferases M.TaqI and M.EcoR1 were able to modify DNA duplexes containing the respective recognition sites [68]. The same SAM analogue was also utilized by the rebeccamycin O-methyltransferase RebM for the formation of new rebeccamycin derivatives [69].

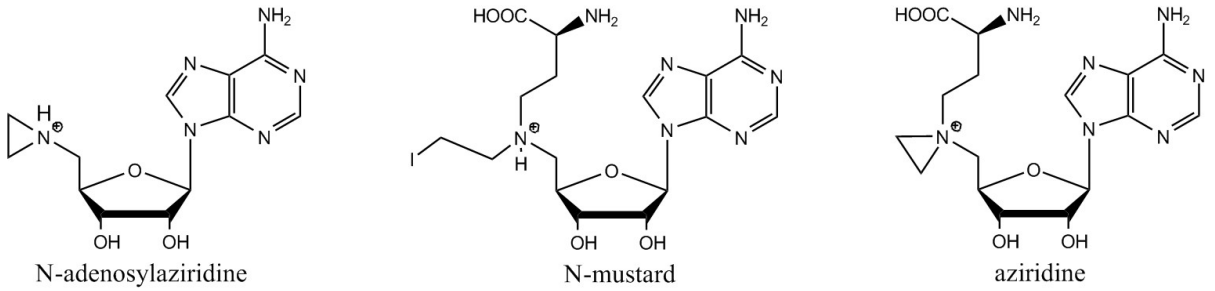

Figure 4: S-adenosyl-L-methionine and aziridine analogues. For enzymatic transfer reaction the aziridine ring is activated for nucleophilic attack by protonation of the ring nitrogen atom. N-mustard is probably transformed to aziridine prior to the methyltransferase catalyzed reaction. In contrast to methylation reactions, the whole aziridine cofactors are transferred to the respective substrates.

Modifications of SAM with extended carbon chains revealed the ability of methyltransferases to transfer other alkyl groups than methyl to DNA [70]. This study also disclosed the advantage of carbon carbon double bonds of the transferred alkyl group in contrast to the methyl group. The same authors could also prepare SAM analogues with extended propargylic side chains carrying a primary amino group, which can be used for chemoligation reactions with amine-reactive probes to attach desired reporter groups onto DNA [71].

SAH capture compounds (SAH-CC) were another invention, which described the use of SAM analogues for analysis and discovery of methyltransferases [13]. The SAH capture compounds contain three functional parts: First, the cofactor product S-adenosyl-L-homocysteine enables directed, non-covalent pre-binding to the enzyme. Second, a photoreactive group facilitates covalent cross linking between the cofactor analogue and the protein. The third part is used for isolation with streptavidin-coated magnetic beads that bind to biotin. It was shown that these SAM analogues can be used for determination of

dissociation constants of several methyltransferases and the demethylated cofactor SAH. Moreover, the isolation of SAH-binding proteins from *E. coli* lysates was also described [13].

Another investigation showed that DNA methyltransferases are also able to accept aldehydes as co-substrates for DNA modifications. The aldehyde transfer catalyzed by the DNA-methyltransferase M.HhaI results in an intermediate compound that is further transformed to yield 5-α-hydroxyalkylcytosine. Furthermore the same study revealed the ability of M.HhaI to catalyze the reverse reaction and re-establishment of unmodified DNA [23].

1.6.3 S-methyl-L-methionine

Some reactions of higher eukaryotes require S-methyl-L-methionine (SMM), also termed vitamin U, for donation of a methyl group in the formation of methionine from homocycteine (Figure 5). The enzyme capable of performing this reaction is called S-methylmethionine (or S-adenosylmethionine): homocysteine S-methyltransferase (HMT). In the plant model organism *Arabidopsis thaliana* the enzyme AtHMT performs this reaction. It is noteworthy that this organism is also capable of performing the utilization of methionine and SAM for production of SMM via the S-adenosylmethionine:methionine S-methyltransferase (MMT) [56],[72]. In humans the enzyme betaine-homocycteine S-methyltransferase (BHMT) is capable of performing the same reaction as AtHMT, but can also utilize betaine as a methyl donor. Interestingly the isoenzyme BHMT-2 prefers SMM as methyl donor and to some extend accepts SAM too [73]. Szegedi *et al.*, 2008 conclude that BHMT1 has evolved for methylation via betaine, and BHMT-2 is responsible for SMM dependent methylation of homocysteine.

1.6.4 Betaine

Betaine is involved in methylation reactions via the betaine-homocysteine S-methyltransferase (BHMT) in mammalian liver and kidney tissues (Figure 6). BHMT transfers the methyl group from betaine to homocysteine under the formation of methionine and dimethylglycine [74]. This reaction is directly linked to choline oxidation.

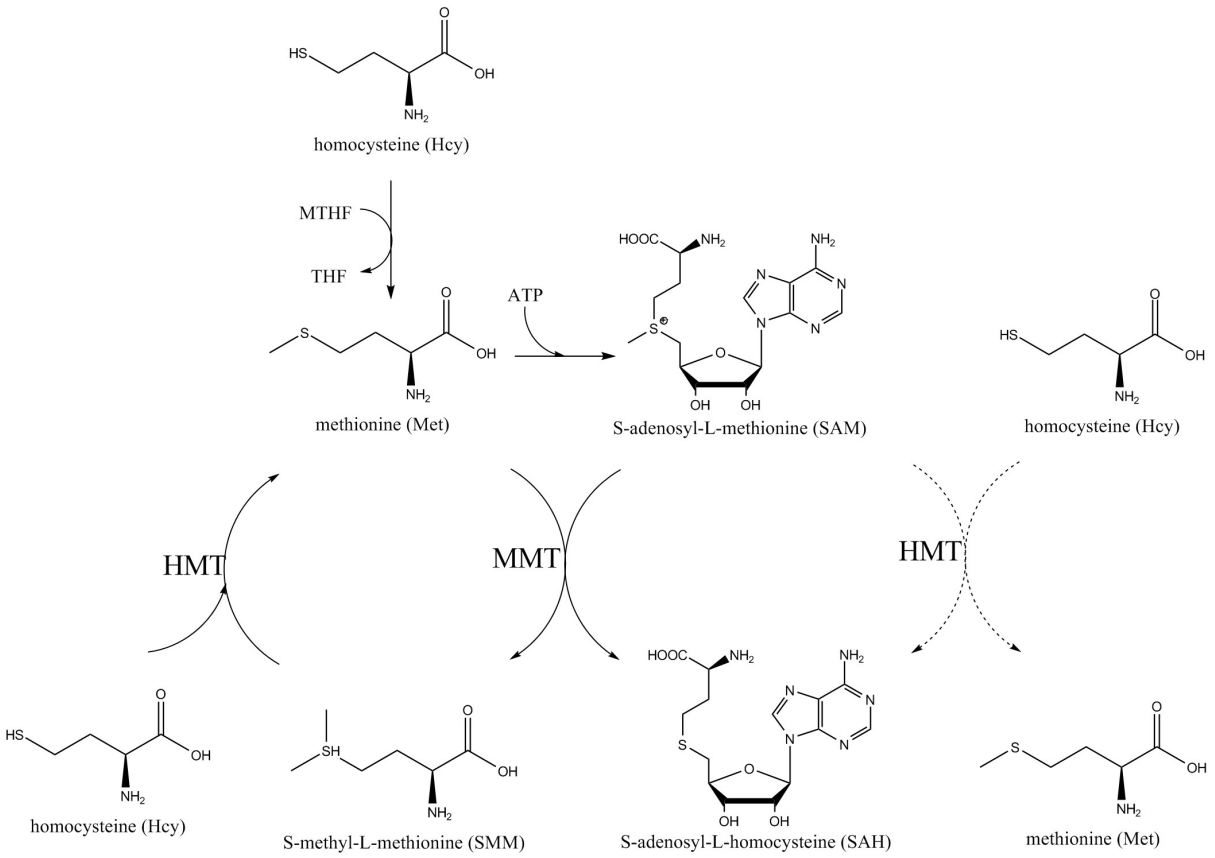

Figure 5: The SAM cycle of higher plants involves SMM as another methyl donor. The formation of SMM depends on the SAM-dependent methionine methyltransferase (MMT) and the substrate methionine. Plants utilize the formation of methionine via the homocysteine methyltransferase (HMT) by transfer of a methyl group from SMM to Hcy. Dotted arrows indicate a possible SAM-dependent methylation of Hcy in the formation of methionine.

Already mentioned before, the isoenzyme BHMT-2 prefers S-methyl-L-methionine (SMM) as a methyl donor for the methylation of homocysteine. The methylation of homocysteine can also be facilitated by methionine synthase via the cofactor methyltetrahydrofolate (MTHF) or methylcobalamin (Figure 3) [75].

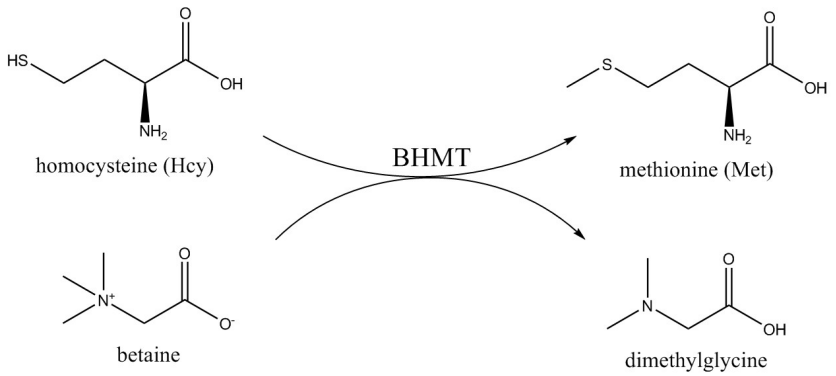

Figure 6: Betaine as methyl donor for the formation of methionine. The methyl group is transferred from betaine to homocysteine under the formation of methionine and dimethylglycine by the methyltransferase betaine-homocysteine S-methyltransferase (BHMT).

1.6.5 Methyltetrahydrofolate

Methyltetrahydrofolate (MTHF) is the methyl donor in the methylation of homocysteine yielding methionine (Figure 8). This reaction is catalyzed by methionine synthase, and is part of the metabolic SAM cycle (Figure 3). MTHF itself is produced by enzymatic methylation of tetrahydrofolate, via DMSP:tetrahydrofolate methyltransferase from dimethylsulfoniopropionate (DMSP) (Figure 8) [76]. MTHF is the methyl donor of an iron-sulfur protein methylation in *Clostridium thermoaceticum*, where the methyl group of MTHF is transferred to a corrinoid/iron-sulfur protein (CFeSP), forming methylcob(III)-amide [77].

1.6.6 Methylcobalamin

Some bacteria and mammals utilize methylcobalamin (MeCbl) for the methylation of homocysteine in the formation of methionine and cobalamin. Cobalamin itself is methylated by donation of the methyl group from MTHF. The enzyme catalyzing these two reaction

consecutively in *E. coli* is the methionine synthase MetH [78],[79]. Methylcobalamin is derived from vitamin B_{12}, which is also the precursor of 5´-deoxyadenosylcobalamin (AdoCbl) that is the cofactor of methylmalonyl-CoA mutase, a mitochondrial enzyme that catalyzes the isomerization of methylmalonyl-CoA to succinyl-CoA [80]. MeCbl and AdoCbl are the two active species of vitamin B_{12}, which displays a corrinoid structure (Figure 7) [81].

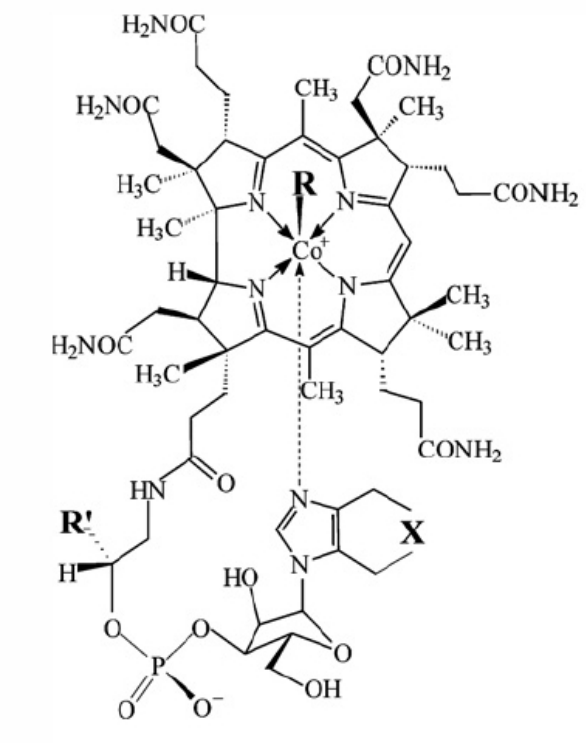

Figure 7: The corrinoid structure is the basis for vitamin B_{12} and its derivatives. Vitamin B_{12}: R = CN, R' = CH_3; Methylcobalamin (MeCbl): R = CH_3, R' = CH_3; 5´-deoxyadenosylcobalamin (AdoCbl): R = 5'-deoxy-5'-adenosyl, R' = CH_3.

1.6.7 Thetin

The role of thetin in methyltransfer reaction has not been drawn much attention (Figure 8). Back in 1959 it was shown that thetin-homocysteine transmethylase catalyzes the transfer of a methyl group from dimethylthetin to homocysteine. The enzyme, which is present in the liver of vertebrates can also use trimethylsulfonium as a methyl donor [82]. Slow *et al.*, 2004 [83] could show that betaine, dimethylthetin, and DMSP (Figure 8),

were accepted as methyl donors for the formation of methionine from homocysteine in rats.

1.6.8 Trimethylsulfonium

Trimethylsulfonium (Me3S) was shown to be a methyl donor for the formation of methyltetrahydrofolate (MTHF) and dimethyl sulfide in *Pseudomonas sp.* [84], (Figure 8).

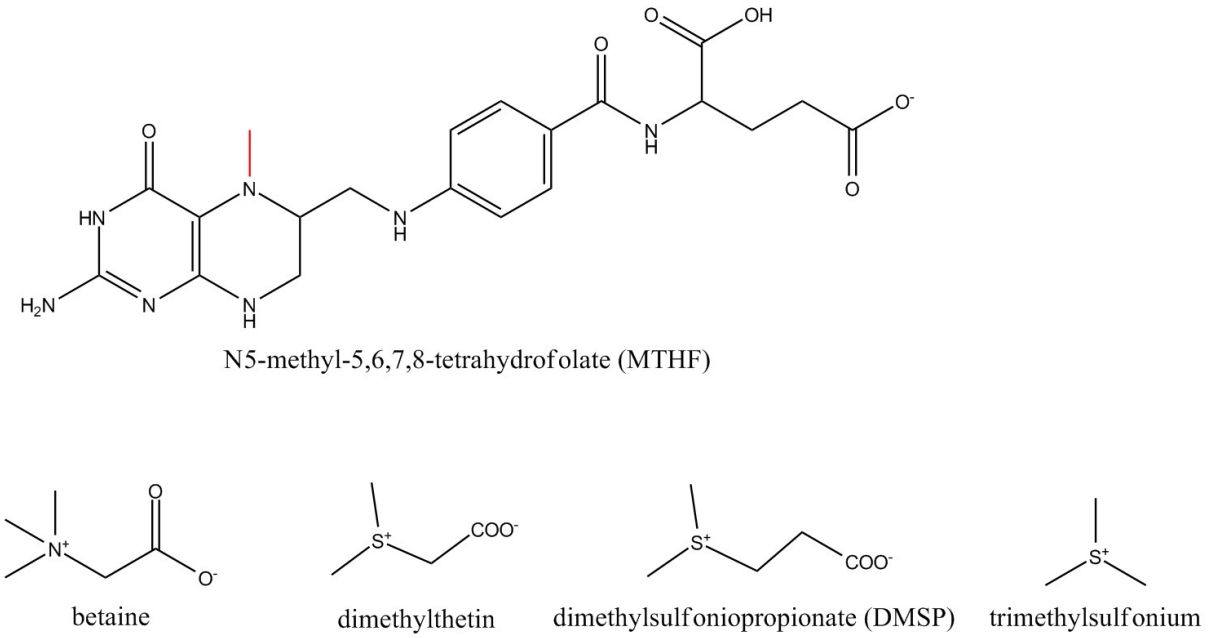

Figure 8: Structures of some cofactors for methyltransferases.

1.7 Structural aspects of methyltransferases

Like other bisubtrate enzymes, the structure of methyltransferases enables the protein to bind two substrates at the same time. As the variety of methyltransferases in means of the diverse substrate scope is tremendous, one would expect a broad range of structural folds. Despite the low sequence identity, methyltransferases incorporate a common architecture consisting of a seven-stranded beta sheet and six alternating alpha helices (Figure 9) [85]. The seventh beta strand is oriented anti parallel to the other. This builds up the double wound open $\alpha\beta\alpha$ sandwich structure. An α/β motif is present in the majority of all enzyme structures [86]. All methyltransferases can bind the cofactor, which in most cases

is SAM, but can also be one of the described alternatives. Most of the so far described methyltransferases use SAM for donation of the methyl group. Therefore the majority of the elucidated structures includes a similar SAM binding pocket. Sterically this cofactor binding pocket is in close proximity to the substrate binding pocket. This is of great importance to facilitate the described reaction mechanism. Whereas the SAM-binding domain is relatively high conserved, the substrate binding site shows a tremendous variety, because of the diverse size, shape, and chemistry of the substrates.

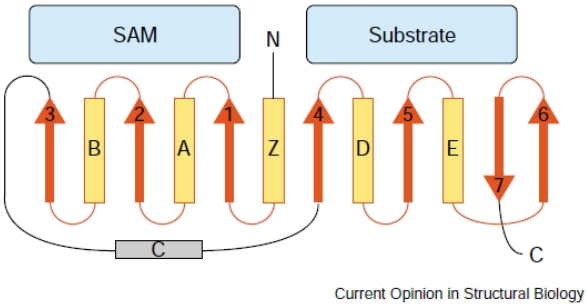

Figure 9: Common architecture of SAM-dependent methyltransferases. Helices are shown as yellow cylinders, strands as red arrows. Alpha C is shown in gray, because it is not always conserved in the core fold. The SAM and substrate binding regions are indicated with light blue bars. Picture taken from Martin *et al.*, 2002 [85].

Five classes of folds have been described so far [87]. Class I, III, and IV show high similarity to NAD(P)-binding Rossmann fold proteins. The overall architecture of both protein types is striking, including at least a six-stranded parallel beta-sheet, and a deep cleft for SAM- or NAD(P)-binding. Keeping in mind the structural similarity of SAM and NAD(P), the relation of these proteins is not surprising. Both cofactors, SAM and NAD(P) consist of an adenosine part that is attached to either methionine (SAM), or nicotinamide (NAD) (Figure 10).

Class I Most of structurally described methyltransferases belong to the class I family, including the prominent proteins COMT, M.HhaI, PRMT, and GNMT. Characteristic of the class I fold is its high similarity to the common core, which represents a typical $\alpha\beta\alpha$ sandwich structure. For example COMT is the best example of this class, because it is almost identical to the core fold [42]. As already described the substrate scope of methyltransferases is very broad. Even within class I the substrate spectrum ranges from small molecules to DNA or RNA. The proteins have evolved to cover such a broad range

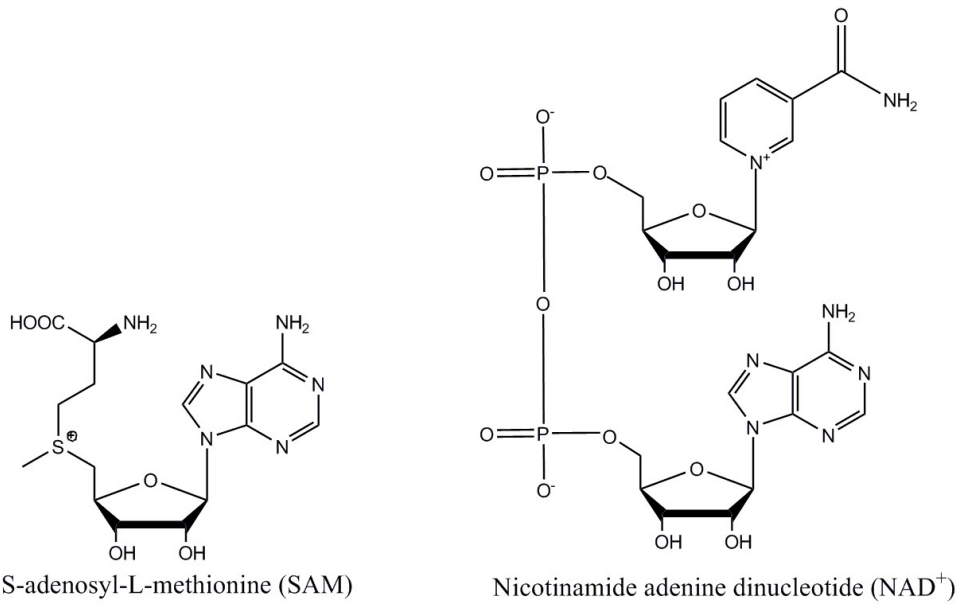

Figure 10: Chemical structures of S-adenosyl-L-methionine (SAM) and nicotinamide adenine dinucleotide (NAD^+). The similartiy of these cofactors is obvious concerning the adenosine and ribose moieties.

of substrate molecules, although they stick to the same core fold. One can imagine that binding a small molecule like catechol depends on less flexibility and rearrangement of the protein structure compared to a nearly unaccessible nucleobase in a DNA double helix. The DNA methyltransferase M.HhaI has solved this problem by a certain mechanism called base flipping. The enzyme gets access to a certain cytosine inside the major groove of the DNA double helix by rotating the target cytosine out of the DNA, without disturbing the integrity of the macromolecule [20]. Conserved domains of class I enzymes are a E/DXGXGXG motif located between β1 and αA, often referred as motif I, which interacts with the methionine part of SAM. It is noteworthy that this sequence motif can vary to some extend. There can also be a lack of the last glycine (GNMT, [88]), an insertion of two more amino acids between E/D and G (NovO, aminocoumarin C-methyltransferase, Section 2.2), or the location of an Y instead of E or D (Vp39, RNA O-methyltransferase [89]). The second conserved domain consists of the acidic amino acids E or D located at the end of β2. This domain interacts with the ribose hydroxyl group of SAM and is known as motif II.

Class II The methionine synthase MetH of *E. coli* is a representative of the class II methyltransferases. Enzymatically this enzyme is very interesting, because it catalyzes

two methyltransfer reactions consecutively and uses three different cofactors. First, the methyl group is transferred from methylcobalamin to homocysteine. Second, cobalamin is methylated via the cofactor methyltetrahydrofolate in a first turnover, and is reactivated via the third cofactor SAM [78]. Its architecture is distinct from class I proteins. The cofactor SAM, which is needed for reactivation, is bound in a groove consisting of long β strands [90].

Class III The precorrin-4 C11-methyltransferase CbiF belongs to the class III methyltransferases. It contains two $\alpha\beta\alpha$ domains which surround the cofactor SAM. Similar to class I, a GXGXG motif is located next to β1, but does not contact the cofactor. The enzyme catalyzes the SAM-dependent methylation of cobalt-precorrin-4 to cobalt-precorrin-5 in the formation of vitamin B_{12} [91].

Class IV A relatively new class was first described in 2002, which did not fit to the three known folds [92],[93]. The SPOUT class of RNA methyltransferases consist of a β-sheet with at least five parallel strands and five alternating helices. A special feature is a deep trefoil knot at its C-terminal that contributes to SAM-binding. Recently the rRNA methyltransferase Nep was crystallized and revealed two structural extensions to the SPOUT class fold. An insertion of a globular loop between β1 and α2 of the core motif and an insertion of a $\beta\alpha\beta$ element between β2 and α5 [94].

Class V Methyltransferases of class V, also called SET-domain proteins, have two separate grooves, one for SAM and the other for substrate binding. These binding pockets are located on different sides of the protein. This type of architecture is very helpful, if mulitmethylation is needed, because otherwise the demethylated cofactor would block the binding pocket, and an incomplete methylated product will be released. Protein lysine N-methyltransferase of the Rubisco complex is a member of this type of enzymes [95]. The topology of SET domain methyltransferases is made of eight curved β strands forming three small sheets and a knot like structure at the C-terminus, similar to the SPOUT fold.

1.8 Aromatic C-methyltransferases

1.8.1 Aminocoumarin methylating enzymes

Methyltransferases that act on bicyclic aromatic compounds can be found in *Streptomyces* species that produce coumarin antibiotics, where these enzymes are involved in the methylation of certain precursors. This type of antibiotics exhibit potent antimicrobial activity by targeting DNA gyrase [96],[97]. Coumermycin, clorobiocin, and novobiocin belong to this family (Figure 11). Novobiocin (Albamycin; Pharmacia & Upjohn) has been licensed

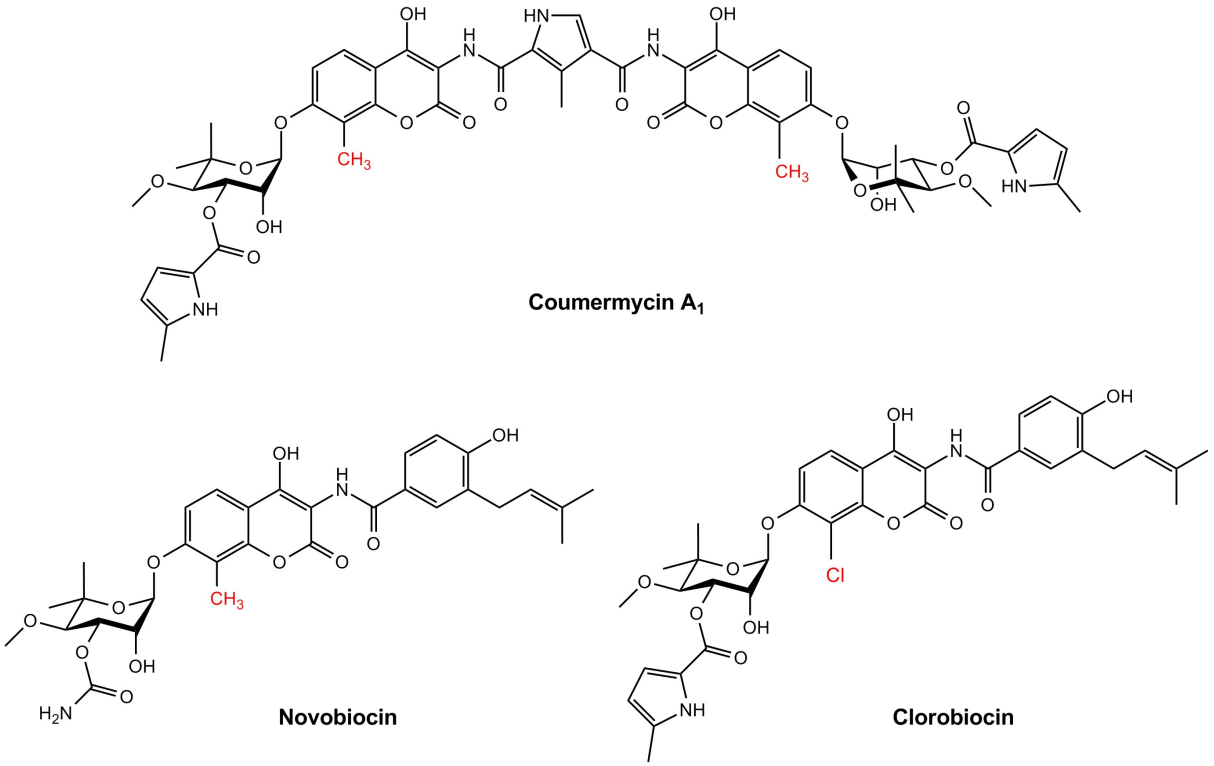

Figure 11: Structures of the aminocoumarin antibiotics coumermycin A_1, novobiocin, and clorobiocin. The position of the methyl group that was transferred via the methyltransferases CouO or NovO to the coumarin derivative structures are highlighted in red. In clorobiocin the position of the chlorine that is attached at the same position as the methyl groups of coumermycin A_1 and novobiocin, is also highlighted in red.

in the United States as an antibiotic for the treatment of infections with multi-resistant gram-positive bacteria, such as *Staphylococcus epidermidis* and *Staphylococcus aureus* [98-100]. It has been shown that subunit B of DNA gyrase is bound by the aminocoumarin moieties and the substituted deoxysugar moieties of coumermycin, clorobiocin, and novobiocin [101]. In case of clorobiocin and novobiocin also the prenylated 4-hydroxybenzoate

moieties interact with the gyrase B protein subunit [102]. Coumermycin and clorobiocin contain another binding site, a methylpyrrole-2-carboxylic acid unit that is attached to the 3-OH of each deoxysugar moiety. It has also been shown that this moiety enables a much higher binding affinity than the prenylated 4-hydroxybenzoate moiety of novobiocin. As coumermycin contains two of these aminocoumarin-deoxysugar moieties it exhibits the highest degree of binding to gyrase B among these three antibiotics [103]. DNA gyrase is a bacterial type II topoisomerase, which introduces negative supercoils into DNA by double strand breakage. Therefore the DNA is rolled around the protein, that consists of two subunits forming an A_2B_2 complex, followed by cleavage of both strands. After passing a segment of DNA through this strand break the gap is sealed and the topology of the DNA contains one negative supercoil. Importantly this reaction depends on the hydrolysis of ATP. For this purpose the enzyme is able to bind ATP for its activity. It has been shown that subunit B is responsible for ATP binding, and that this is also the target for aminocoumarin compounds. Therefore aminocoumarins inhibit bacterial DNA replication by repression of ATP hydrolysis on subunit B of DNA gyrase [101],[102].

In the last decade great effort has been made on the unraveling of the biosynthesis of these antibiotics, leading to an understanding of the involved enzymes and the order of their action [103-106],[60]. Whereas biosynthesis of clorobiocin lacks the action of a C-methyltransferase, coumermycin and novobiocin production depends on two aromatic C-methyltransferases. CouO of *Streptomyces rishiriensis* methylates the precursor of coumermycin A_1 and NovO of *Streptomyces spheroides* methylates the precursor of novobiocin (Figure 11). In clorobiocin a chlorine is attached at position 8 of the aminocoumarin ring, which is the same position of the methyl group in coumermycin and novobiocin. The similarity of these compounds goes in hand with the similarity of responsible biosynthetic gene clusters of respective strains. The gene *clo-hal* of *Streptomyces roseochromogenes* is located relatively at the same position as *couO* and *novO* in *Streptomyces rishiriensis* and *Streptomyces spheroides*, respectively. *clo–hal* is a homologue of the non-haem halogenase genes *comH* of *Streptomyces lavendulae* [107]. Elucidation of the function of enzymes which are involved in the biosynthesis of these aminocoumarins and progress in genetic engineering led to the successful production of chimeric aminocoumarin compounds [108-110],[43]. Wolbert *et al* [11] described the production of chlorinated coumermycin derivatives and their antibacterial activities. These studies intend to give further insights into

structure-activity relationship of aminocoumarin antibiotics.

CouO and NovO share high sequence identity of 85 % on primary protein structure. This high value of identity is not surprising when considering the similarity of the substrates. Previously it has been shown that the enzymes accept both substrates, the coumermycin A_1 and the novobiocin precursor molecule [105]. The protein sequence of both enzymes contain the conserved motif I D/EXXXGXG as DLCCGSG located near the amino terminus. Remarkable two cysteins are inserted between D and G of this motif.

1.8.2 Tyrosine methylating enzymes

Methyltransferases that transfer a methyl group onto the amino acid tyrosine were found in *Pseudomonas fluorescence A1* [44] and in *Streptomyces lavendulae* [45]. The enzymes catalyze the transfer of a methyl group from SAM to C-3' of tyrosine **11** resulting in 3'-methyltyrosine **12** (Figure 38). In the mentioned bacteria this 3'-methyltyrosine is further converted to yield the antibiotics safracin and saframycin, respectively (Figure 12). In both cases the methyltransfer reaction is the first enzymatic step in the biosynthetic pathway, which include non-ribosomal peptide synthetases (NRPS) and tailoring enzymes. Both compounds belong to the class of isoquinoline alkaloids that exhibit antibiotic and antitumor activities [111],[112]. Since the report of these compounds similar ones have been found including ecteinascidin. Ecteinascidin 743 (ET743) , isolated from marine invertebrates, has a core that is structurally similar to that of saframycin and is currently in clinical trails as an anticancer drug [113]. Functionally these compounds are thought to interact with DNA and thereby forming covalent bonds that are essential for cytotoxicity [114]. Other reports suggest an interaction of a drug-DNA-complex with GAPDH (glycerinaldehyde-3-phosphate dehydrogenase) [115]. A review published in 2002 gives a detailed overview about structure and function of this class of drugs [116]. Coding sequences of putative tyrosine-C-methyltransferases were designated to *sacF* of *Pseudomonas fluorescence A1* and *sfmM2* of *Streptomyces lavendulae*. The resultant proteins reveal 64 % sequence identity and contain the conserved sequence motif I D/EXXXGXG as DAGGGDA and DCGGGDA, respectively. In contrast to the coumarin methylating enzymes NovO and CouO, which locate motif I near their amino terminus, it is located right in the middle of the whole sequence of SacF and SfmM2.

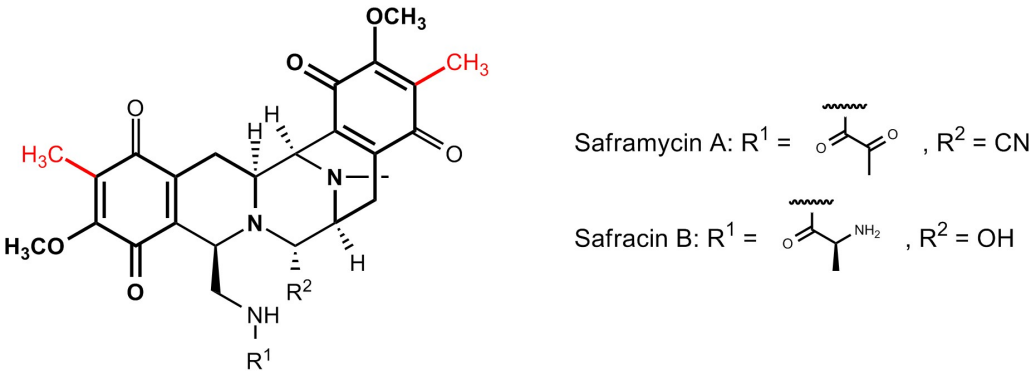

Figure 12: Structures of the isoquinoline alkaloid antibiotics safracin and saframycin. The position of the methyl group which is transferred to tyrosine during biosynthesis via the methyltransferases SacF or SfmM2 of the respective compound is highlighted in red.

1.8.3 Hydroxykynurenine methylating enzymes

Another type of methyltransferases that transfer the methyl group of SAM on small aromatic substrates was found in the biosynthesis of the antibiotics actinomycin, anthramycin, and sibiromycin. Actinomycin, a bicyclic chromopeptide lactone, which is produced by *Streptomyces chrysomallus* [117] and *Streptomyces antibioticus* [118], is structurally different from both anthramycin and sibiromycin (Figure 13, 15). Actinomycin intercalates into GC-rich regions of DNA and thereby inhibits transcription in both prokaryotes and eukaryotes [119]. Due to high toxicity of the compounds tumor therapy is only possible for a few tumor types [120]. Anthramycin produced by *Streptomyces refuineus* [121] and sibiromycin produced by *Streptosporangium sibiricum* [122] belong to the group of pyrrolobenzodiazepines and therefore share high structural similarities including a methylated aromatic structure (Figure 15). Anthramycin exhibits a variety of antimicrobial, antiviral , and anti-tumor activities. Its activity results from non-covalent binding to TA-rich regions in the minor groove of DNA followed by irreversible covalent modification of the N2-amino group of a vicinal guanine [123]. Sibiromycin follows the same way of action on DNA, but has an even higher binding affinity to its target, because of an O-glycosylation at C7 [124]. However, the biosynthesis of all three antibiotics involve a similar methyl transfer reaction. Several studies claimed that the biosynthesis of actinomycin [118], anthramycin [121], and sibiromycin [122] involves the methylation of 3-hydroxyanthranilic acid (3-HA) that is derived from 3-hydroxykynurenine (3-HK). Recently Crnovčić *et al.*, 2011 [117] described that the biosynthesis of actinomycin in *Strep-*

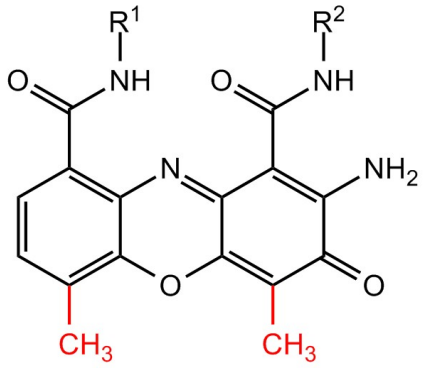

Figure 13: Structure of the bicyclic chromopeptide lactone actinomycin. The position of the methyl group which is transferred to the 3-hydroxykynurenine moiety is highlighted in red.

tomyces chrysomallus depends on the methylation of 3-hydroxykynurenine (Figure 14). Orf19, the methyltransferase of *Streptomyces refuineus* shares 60 % sequence identity with

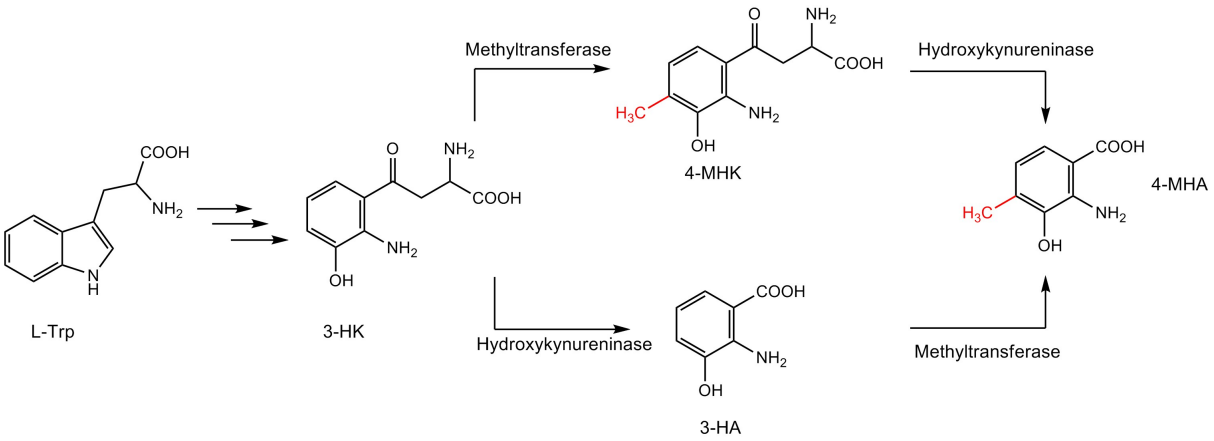

Figure 14: Methyltransfer catalyzed by the methyltransferases of *Streptomyces chrysomallus, -antibioticus, -refuineus*, and *Streptosporangium sibiricum*. Tryptophan is the starting compound that is converted in three steps to 3-hydroxykynurenine (3-HK). For the formation of 4-methyl-3-hydroxyanthranilic acid (4-MHA) two directions are possible. First, via methylation of 3-HK and subsequent kynureninase activity Second, via kynureninase activity on 3-HK and subsequent methylation of 3-hydroxyanthranilic acid (3-HA). The position of the methyl group which is transferred to the 3-HA or to the 3-HK moiety is highlighted in red.

SibL, the methyltransferase of *Streptosporangium sibiricum*. Similar to the described tyrosine methylating enzymes, the conserved sequence motif I is located in the middle of the protein sequence, and in both cases consists of the amino acids DVGGGDA. Moreover, Orf19 shares 47 % sequence identity with SfmM2 and 44 % with SacF. An sequence alignment of all four enzymes Orf19, SibL, SacF, and SfmM2 results in 30 % identity. Keeping

in mind, that although methyltransferases share a common structural architecture and their primary sequences do not show much identity, this relatively high identity could be a hint for some functional similarity. Generally a structure-guided sequence alignment would state the sequence identity of structurally similar methyltransferases below 17 %. Only the conserved domains, motif I and motif II, outstand this low similarity.

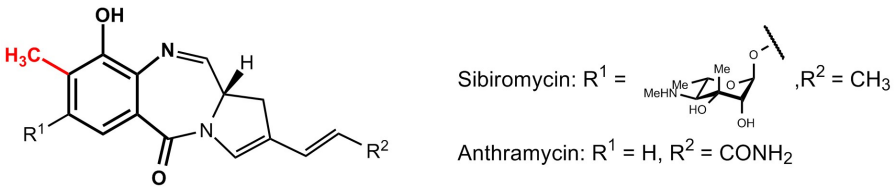

Figure 15: Structures of the pyrrolobenzodiazepines anthramycin and sibiromycin. The position of the methyl group which is transferred to 3-hydroxykynurenine moiety via the methyltransferases Orf19 and SibL is highlighted in red.

1.8.4 Tryptophan methylating enzymes

Methylation of tryptophan is also an essential step in the biosynthesis of antimicrobial agents. The production of thiostrepton involves several enzymatic steps including the methyltransfer on tryptophan, which is the first step in this biochemical pathway (Figure 17). Thiostrepton inhibits bacterial protein synthesis by binding to 23S rRNA and protein L-11. This complex reacts with elongation factor G and translocation along the mRNA transcript, and at the same time interacts with the large ribosomal subunit where it blocks GTP hydrolysis of elongation factor Tu [125],[126]. First reports of isolation of thiostrepton go back to the 1950's where *Streptomyces azureus* was identified as producer strain [127-129]. Later also *Streptomyces laurentii* [130] and *Streptomyces hawaiensis* were reported as producer strains of thiostrepton [131]. The methyltransferase of *Streptomyces laurentii* responsible for the methylation of tryptophan was characterized by Frenzel and co-workers in 1990 [132]. Although purification of an active enzyme was not possible, some characteristics could be determined, which stated the SAM-dependent methyltransferase to use an unusual mechanism for the methyltransfer reaction. Unlike the great majority of all other methyltransferases, this enzyme transfers the methyl group of SAM with net retention of configuration. Also other antimicrobial agents consist of a quinaldic acid moiety like thiostrepton. It is assumable that synthesis of these compounds must depend on the

action of a tryptophan-C-methyltransferase too. *Streptomyces sioyaensis* which produces the antibiotic siomycin could exhibit this feature (Figure 16). Recently biosynthetic gene

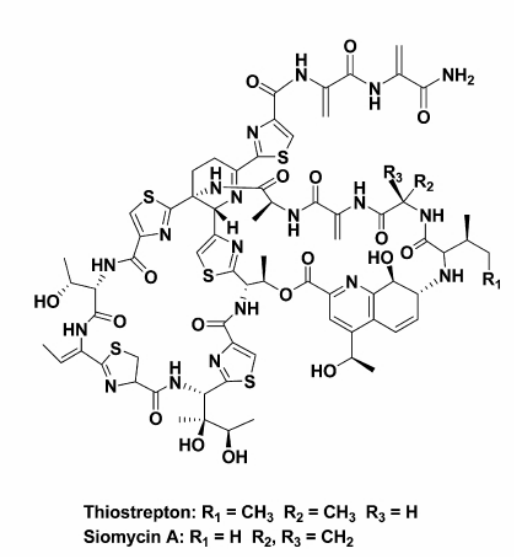

Figure 16: Structures of the thiopeptide antibiotics thiostrepton and siomycin.

clusters of thiostrepton and siomycin producer strains *Streptomyces laurentii* and *Streptomyces sioyaensis* were identified, respectively [133],[62]. It was shown that all involved enzymes exhibit high similarity and that both clusters include two C-methyltransferases. One of each is meant to be a radical SAM-dependent methyltransferase. SioF of *Streptomyces sioyaensis* and TsrP of *Streptomyces laurentii* share 80 % sequence identity. Kelly *et al.*, 2009 [62] claimed that TrsP fails to meet the expectation for methylation of tryptophan, but proposed that TsrM could catalyze this reaction via a radical mechanism and retention of the methyl group stereochemistry. SioT of *Streptomyces sioyaensis* that shares 81 % identity with TsrM could be responsible for the same reaction in the production of siomycin. So far no enzymatic data is available about the characteristics of these methyltransferases.

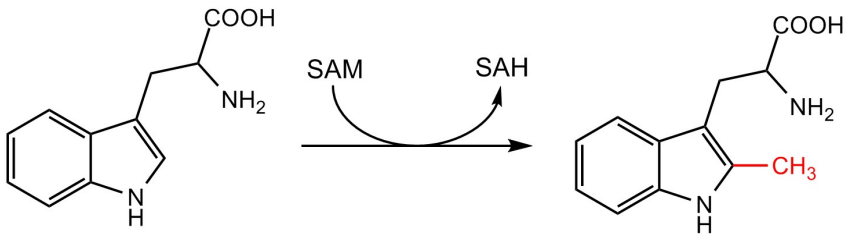

Figure 17: Methyltransfer catalyzed by tryptophan-C2-methyltransferases of *Streptomyces* species The transferred methyl group to tryptophan is highlighted in red.

1.8.5 Ubiquinone methylating enzymes

The gene product of the *E. coli* gene *ubiE* catalysis the methylation of 2-methoxy-6-polyprenylbenzene-1,4-diol under formation of 2-methoxy-5-methyl-6-polyprenylbenzene-1,4-diol and the methylation of 2-polyprenylnaphthalene-1,4-diol under formation of 3-methyl-2-polyprenylnaphthalene-1,4-diol in the biosynthesis of ubiquinone (coenzyme Q) and menaquinone (vitamin K_{12}), respectively [134]. Ubiquinone and menaquinone

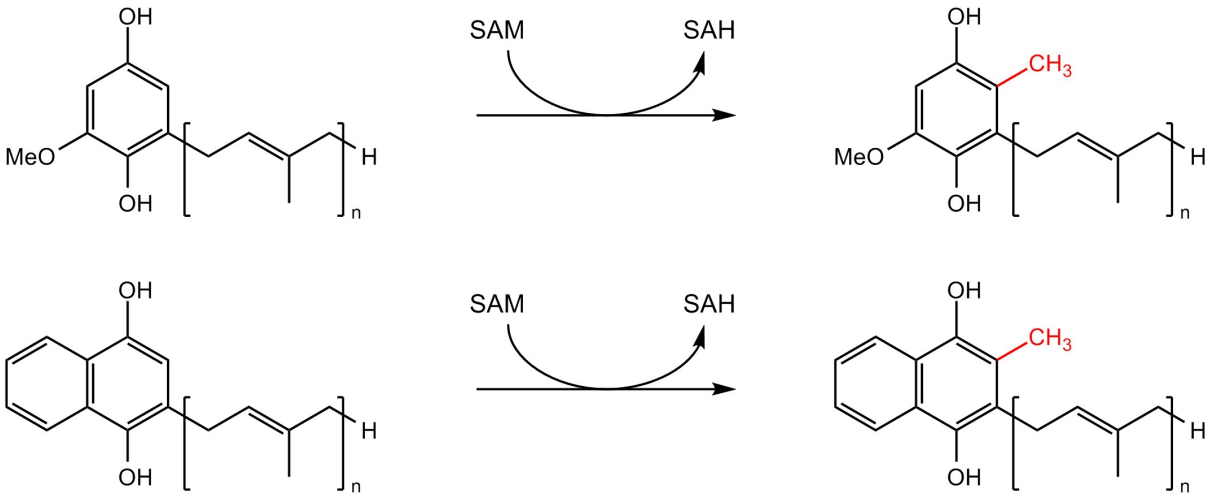

Figure 18: Methyltransfer catalyzed by the methyltransferase UbiE to 2-methoxy-6-polyprenyl-1,4-benzoquinol and 2-polyprenylnaphthalene-1,4-diol in the biosynthesis of ubiquinone and menaquinone, respectively.

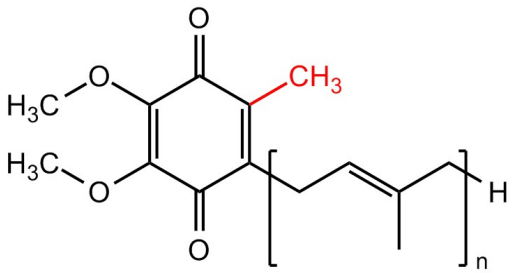

Figure 19: Structure of ubiquinone (coenzyme Q). The position of the methyl group which is transferred to the ubiquinone precursor via the methyltransferases UbiE is highlighted in red.

play essential roles in the respiratory pathway in both prokaryotes and eukaryotes [135]. In prokaryotes the genes involved in this biosynthesis are designated *ubi* and in eukaryotes *coq*. The C-methylation is the only step, which the ubiquinone and menaquinone pathways

have in common [136]. The eukaryotic analogue of UbiE is the Coq5 protein of *Saccharomyces cerevisiae* [137]. Ubiquinone biosynthesis also involves two O-methylations, which are catalyzed by the methyltransferases UbiG or Coq3. UbiE/Coq5 and UbiG/Coq3 are SAM-dependent methyltransferases. In *E. coli* ubiquinone serves as a redox mediator in aerobic respiration and performs this function via reversible redox cycling between hydroquinone and ubiquinone in the plasma membrane. In eukaryotes ubiquinone is responsible for transport of electrons from Complex I or II to the cytochrome bc_1 complex in the inner mitochondrial membrane. Despite its role in electron transfer, ubiquinone acts a a lipid-soluble antioxidant that scavenges lipid peroxyl radicals in the membrane in the same manner as vitamin E [138].

1.9 Aim of this work

The Friedel-Crafts reaction describes the alkylation of aromatic compounds. In nature alkylation occurs via the transfer of a methyl group to various substrates, catalyzed by methyltransferases EC [2.1.1]. Some of these proteins accept small aromatic compounds as substrates for methylation.

This work aims to establish an enzymatic equivalent to the Friedel-Crafts alkylation. In order to achieve this goal, two major topics have to be addressed. First, the isolation and characterization of certain methyltransferases and second, the analysis of the substrate scope and the acceptance of modified cofactors.

Both fundamental and applied aspects of enzymology are addressed in this thesis. Information about enzyme basics, classification and prospective application is gathered, analyzed and reflected.

To date several methyltransferases are described in literature and enzyme databases, which provide information about genetic-, biochemical-, and structural data. This information is used to isolate enzymes that are able to fulfill the abovementioned demands.

In order to achieve the objectives several techniques ranging from DNA manipulation and protein purification to analytical methods, which all include bioinformatic tools, are used.

2 Results

2.1 Biocatalytic Friedel-Crafts Alkylation using Non-natural Cofactors**

*Harald Stecher[1,2], Martin Tengg[1,3], Bernhard J. Ueberbacher[1], Peter Remler[1], Helmut Schwab[3], Herfried Griengl[1], and Mandana Gruber-Khadjawi[1,2]**

[1]Research Centre Applied Biocatalysis, Petersgasse 14, A-8010-Graz, Austria

[2]Institute of Organic Chemistry, Graz University of Technology, Stremayrgasse 16, A-8010 Graz, Austria

[3]Institute of Molecular Biotechnology, Graz University of Technology, Petersgasse 14, A-8010-Graz, Austria

Keywords: biocatalysis, C-C coupling, Friedel–Crafts alkylation, S-adenosyl-L-methionine, sustainable chemistry

Angew. Chem. Int. Ed. **2009**, 48(50), 9546 – 8

Contribution of Martin Tengg to this work:
Experimentals: Cloning, expression, protein purification, enzyme kinetics and HPLC analytics
Setup of these experiments and interpretation of results, as well as writing of the respective supporting information.
The authors Harald Stecher and Martin Tengg contributed equally to this work.

The formation of C-C bonds is a central aspect of synthetic organic chemistry. However, in biocatalysis only few enzymes capable to perform this reaction are known, among which aldolases, transketolases, and hydroxynitril lyases have been investigated thoroughly [1],[139-148]. Some have even found their way into industrial applications [2],[149],[150]. Friedel–Crafts alkylation is a classic organic reaction of great importance. However, in particular for large scale application, this transformation is ecologically very critical and regiospecific monoalkylation is difficult to achieve. Therefore, an environmentally friendly

and selective alternative would be highly desirable. In nature methyl groups are selectively introduced into reactive aromatic rings by methyltransferases (Mtases), in particular with S-adenosyl-L-methionine (SAM) as the cofactor. Furthermore, enzyme-catalyzed reactions are important for access to isoprenoids. Also, prenylation of aromatic rings has been performed [151]. For phenylalanine ammonia lyases a Friedel–Crafts-type mechanism has been proposed [152]. Recently, it has been shown that besides the methyl group other alkyl, alkenyl, and alkinyl groups can be introduced into S-adenosyl-L-homocysteine. These modified cofactors of transferases were used for a sequence-specific alkylation of DNA [153].

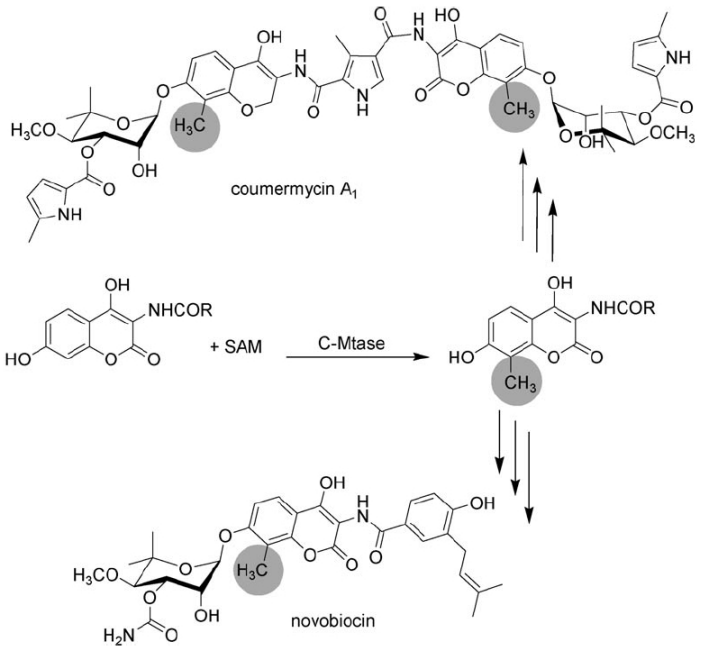

Figure 20: C-Mtases involved in the biosynthesis of the antibiotics Coumermycin A_1 in *Streptomyces rishiriensis* and Novobiocin in *Streptomyces spheroids*.

Having cofactor and modified cofactors in hand, we investigated the possibility of alkylation of aromatic substrates, thus transferring the biosynthesis into the laboratory (Figure 20). Aminocoumarins are antibiotics produced by some Streptomyces species and are targets for the methyl transfer from the natural cofactor SAM. The Mtase A and B are involved in the biosynthesis [105] of the antibiotics coumermycin A_1 [154] (produced by *Streptomyces rishiriensis*) and novobiocin [155],[156] (produced by *Streptomyces spheroides*; Figure 20).

SAM analogues were synthesized by modifying the strategy published by Klimašauskas,

Weinhold, and co-workers [70]. S-Adenosyl-L-homocysteine (SAH) was alkylated by seven different alkyl bromides using formic acid as the solvent and AgOTf as a Lewis acid activator and catalyst. We observed quantitative conversion in less than 2 days (average reaction time 24 h; Figure 21). The chemical synthesis of SAM analogues results in approximately 1:1 diastereomeric mixtures at the sulfonium center. In the first screenings the diastereomers were separated by preparative HPLC and used as cofactors for the alkylation of coumarin compound **3a**. Both epimers were accepted by the enzymes NovO and CouO (Mtase A and B) with only slight difference in the conversion after 24 hours. Therefore, the tedious epimer separation was not undertaken. For all following experiments the crude diastereomeric mixture of SAM analogues were performed without further purification and separation of the diastereomers.

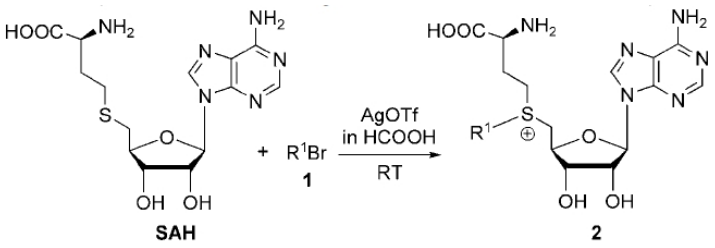

Alkyl halide	R^1	Product
1a	CH_3	**2a**
1b	$CH_2{=}CHCH_2$	**2b**
1c	$CH_3CH{=}CHCH_2$	**2c**
1d	$CH{\equiv}CCH_2$	**2d**
1e	$CH_3C{\equiv}CCH_2$	**2e**
1f	$C_6H_5CH_2$	**2f**

Figure 21: Synthesis of SAM analogues. Tf=trifluoromethanesulfonyl.

The methyltransferase gene *novO* found in *Streptomyces spheroides* [157] shows higher sequence homology to *couO*, which is the methyltransferase gene in *Streptomyces rishiriensis* (84 % identity on protein level) [103],[110],[158],[159]. These Mtases were heterologously expressed in *E. coli*. Both enzymes were purified as Strep-tagged proteins by affinity chromatography. NovO shows a K_M value of 26.7 μM for substrate **3b** and the K_M value of CouO for substrate **3a** is 64.4 μM. The activity assay is based on HPLC/MS analysis of the enzymatic transformation. For the activity screening model substrates with high similarity to the natural substrates of these enzymes were chosen and synthesized (e.g. **3a** and **3b**; see the Supporting Information).

The biocatalytic transformations were performed in small shaked vials on a 1 mL scale (1

mM substrate) using the crude lysate of the expression in *E. coli* in the presence of 10 % DMSO (dimethyl sulfoxide) at 35 °C for 24 hours (see the Supporting Information). Some of the reactions were performed on a larger scale (30 mg substrate, 3 mM solution) and the products were isolated. At first coumarin derivatives were chosen as substrates and the results are given in Figure 22. The methylation of coumarin **3a** is not surprising owing to the high structural similarity to the natural substrate. However, besides methyl other alkyl groups can be introduced regiospecifically into C8 of the 4,7-dihydroxycoumarin system. Furthermore, other substituent patterns at C3 are possible. These transformations are interesting because they are the first examples of biocatalytic Friedel–Crafts alkylations. It was therefore very gratifying that also other substrates were accepted by CouO as shown in Figure 23.

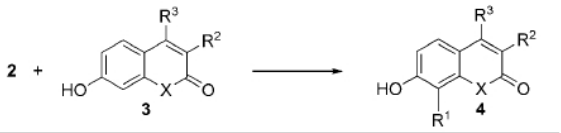

	Substrate			Product
	X	R^2	R^3	R^1=CH_3
3 a	O	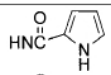	OH	**4 a**
3 b	O	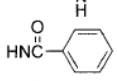	OH	**4 b**
3 c	O	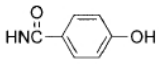	OH	**4 c**
3 d	O		OH	**4 d**
3 e	O	CH_2COOH	CH_3	**4 e**
3 f	NH	H	CH_3	**4 f**

Substr.	Product	NovO[a]	CouO[a]	Substr.	Product	NovO[a]	CouO[a]	Substr.	Product	NovO[a]	CouO[a]
2a **3a**	**4a**: $R^1=CH_3$	>99	>99	**2a** **3b**	**4b**: $R^1=CH_3$	>99	96	SAM **3c**	**4c**: $R^1=CH_3$	>99	>99
2b **3a**	**4a**: $R^1=CH_2{=}CHCH_2$	>99	>99	**2b** **3b**	**4b**: $R^1=CH_2{=}CHCH_2$	96	42	SAM **3d**	**4d**: $R^1=CH_3$	>99	>99
2c **3a**	**4a**: $R^1=CH_3CH{=}CHCH_2$	42	38	**2c** **3b**	**4b**: $R^1=CH_3CH{=}CHCH_2$	30	11	SAM **3e**	**4e**: $R^1=CH_3$	–	30
2d **3a**	**4a**: $R^1=CH{\equiv}CCH_2$	99	99	**2d** **3b**	**4b**: $R^1=CH{\equiv}CCH_2$	35	11	SAM **3f**	**4f**: $R^1=CH_3$	–	10
2e **3a**	**4a**: $R^1=CH_3C{\equiv}CCH_2$	41	77	**2e** **3b**	**4b**: $R^1=CH_3C{\equiv}CCH_2$	28	–				
2f **3a**	**4a**: $R^1=C_6H_5CH_2$	40	45	**2f** **3b**	**4b**: $R^1=C_6H_5CH_2$	24	21				

[a] % conversion was determined by HPLC analysis.

Figure 22: Enzymatic synthesis of alkyl coumarin derivatives.

There seem, however, to be quite stringent structure requirements since naphthalenediols with a 1,2-, 1,3-, 1,4-, 1,5-, 1,6-, or 2,3-substitution pattern gave no reaction. In addition, resorcinol and phloroglucinol were not accepted.

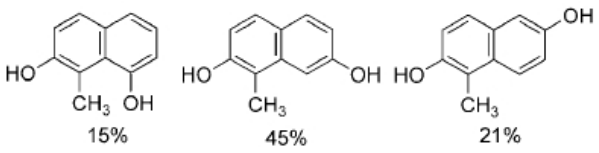

Figure 23: Methylation products of naphthalenediols catalyzed by CouO (% conversion after 24 h).

In summary a biocatalytic equivalent for the Friedel– Crafts alkylation is described. The enzymes are SAM dependent methyltransferases which are capable of accepting modified cofactors and yield not only methylated but also allyl, propargyl, and benzylated arenes in moderate to high yields with excellent regioselectivity. Only monosubstituted products were formed, even if a large excess of SAM and analogues was applied. Gratifyingly, the substrate acceptance of the Mtases is broader than expected. Naphthalene derivatives can replace the coumarin scaffold. This concept may serve as the beginning of a "green" and selective Friedel– Crafts alkylation.

Footnotes

*To whom correspondence may be addressed: mandana.gruber@a-b.at

**The Österreichische Forschungsförderungsgesellschaft (FFG), the Province of Styria, and the Styrian Business Promotion Agency (SFG)—within the framework of the Kplus programme as well as GASS programme within NAWI Graz - are acknowledged for financial support, as well as Birgit Krenn for technical support. M.G.-K. thanks Prof. Dr. Rolf Breinbauer for his fruitful contribution to this manuscript.

2.1.1 Supporting information

Cloning and Expression

For cloning and heterologous expression of the methyltransferase encoding genes *novO* and *couO*, the genomic DNA of strains *Streptomyces spheroides* (DSMZ 40292) and *Streptomyces rishiriensis* (DSMZ 40489) were isolated following the protocol of Kieser *et al.*, 2000 [160]. The genes were amplified by standard PCR conditions using the forward

primer 5'- AATCTGCATATGAAGATTGAACCGATTAC-3' and the reverse primer 5'-TAGGTAAAGCTTTCAGGCAGCGGCCCGACGGG-3'. These primers introduced the respective *NdeI* and *HindIII* restriction sites (underlined above) for subsequent cloning into the expression vector pET26b(+). The PCR products were gel-purified, digested with *NdeI* and *HindIII*, and ligated into the linearized pET26b(+) vector. The use of these primers for both genes resulted in two amino acid exchanges (A5P and S223C) in case of NovO. The expression constructs pET26b(+)-couO, and pET26b(+)-novO were transformed into *E. coli* BL21 Gold (DE3) electrocompetent cells for protein overexpression. Transformants harbouring the desired constructs were grown at 30°C in LB medium supplemented with 40 µg/ml kanamycin to an OD_{600} of 0.8, then shifted to 25°C and induced with isopropyl-Dthiogalactopyranoside (IPTG) to a final concentration of 100µM, and grown for an additional 16 h at 25°C. The cells were harvested by centrifugation (10 min at 6000 x g), resuspended in buffer A: 50mM Na-phosphate pH7 (pH6.5 for NovO), and lysed by sonication for 6 minutes. The resultant cell debris was removed by centrifugation (60 min at 50000 x g). The supernatant was analyzed by SDS-PAGE and kept at 4°C for enzymatic reactions. The cell pellets were resuspended in buffer A and analyzed by SDS-PAGE.

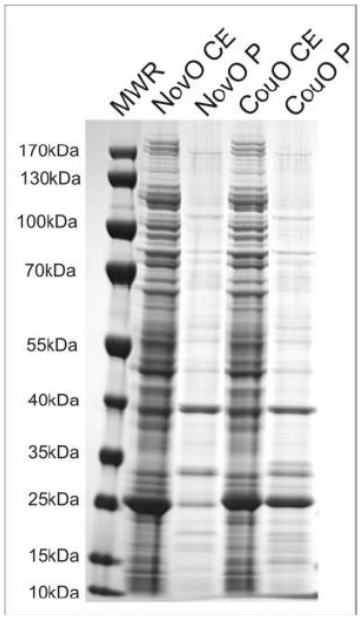

Figure 24: SDS-PAGE of CouO and NovO expression in *E. Coli* BL21 Gold (DE3), CE crude lysate, P resuspended pellet. The yield of CouO and NovO expression in *E. Coli* is about 160mg per liter culture volume, which is nearly a third of the whole protein content obtained.

Purification of CouO and NovO

For an efficient purification procedure, C-terminal Strep Tag II was introduced into both CouO and NovO by a two-step side-directed mutagenesis, based on the QuikChange® method, of the constructs pET26b(+)-couO and pET26b(+)-novO using the forward primer 5'-GCCCGTCGGGCCGCTGCCAGCGCTTGGAGCCACCCGCAGT TCGAAA AATGAAAGCTTGCGGCCGCACTCGAGC-3' and the reverse primer 5'- GCTCGAGT GCGGCCGCAAGCTTTCATTTTTCGAACTGCGGGTGGCTCCAAGCGCTGGCAG CGGCCCGACGGGC-3'. The expression constructs pET26b(+)-couO-Strep, and pET26b(+)-novO-Strep were transformed into *E. coli* BL21 Gold (DE3) electrocompetent cells. Protein expression was achieved as described above, whereas cells were sonicated in Strep Tag binding buffer W: 100mM Tris-HCl pH8, 150mM NaCl, 1mM EDTA. The cleared lysate was immediately used for affinity purification using a Strep-Tactin Superflow High- Capacity column from IBA following the manual of the supplier. After pooling the eluted fractions protein aliquots were analyzed by SDS-PAGE and stored at -20°C.

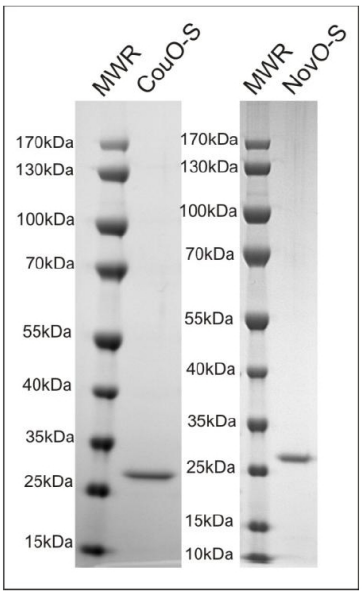

Figure 25: SDS-PAGE of purified strep-tagged CouO and NovO. Both enzymes show high purity and were concentrated to 10mg/ml The yield of Strep-tagged enzymes were not as high as the wildtype CouO and NovO expression in *E. coli*. NovOStrep yield was 120mg per liter and CouO-Strep only 30mg per liter culture volume.

Determination of K_M, Vmax, kcat

For determination of kinetic parameters the reactions were performed as described in Assay, besides resigning the use of DTT. The reactions were carried out in a 100µl scale of triplicate measurements using two separate substrate stock solutions of 1mM 3k or 3j respectively. The SAM concentration was kept constant at 2mM, substrate concentrations were varied from 15 to 500 µM. Reactions were initiated with 50µg CouO-Strep or 47µg NovO-Strep and stopped after 5, 10, 20, 30, and 60 minutes.

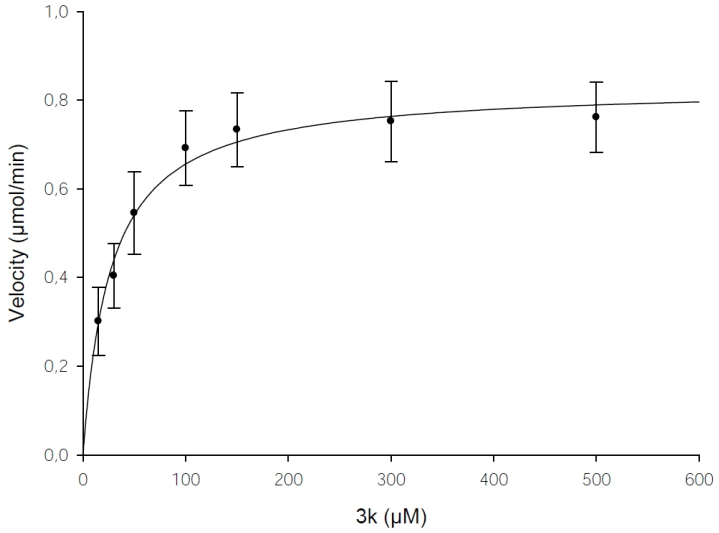

Figure 26: Michaelis-Menten graph of NovO-Strep methylation of substrat 3k. The Michaelis-Menten graph led to the determination of Vmax = 831 nmol/min and K_M = 26.7 µM. According to the 47 µg of enzyme the specific activity could be calculated as 16 U/mg.

Synthesis of aminocoumarin substrates

2,4-diacetoxybenzoic acid [161]

To a stirred and light protected solution of 5.0g 2,4-dihydroxybenzoic acid (32.4mmol, 1eq.) in 30mL pyridine, 15.3mL acetic anhydride (16.6g, 162mmol, 5eq.) and 0.40g DMAP (3.24mmol, 0.1eq.) were added. After 24h ice was added to the reaction mixture and it was acidified with aqueous 3N HCl. The resulting suspension was extracted three times with ethyl acetate. The organic layers were pooled and washed once with brine. After drying over Na_2SO_4 the solvent was reduced to a volume of approximately 15mL, which were allowed to crystallize. The resulting crystals were collected and dried

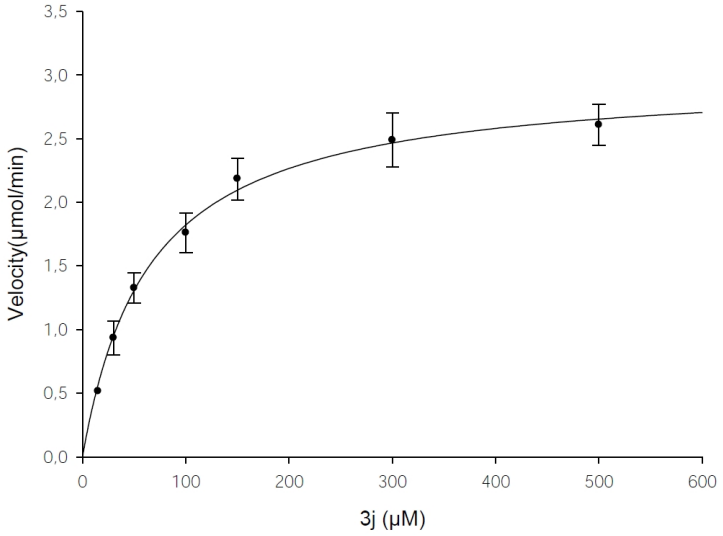

Figure 27: Michaelis-Menten graph of CouO-Strep methylation of substrat 3j. Measurements of the kinetic parameters of CouO-Strep methylating substrate 3j yielded significant higher values for Vmax = 2996 nmol/min, K_M = 64.4 µM, and the specific activity of 51 U/mg.

over $CaCl_2$, further product was crystallized from the mother liquor. In total 7.2g (93%) off-white crystals were collected. 1H NMR (300MHz, DMSO-d6) ppm: 13.12 (br, 1H, -COOH), 7.98 (d, J = 8.6Hz, 1H, -CH_{ar}-), 7.18 (dd, J_1 = 8.6, J_2 = 2.3Hz, 1H, -CH_{ar}-), 7.09 (d, J = 2.2Hz, 1H, -CH_{ar}-), 2.29 (s, 3H, -CH_3), 2.25 (s, 3H, -CH_3). 13C (75MHz) ppm: 169.0, 168.6, 165.0, 154.0, 151.1, 132.5, 121.6, 119.7, 117.6, 20.8, 20.8.

2,4-diacetoxybenzoyl chloride [161]

2.0g 2,4-diacetoxybenzoic acid (8.4mmol, 1eq.) was solved in 20mL CH_2Cl_2. 12mL $SOCl_2$ (20g, 165mmol, 20eq.) was added to the stirred solution. The mixture was heated to reflux for 5h before CH_2Cl_2 and $SOCl_2$ were distilled off. The resulting brown solid was directly used for the next step and not further characterized.

2-(tert-butoxycarbonylamino)-3-ethoxy-3-oxopropanoic acid [162]

To a suspension of 4.49g KOH (80mmol, 1eq.) in 100ml EtOH 20.4mL diethyl 2-(tert-butyloxycarbonylamino) propandioate (22.0g, 80mmol, 1eq.) was added. The mixture was stirred for 3h before about ninety percent of the solvent was removed. 150mL of aqueous 1M $NaHCO_3$ was added and washed twice with ethyl acetate to remove the unreacted educt. The solution was cooled to 0°C, acidified with $KHSO_4$ and extracted three times with ethyl acetate. The combined organic layers were washed once with brine and dried over Na_2SO_4. The solvent was evaporated under reduced pressure (bath temperature 20°C). The resulting oily residue was dried in vacuo to give 14.45g (73%) of a white

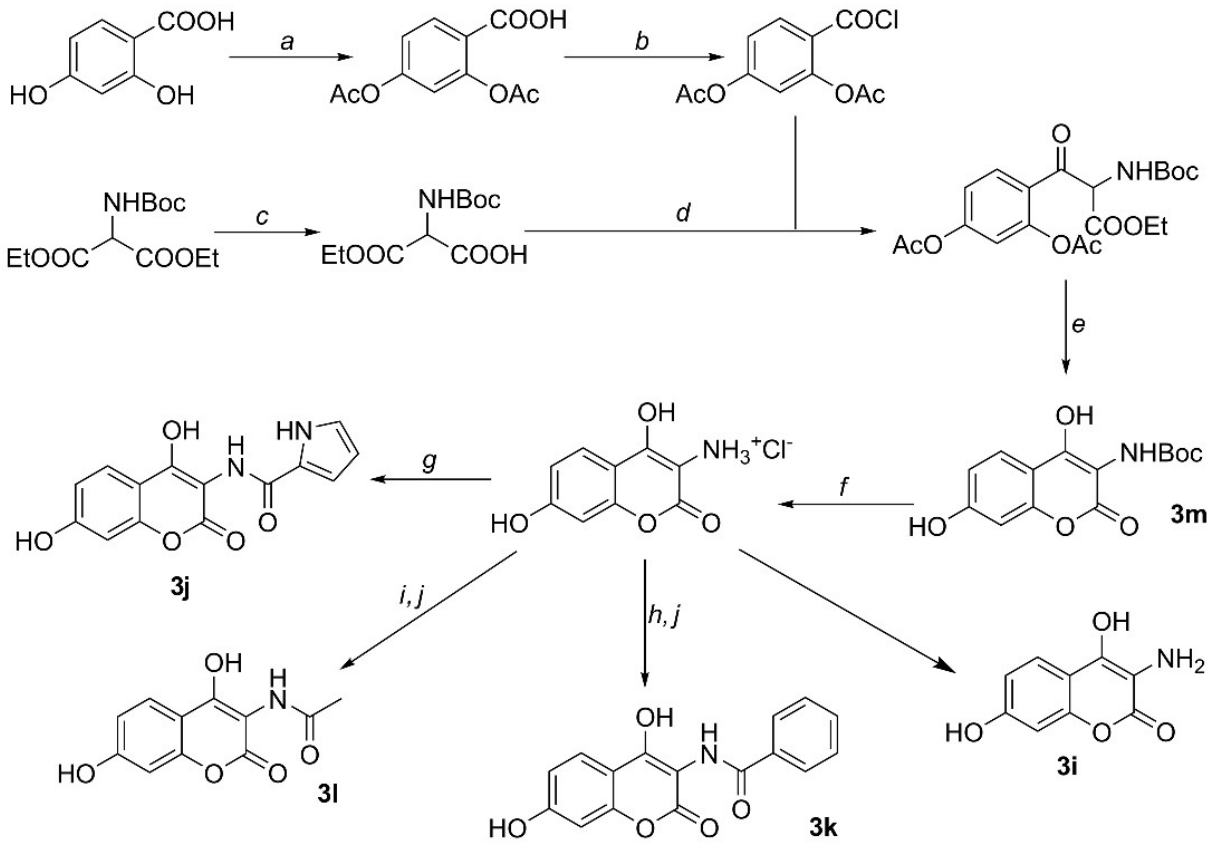

Figure 28: Synthesis of substrates for CouO and NovO. a Ac2O(acetic anhydride), pyridine, DMAP (4-(Dimethylamino)pyridine, room temperature (rt), 24h, 93% b $SOCl_2$, CH_2Cl_2, reflux, 5h c KOH, MeOH, rt, 3h, 73% d Et3N, $MgCl_2$, THF, 2h at 0°C, 16h at rt, 73% e aqueous NaOH, MeOH, rt, 16h, 92% f 1N HCl, MeOH, rt, 24h, 67% g Pyrrol-2-carboxylic acid, PyBOP((Benzotriazol-1- yloxy)tripyrrolidinophosphonium hexafluorophosphate), NMM (N-methyl morpholine), DMF, rt, Ar atmosphere, 48h, 78% h PhCOCl, pyridine, DMF, rt, 24h i Ac2O, pyridine, DMF, rt, 24h j 3*N* NaOH / MeOH 1:1, rt, 72h, (h+j >99%), (i+j 66%).

powder. 1H NMR (500MHz, $CDCl_3$) ppm: 7.73 (d, J = 4.4Hz, 0.6H, -NH-), 5.65 (d, J = 6.8Hz, 0.4H, -NH-), 4.98 (d, J = 7.3Hz, 0.4H, -CH-), 4.77 (d, J = 4.9Hz, 0.6H, -CH-), 4.23-4.31 (m, 2H, -CH_2-), 1.42 (s, 9H, 3 –CH_3), 1.31 (t, J = 7.3Hz, 3H, -CH_3). 13C (125MHz) ppm:168.5, 166.9, 156.4, 83.0, 63.0, 58.9, 28.3, 14.3.

4-(2-(tert-butoxycarbonylamino)-3-ethoxy-3-oxopropanoyl)-1,3-phenylene diacetate [163]

To an ice-cooled solution of 2-(tert-butyloxycarbonylamino)-3-ethoxy-3-oxopropanoic acid (2.91g, 11.8mmol, 1.4eq.) in dry THF (30mL), 7.4mL triethylamine (5.36g, 52.8mmol, 6.3eq.) and 2.69g MgCl2 (28.3mmol, 3.4eq.) were added and the resulting slurry was stirred vigorously for 2h. Then crude 2,4-diacetoxybenzoyl chloride (theoretical amount 8.4mmol, 1eq.) in 50mL dry THF was added and the resulting suspension was stirred overnight at room temperature. The reaction mixture was quenched with saturated aqueous NH_4Cl until the suspension clarified. The solution was extracted three times with ethyl acetate. The combined organic layers were dried over Na_2SO_4. Removal of the solvent yielded 4.31g (121%) of darkbrown oil, which was used for the next step without further purification.

***tert*-butyl 4,7-dihydroxy-2-oxo-2*H*-chromen-3-ylcarbamate 3m** [163]

The crude 4-(2-(tert-butyloxycarbonylamino)-3-ethoxy-3-oxopropanoyl)-1,3-phenylene diacetate (4.31g) was dissolved in 24mL MeOH and 30mL 1.5N NaOH was added. The solution was stirred for 3h at room temperature. Then the solution was acidified with 1N HCl to pH3 and extracted three times with ethyl acetate. The combined organic layers were washed with brine, dried over Na_2SO_4 and the solvent was removed in vacuo. The crude product was purified by column chromatography to give 1.24g (50% over three steps) of an orange solid. 1H NMR (500MHz, DMSO-d6) ppm: 7.78 (s, 1H, -NH-), 7.64 (d, J = 8.8Hz, 1H, -CH_{ar}-), 6.77 (dd, J_1 = 8.8, J_2 = 2.0Hz, 1H, -CH_{ar}-), 6.66 (d, J = 2Hz, 1H, -CH_{ar}-), 1.40 (s, 9H, -CH_3). 13C NMR (125MHz) ppm: 166.4, 161.9, 161.6, 155.4, 154.1, 125.7, 113.5, 108.7, 102.5, 100.8, 79.3, 28.9.

3-amino-4,7-dihydroxy-2*H*-chromen-2-one hydrochloride [163]

To a cooled mixture of 25mL Et2O and 5mL MeOH 4.3mL acetyl chloride was carefully added. This acidic mixture was poured onto a stirred and cooled solution of 1.24g tert-butyl 4,7-dihydroxy-2-oxo-2*H*-chromen-3-ylcarbamate in 25mL Et2O and 5mL MeOH (1N HCl in the reaction mixture). The solution was allowed to stir for 24h at room

temperature. The precipitate formed was collected and dried to give 0.52g (53%) light brown solid. 1H NMR (500MHz, DMSO-d6) ppm: 7.96 (d, J = 8.8Hz, 1H, -CH_{ar}-), 6.84 (dd, J_1 = 8.8Hz, J_2 = v2.0Hz, 1H, -CH_{ar}-), 6.75 (d, J = 2.0Hz, 1H, -CH_{ar}-). 13C NMR (125MHz) ppm:162.7, 161.5, 160.4, 154.2, 126.4, 113.9, 108.7, 103.0, 95.5.

N-(4,7-dihydroxy-2-oxo-2*H*-chromen-3-yl)benzamide 3k

To a stirred solution of 200mg 3-amino-4,7-dihydroxy-2H-chromen-2-on hydrochloride (0.87mmol, 1eq.) in 10mL ethyl acetate 0.51 mL benzoyl chloride (0.61g, 4.4mmol, 5eq.) and 1.22mL triethylamine (0.88g, 8.7mmol, 10eq.) were added. The suspension was stirred overnight at room temperature. After removal of the solid by filtration the solvent was removed by evaporation. The resulting residue was dissolved in 10mL MeOH and 10mL 1N NaOH was added. The reaction mixture was stirred for 24h, subsequently the mixture was acidified with 1N HCl to pH3 and extracted three times with ethyl acetate. The combined organic layers were washed once with brine and dried over Na2SO4. Celite was added and the solvent was removed in vacuo. The resulting fine brown powder was used for purification by column chromatography to give 243mg (94%) of an orange solid. mp 283-285°C, ESI-MS 298.0 and 320.0, 1H NMR (500MHz, DSMO-d6) ppm: 11.82 (s, 1H, -OH), 10.56 (s, 1H, - OH), 9.42 (s, 1H, -NH-), 8.00 (d, J = 7.3Hz, 2H, -CH_{ar}-), 7.72 (d, J = 8.8Hz, 1H, -CH_{ar}-), 7.58 (t, J = 7.3Hz, 1H, -CH_{ar}-), 7.51 (t, J = 7.6Hz, 2H, -CH_{ar}-), 6.83 (dd, J_1 = 8.8Hz, J_2 = 2.0Hz, 1H, -CH_{ar}-), 6.74 (d, J = 2.4Hz, 1H, -CH_{ar}-). 13C (125MHz) ppm: 166.6, 161.4, 160.8, 160.3, 153.5, 133.9, 131.6, 128.2, 128.0, 125.0, 113.0, 107.9, 101.9, 100.1.

***N*-(4,7-dihydroxy-2-oxo-2*H*-chromen-3-yl)acetamide 3l**

To a stirred solution of 100mg 3-amino-4,7-dihydroxy-2H-chromen-2-on hydrochloride (0.44mmol, 1.0eq.) in 1mL DMF, 38.7µL pyridine (38mg. 0.48mmol, 1.1eq.) and 41.3µL acetic anhydride (45mg, 0.44mmol, 1.0eq.) were added. After 19h further 82.6µL acetic anhydride (89mg, 0.88mmol, 2eq.) and 116µL pyridine (114mg, 1.46mmol, 3.3eq.) were added and the reaction mixture was stirred for 5h. 1ml MeOH and 44µL NaOMe were added and the mixture was stirred overnight. Then the solution was diluted with ethyl acetate and acidified with 1N HCl. After separation of the phases the aqueous phase was extracted twice with ethyl acetate. The combined organic layers were dried over Na_2SO_4 and the solvent was removed in vacuo. The resulting residue was dried in vacuo to give 68mg (66%) of an offwhite solid. mp 255-257°C, ESI-MS 236.1 and 258.0, 1H

NMR (500MHz, DMSO-d6) ppm: 12.06 (s, 1H, -OH), 10.51 (s, 1H, -OH), 9.30 (s, 1H, -NH-), 7.66 (d, J = 6.8Hz, 1H, - CHar-), 6.79 (dd, J_1 = 8.8, J_2 = 2.0Hz, 1H, -CH_{ar}-), 6.68 (d, J = 2Hz, 1H, -CH_{ar}-), 2.05 (s, 3H, - CH_3). 13C NMR (125Hz) ppm: 171.7, 162.0, 161.2, 158.9, 153.7, 125.7, 113.7, 108.7, 102.5, 101.4, 23.3.

***N*-(4,7-dihydroxy-2-oxo-2*H*-chromen-3-yl)-1*H*-pyrrol-2-carboxamide [108] 3j**

A mixture of 200mg 3-amino-4,7-dihydroxy-2*H*-chromen-2-on hydrochloride (0.87mmol, 1eq.), 97mg 1*H*-pyrrole-2-carboxylic acid (0.87mmol, 1eq.), 454mg PyBOP (0.87mg, 1eq.) and 770µL *N*-methylmorpholin (707mg, 7.0mol, 8eq.) in 12 mL DMF was stirred for 27h at room temperature under an argon atmosphere. After addition of further 227mg PyBOP (0.44mmol, 0.5eq.) the solution was again stirred for 66h. The reaction mixture was acidified with 1N HCl and extracted three times with ethyl acetate. The combined organic layers were washed once with brine. After drying over Na_2SO_4 the solvent was removed under reduced pressure. The resulting brown oil was dissolved in ethyl acetate yielding a suspension. The solid was collected to give the desired product. Further product was precipitated from the mother liquor by addition of cyclohexane. Both fractions were dried in vacuo to yield overall 180mg (72%) of a brown solid. mp 278-279°C, ESI-MS 287.0 and 309.1, 1H NMR (500MHz, DMSO-d6) ppm: 12.01 (br, 1H, -OH), 11.65 (s, 1H, -NH-) 10.57 (br, 1H, -OH), 9.30 (s, 1H, -NH-), 7.69 (d, J = 8.3Hz, 1H, -CH_{ar}-) 7.01 (s, 1H, -CH_{pyrr}-), 6.94 (s, 1H, -CH_{pyrr}-), 6.81 (dd, J_1 = 8.8, J_2 = 2.0Hz, 1H, -CH_{ar}-), 6.71 (d, J = 2Hz, 1H, -CH_{ar}-), 6.15 (s, 1H, -CH_{pyrr}-). 13C NMR (125Hz) ppm: 162.0, 161.6, 161.5, 160.3, 154.0, 126.2, 125.7, 123.1, 113.7, 112.9, 109.7, 108.8, 102.6, 100.9.

Assay

Crude lysate of CouO and NovO was prepared by sonication of the harvested recombinant *E. coli* cells resuspended in 50mM sodium phosphate buffer pH7 for CouO and pH6.5 for NovO after centrifugation and separation from cell debris. The reaction was performed in 1ml scale in a thermomixer at 35°C and 1000 per minute (mixing frequency) for 24h containing 1mM (mmolar) substrate from a 10mM DMSO stock (dimethyl sulfoxide), 2mM SAM (A7007 from Sigma)(or analog) from a 20mM phosphate buffer stock, 1mM DTT (1,4-Dithioerythritol 43796 from Fluka) from a 10mM phosphate buffer stock, 1mg/ml BSA (bovine serum albumin A3294 from Sigma) and crude lysate of CouO and NovO

respectively. The assay was stopped by heating the vials for 10 minutes at 80°C, followed by maintaining the vials in the refrigerator for 15 minutes. Subsequently the mixtures were centrifugated at 14.000rpm for 15 minutes. 5µl of the aqueous solution was injected to the HPLC without further dilution. The assay was developed after trying several

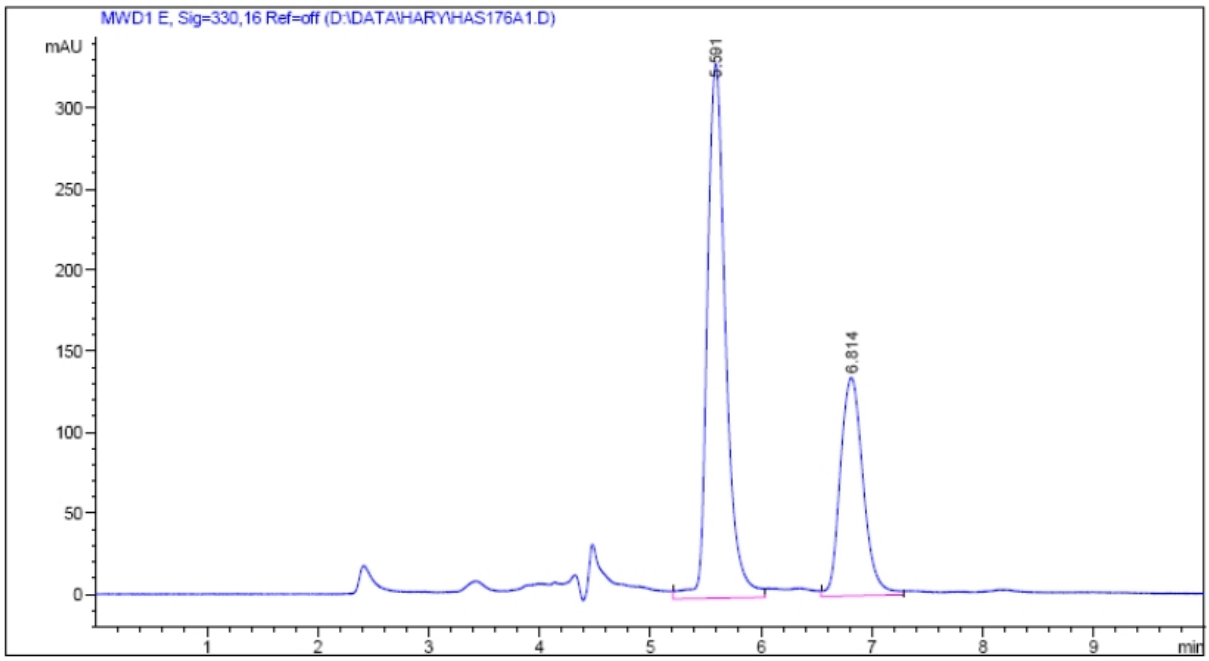

Figure 29: Chromatogram of methyltransferase activity assay of CouO with substrate 3k. Purosphere Star® C-18 column, eluent: 10mM NH_4COOH pH 6 / MeOH 7:3, flow 0.6ml/min, 30°C. Peak at R_t 5.59min is the substrate, R_t 6.61min peak shows the product.

conditions. The addition of DTT and BSA to the assay proved to be beneficial, probably due to the protection of cysteine residues in the enzyme in the case of DTT and structure stabilisation effects in the case of BSA. Two negative controls were performed for each assay, one contained all ingredients except lysate, the other a heated lysate preparation (heat deactivated enzyme).

Synthesis of alkylated aminocoumarines catalyzed by methyltransferase

Typical procedure for the synthesis of an alkylated aminocoumarin, as example crotylated derivative:

25 mg (84µmol , 1eq.) 3j, 40 mg Crotyl-SAH 2c (91µmol,1.1eq.) und 25 mg BSA Albumin from bovine serum were solved in 25 ml NovO crude lysate (6mg/ml protein) or CouO

crude lysate (4mg/ml protein) + 2.5 ml DMSO (D8418 from Sigma) and stirred at 35°C for 24 h. Conversion was followed by HPLC. To stop the reaction, the solution was heated at 80°C for 10 minutes. After heating, the solution was kept in the refrigerator for 15 minutes before it was centrifugated at 14000 rpm for 20 minutes. The soluble part was extracted 3 times with 50ml ethyl acetate each. The precipitate was suspended in 50ml ethyl acetate, vortexed thoroughly followed by centifugation. The combined organic solutions were dried over anhydrous Na2SO4 and the solvent removed under reduced pressure. The crude product was performed to flash chromatography (methylene chloride/MeOH 20:1) to yield 30mg (>100%) slightly impure product. A second round of chromatography was necessary to purify the product.

HPLC: Purosphere Star® C-18 column, eluent: 10mM NH_4COOH pH 7.2 / MeOH 7:3, flow 0.5 ml/min, 40°C, Rt 13,8min 1H NMR (500 MHz), DMSO-d6 δ (ppm) 1.5 (d, J=5Hz, 3H), 3.36 (m, 2H), 5.40 (m, 1H), 5.52 (m, 1H), 6.14 (s, 1H), 6.85 (d, J=10Hz, 1H), 6.93 (s, 1H), 7.00 (s, 1H), 7.57 (d, J=10Hz, 1H), 8.95 (br, 1H), 10.38 (br, 1H), 11.63 (br, 1H), 11.87(br, 1H)

Synthesis of SAM analogs

Typical procedure for the synthesis of SAM analogs, as example crotyl SAH (S-Adenosyl-Scrotyl homocysteine):
SAH 40 mg (0,1mmol , 1eq.) SAH (S-Adenosyl homocysteine A9384 from Sigma) was solved in 2ml formic acid (06440 from Fluka), 80 mg (0,3mol, 3eq.) silver triflate (AgOTf = silver trifluoromethanesulfonate 85325 from Fluka) and 600µl (5,8mmol , 60eq.) crotyl bromide (C86405 from Aldrich) were added and stirring continued for 24h. Conversion was controlled by HPLC (conditions: Purosphere Star® C-18 column, eluent 10mM NH_4COOH pH 6 / MeOH 7:3, flow 0.6ml/min, 30°C). If necessary again 80mg AgOTf and 600µl crotyl bromide were added and the conversion was controlled further by HPLC. As soon as no SAH could be detected in the chromatogram, the work up began as following: addition of 10ml water and subsequent 3x extraction with 10ml diethyl ether each for the separation of residual alkyl bromide and partially formic acid from the mixture. The aqueous phase was then lyophilized. Yield 44mg (96%)

Synthesis of 2,7-dihydroxy-1-methylnaphthalene

20mg (0.12mmol, 1eq.) 2,7-dihydroxynaphthalene (D116408 from Aldrich), 12mg BSA and 2mg DTT (1,4-dithio-DL-threitol 43815 from Fluka) were solved in 12ml crude lysate of CouO (7.5mg/ml protein content). 100mg (0.23mmol, 2eq.) SAM-Cl (A7007 from Sigma) were added. The crude lysate was prepared by centrifugation of cell debris after ultra sonic cell disruption of suspended cells in 50mM sodium phosphate buffer pH 7.0. The reaction mixture was placed in a thermo-shaker at 35°C and 150rpm. After 48h about 50% conversion was detected by HPLC. 12ml lysate, 12mg BSA and 2mg DTT and further 45mg SAM-Cl were added. After further 3days the conversion was almost complete. The work-up started with 20min centrifugation at 10.000rpm. The aqueous phase was extracted 3x with 25ml diethylether each. The combined organic solutions were dried over anhydrous Na_2SO_4 and evaporated to dryness after filtration. 22mg of a yellow oil was obtained as crude product. Flash chromatography on silica gel with cyclohexane / ethyl acetate as mobile phase yielded 20mg of a white solid.

^{1}H NMR (500 MHz), DMSO-d6: δ (ppm) 2.28 (s, 3H, -CH3), 6.82 (dd, J=8.7Hz, J=2.0Hz, 1H, 6-H), 6.90 (d, J=8.7Hz, 1H, 3-H), 7.03 (s, 1H, 8-H), 7.44 (d, J=8.7Hz, 1H, 4-H), 7.58 (d, J=8.7Hz, 1H, 5-H), 9.31 (s, 1H, 2-OH), 9.53 (s, 1H, 7-OH).

^{13}C NMR (125MHz), DMSO-d6: δ (ppm) 11.2 (-CH3), 105.2 (C-8), 113.2 (C-1), 115.3 (C-3 or C-6), 115.4 (C-6 or C-3), 123.3 (C-4a), 127.2 (C-4), 130.4 (C-5), 136.2 (C-8a), 153.1 (C- 2), 156.2 (C-7).

2.2 Methyltransferase NovO - a versatile catalyst for enzymatic Friedel-Crafts alkylation*

Martin Tengg[1,2], Harald Stecher[1], Peter Remler[1], Inge Eiteljörg[1], Helmut Schwab[1,2] and Mandana Gruber-Khadjawi[1]

[1]ACIB GmbH, Petersgasse 14, A-8010-Graz, Austria

[2]Institute of Molecular Biotechnology, Graz University of Technology, Petersgasse 14, A-8010-Graz, Austria

Running title: *Methyltransferase NovO – Enzymatic Friedel-Crafts Alkylation*

Keywords:*Methyltransferase, Friedel-Crafts reaction, S-adenosyl-*L*-methionine, kinetic studies, mutational analysis*

Manuscript submitted to *J. Biol. Chem.* **2011** (299800)

Contribution of Martin Tengg to this work:

Experimentals: Cloning, mutagenesis, expression, protein purification, methyltransferase assay, determination of temperature and pH optimum, stability assay, determination of kinetic parameters, and HPLC analyses

Setup of these experiments and interpretation of results, as well as conception and writing of the manuscript.

Background: Methyltransferase NovO from *Streptomyces spheroides* catalyzing an enzymatic Friedel-Crafts alkylation.

Results: Mutational analysis and kinetic studies provided insight into essential elements of the protein and on substrate and co-substrate utilization.

Conclusion: Transfer of non-natural allyl groups is very efficient assigning the methyltransferase NovO as effective "alkyltransferase"'

Significance: Enzyme-catalyzed alkylation of aromatic compounds has high potential for the synthesis of fine chemicals.

2.2.1 Summary

The alkylation of aromatic compounds, known as Friedel-Crafts alkylation is a reaction of great importance in organic chemistry. The transfer of methyl- and allyl groups to coumarin- and naphthalene containing substrates was accomplished by the methyltransferase NovO cloned from *Streptomyces spheroides*. The NovO protein could be heterologously produced as soluble and active enzyme in *Escherichia coli*. Characterization of NovO revealed a type I methyltransferase that performs its action as a dimer in solution. Functional elements include the conserved S-adenosyl-l-methionine (SAM) binding site E/DXXXGXG as DLCCGSG (residues 45 to 51). A histidine at position 15 was identified as the catalytic base in the alkyl transfer reaction. Determination of kinetic parameters revealed a K_m value of 0.036 mM for the coumarin derivative substrate, in contrast to a much higher K_m of 2.5 mM for the non-natural 2,7-dihydroxynaphthalene. In contrast, the k_{cat} of $37*10^{-4}$ was significantly higher for 2,7-dihydroxynaphthalene compared to the k_{cat} of $5.2*10^{-4}$ for the coumarin derivative. The transfer of allyl groups via the SAM analogue allyl-SAH occurs with a fourfold increased k_{cat} of $11*10^{-3}$ compared to $3.2*10^{-3}$ for methyl transfer. The evolutionary design towards SAM is obviously concerning the K_m value of 0.06 mM compared to 0.22 mM for allyl-SAH .

2.2.2 Introduction

Methylation is one of the key reactions in all living organisms. Methyl groups cause steric and electronic effects in small molecules and on biomolecules, which leads to consequences in biological behavior like selectivity among receptors, activity and protection strategies [164]. The transfer of methyl groups is catalyzed by methyltransferases. These enzymes need cofactors such as tetrahydrofolic acid, betaine and vitamin B12 but the majority of these enzymes use S-adenosyl-L-methionine (SAM) as methyl donor, which is the second most widely used cofactor in nature [14]. The SAM-dependent methyltransferases act on different substrates including DNA, RNA, proteins, lipids, carbohydrates

and small molecules. The enzymes are highly specific for the atom they methylate. The methyl group can be transferred to S-, N-, O-, C- and even halogen atoms [17]. The methyl transfer from SAM to its substrate is incident with very favorable enthalpy (≈ -70kJ/mol) and leads to selective methylation [87]. Due to their versatile substrates the role of the enzymes is diverse, including for example functions such as regulation, signaling, storage and biosynthesis. Several SAM dependent C-methyltransferases (sterol-C-, RNA- and DNA-nucleoside-C-methyltransferases) are known [54],[165],[19]. Apart from methyltransferases involved in the biosynthesis of polyketides [166], ubiquinone and its analogues [134] until now only few C-methyltransferases, which act on small aromatic substrates, were identified [121],[132],[167]. In nature the production of antibiotics very often depends on the methylation of precursors. A special group of these antibiotics, which are produced by *Streptomyces* species, exhibits potent antimicrobial activity by targeting DNA gyrase [96]. Coumermycin, clorobiocin, and novobiocin belong to this family of coumarin antibiotics. Novobiocin (Albamycin; Pharmacia & Upjohn) has been licensed in the United States as an antibiotic for the treatment of infections with multi-resistant gram-positive bacteria such as *Staphylococcus epidermidis* and *Staphylococcus aureus* [98-100]. In the last decade great effort has been made to unravel the biosynthesis of these antibiotics, leading to an understanding of the involved enzymes and the order of their action [103-106],[60]. Concerning the biosynthesis of novobiocin it has been shown that NovO is the methyltransferase that is required for methylation of desmethylnovobiocic acid [105]. Recently, we reported on a novel enzymatic C-C bond formation, namely the Friedel-Crafts alkylation catalyzed by SAM-dependent methyltransferases (Figure 30). The substrate acceptance of these enzymes was broader than expected and more surprisingly, the enzymes also accepted chemically modified cofactors as alkyl donors. Thus, alkylation of aromatic substrates was not restricted to methylation [168]. In general, cofactors are highly conserved mediators of biological processes and the cofactor dependence of enzymes is thus highly restricted. Modified cofactors decorated with allyl, propargyl and benzyl residues were used for Friedel-Crafts alkylation and extended the formation of aromatic compounds beyond the natural methylation reaction. Here we present the detailed molecular and biocatalytic characterization of the SAM-dependent methyltransferase NovO in order to rationalize its role and mode of action in the enzymatic Friedel-Crafts alkylation.

2.2.3 Experimental procedures

Cloning, heterologous expression and purification

Cloning, heterologous expression and purification of the methyltransferase NovO of *Streptomyces spheroides* (DSMZ 40292) was done as described previously [168], with the exception that no inducer was added to recombinant *E. coli* cultures. Two alternative primer pairs were used to check the correctness of the amplified *novO* gene (Table 2 #25 - 28). NovO variants were generated by site-directed mutagenesis using the appropriate primers listed in Table 2 [169]. Lysis of pET26b(+)-novO-variants, and pET26b(+)-novO-Strep-variants was achieved by incubation in 20 ml of 50 mM sodium phosphate buffer pH 6.5 with 6 mg lysozyme (Roth, Karlsruhe, Germany) per gram wet cell paste at room temperature for 20 minutes and subsequent incubation with 250 U Benzonase® (Merck, Darmstadt, Germany) per gram wet cell paste at room temperature for another 20 minutes. Aliquots of total crude extracts were analyzed on SDS-PAGE. The resultant cell debris was removed by centrifugation (60 min at 50000 x g). The supernatant was analyzed by SDS-PAGE and kept at 4 °C for enzymatic reactions and further affinity chromatography. Purified fractions were pooled and concentrated with Ultra-filtration spin columns from Vivaspin (cut-off 10.000 Da) to a final concentration of 5 to 10 mg/ml. For storage at -20 °C glycerol was added to a final concentration of 50 %. Total protein concentrations were determined by Bradford assay (BioRad, Hercules, USA) using bovine serum albumin, (Thermo Fisher, Waltham, USA) as reference protein. Quantitation of respective protein bands in SDS-PAGE was done with the GeneTools software from SynGene® (Syngene, Cambrigde, UK).

Methyltransferase assay

Soluble protein fractions of recombinant *E. coli* expressing NovO or its variants were incubated in 0.1 ml scale in a thermomixer at 35 °C and 1000 rpm for 16 hours. The reactions contained 0.5 mM substrate from a 10 mM stock solution prepared in DMSO, 2 mM SAM **a** (Sigma-Aldrich, St. Louis, USA) or allyl-SAH **b** from a 20 mM stock solution prepared in 50 mM sodium phosphate buffer pH 6.5, and 0.1 mg/ml BSA from a 2 mg/ml

stock solution prepared in 50 mM sodium phosphate buffer pH 6.5. Allyl-SAH **b** was prepared as described previously [168]. The amount of soluble protein fractions was set to 80 % of the total reaction volume. The reaction was stopped by heating at 80 °C for 10 minutes. Subsequently the mixtures were centrifuged at 16.000 x g for 15 minutes. Two to 20 μl of the aqueous solution was analyzed by HPLC. Specific activities were calculated based on determining the content of NovO in total protein by gel quantitation.

Determination of temperature and pH optimum

Temperature and pH optimum were determined with 1 mM coumarinbenzamide **3** (Figure 30) as substrate. For determination of the optimal reaction temperature 12 different temperatures were chosen between 27 and 48 °C. Reactions were initiated with 0.23 mg of soluble protein fractions and incubated for 4 or 24 hours. To find the optimal buffer and pH conditions soluble protein fractions containing NovO were prepared in 50 mM sodium phosphate buffer with pH values of 5, 5.5, 6, 6.5, 7, 7.5, and 8, or in 50 mM Tris-HCl buffer with pH values of 7.5, 8, 8.5, and 9. Reactions were initiated by adding 0.23 mg of corresponding soluble protein fractions and incubated for 24 hours.

Stability assay

The oxidation state of the cysteine residues of NovO was analyzed by incubation of the enzyme under oxidative or reductive conditions. Reactions were prepared as described for the methyltransferase assay containing 0.5 mM 2,7-dihydroxynaphthalene **5** (Figure 30), with or without additional DTT (1,4-dithiothreitol, Roth, Karlsruhe, Germany). DTT was added to a final concentration of 1 mM, and 0.1 ml reactions were incubated in 15 ml or 0.2 ml reaction tubes. Reactions were initiated by adding 0.05 mg (1.9 nmol) of purified Strep-tagged NovO and incubated for 16 hours. In another experiment the enzyme was pre-incubated for 4 hours under the described conditions before substrate and cofactor were added and further incubated for 16 hours.

Determination of kinetic parameters

For the determination of kinetic parameters the reactions were performed as described (Section 4.7) using purified Strep-tagged NovO protein. It has to be mentioned that though in soluble protein fractions no difference between tagged and untagged NovO proteins was observed, purified Strep-tagged NovO had a lower k_{cat} (compare Figure 33 and Table 1). The reactions were carried out in triplicate using substrate stock solutions of 10 mM coumarinbenzamide **3** (prepared in DMSO) or 40 mM 2,7-dihydroxynaphthalene **5** (prepared in 10 % of DMSO, 90 % of 50 mM sodium phosphate buffer pH 6.5). The SAM concentration was kept constant at 2 mM. Substrate concentrations were varied from 0.015 to 0.5 mM for coumarinbenzamide **3** and 0.02 to 20 mM in case of 2,7-dihydroxynaphthalene **5**, keeping the DMSO concentration constant at 5 %. Reactions were initiated with 0.05 mg (1.9 nmol) of purified Strep-tagged NovO protein and stopped after 5, 10, 20, 30, and 60 minutes. When kinetic parameters of co-substrates were investigated, the concentration of coumarinbenzamide **3** was set 4 times higher than the respective co-substrate concentration with a maximum of 2 mM leading to a DMSO concentration of 20 %. The SAM **a** concentration was varied from 0.03 to 1 mM and the allyl-SAH **b** concentration from 0.03 to 2 mM. Reactions were initiated by adding 0.05 mg (1.9 nmol) of Strep-tagged NovO (SAM **a**) or 0.0125 mg (0.47 nmol) of Strep-tagged NovO (allyl-SAH **b**) and stopped after 2.5, 5, 10, 20, 30, and 60 minutes.

HPLC analyses

HPLC analyses were performed on an Agilent 1100 instrument equipped with autosampler and diode array detector (DAD). Samples were analyzed on a Merck Chromolith® Performance RP-18e endcapped 100 x 4.6 mm column. Coumarinbenzamide **3** and 8-alkylated derivative **4** were separated with the eluent system 10 mM ammonium acetate (NH_4OAc) pH 5.5 and acetonitrile (AcCN) 93:7, flow 2 ml/min, 40 °C and $\lambda = 305$ nm. 2,7-dihydroxynaphthalene **5** and 1-alkylated derivative **6** were separated with the eluent system 10 mM NH_4OAc pH 5.5 and AcCN 9:1, flow 2.5 ml/min, 40 °C and $\lambda = 254$ nm.

Gel-filtration chromatography

Gel-filtration (Superdex 75 HR 10/30, GE Healthcare) using 50 mM Tris-HCl buffer containing 150 mM NaCl at pH 8.0 was applied. 0.25 ml of 2 mg/ml Strep-tagged NovO was loaded at a flow rate of 0.5 ml/min. Analysis and correlation of the elution profile to the chromatogram of a molecular weight standard (GE Healthcare, Uppsala, Sweden) yields the mass and the dimeric state of the native protein (Figure 32).

2.2.4 Results

Cloning and heterologous expression

The gene *novO* of *Streptomyces spheroides* [104], which encodes a methyltransferase, was cloned by PCR and heterologously expressed in *E. coli* as described previously [168].

Sequencing of the cloned *novO* gene showed differences to data present in the GenBank entry AAF67508.1. One exchanged base at position 13 from a guanosine to a cytosine resulting in the amino acid exchange A5P was intentionally introduced by the primers used for PCR amplification. Two further base exchanges at position 668 and 669 from a guanosine to a cytosine and a cytosine to a guanosine, respectively, resulted in the amino acid exchange S223C. Moreover, six additional silent base exchanges were identified in the cloned *novO* gene. These sequence differences were verified by sequencing several clones and by direct sequencing of the PCR amplified DNA. The revised *novO* sequence was submitted to GenBank (GenBank Accession number JN606326).

As already described previously, the cloned *novO* is readily expressed in *E. coli* resulting in up to 160 mg of soluble protein per liter culture, and showing high conversion rates for selected substrates [168]. Mutagenesis of these amino acids to create a protein, which is identical to that of GenBank entry AAF67508.1, resulted in the production of mostly insoluble NovO protein. Only small amounts of the protein were detected in the soluble fraction (Figure 31). In order to determine which of the two residues is responsible for this effect, single amino acid exchanges of P5A or C223S were created. Expression analysis showed that cysteine 223 plays a crucial role in the production of soluble protein, whereas proline and alanine at position 5 are interchangeable (Figure 31).

Biochemical characterization

NovO showed highest conversion rates at 35 °C, and lost all its activity above 44 °C. Sodium phosphate buffer at pH 6.5 provided optimal reaction conditions, whereas incubation below pH 5 almost eliminated all activity due to precipitation of the protein. In addition, the use of Tris-HCl buffer was less favorable, because at identical pH values

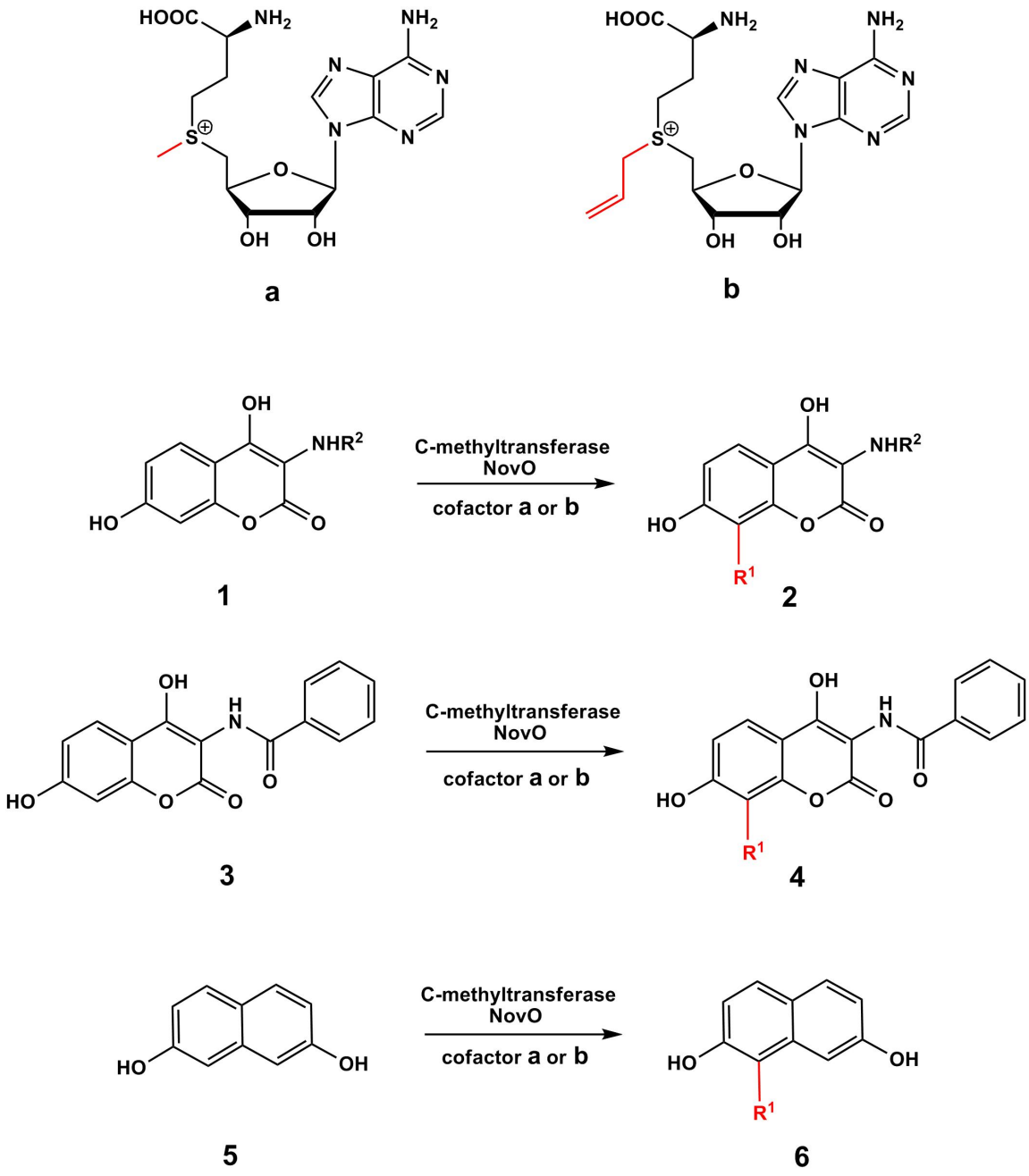

Figure 30: Alkyltransfer catalyzed by NovO illustrated with cofactors SAM a and Ally-SAH b. SAM **a** was purchased and Ally-SAH **b** synthesized as described previously [168]. R^1 = methyl, allyl, crotyl, propynyl, butynyl, benzyl. **1**: coumarin derivative, **2**: 8-alkylated coumarin derivative, **3**: *N*-(4,7-dihydroxy-2-oxo-2*H*-chromen-3-yl) benzamide,**4**: *N*-(4,7-dihydroxy-8-alkyl-2-oxo-2*H*-chromen-3-yl) benzamide, **5**: 2,7-dihydroxynaphthalene, **6**: 1-alkyl-2,7-dihydroxynaphthalene.

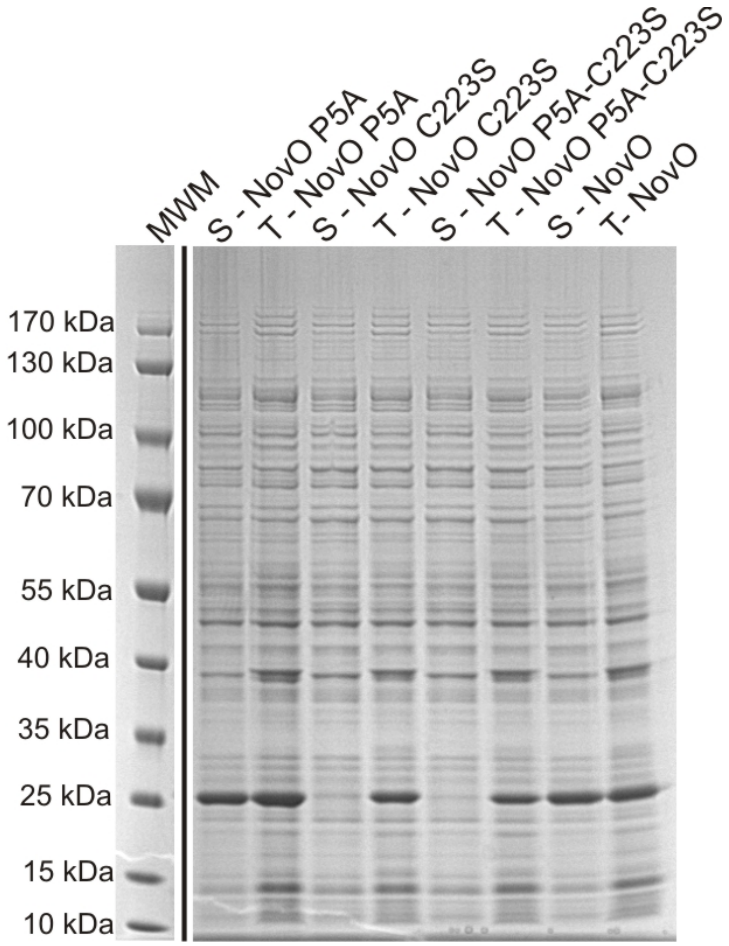

Figure 31: 4-12 % SDS-polyacrylamide gel of heterologous expression of NovO variants in *E. coli* BL21 Gold (DE3). Soluble protein fractions (S) and total crude extracts (T) of the NovO variants P5A, C223S, P5A-C223S, and the wild-type NovO protein are shown. Bands corresponding to NovO and its variants appear at the same position as the 25 kDa band of the molecular weight marker (MWM).

of 7.5 the conversion rate was decreased by 60 % when compared to sodium phosphate buffer (data not shown). The stability of the protein turned out to be a critical point in terms of storage and temperature conditions. As mentioned above it was observed that the protein was completely inactivated above 44 °C. Freezing and subsequent thawing of soluble protein fractions and purified protein decreased the enzyme activity drastically, leading to precipitation and inactivation. Storage of the purified protein at 4 °C led to a reduction of activity of 50 % within two weeks. If the purified protein was stored in the elution buffer supplemented with 50 % glycerol, no decrease of activity was observed after 18 months of storage at -20 °C.

Due to the fact that the NovO protein contains four cysteine residues including C223, and the observation of a dimeric state in gel-filtration chromatography (Figure 32) the possibility of disulfide bond formation or oxidation of cysteines had to be investigated. The incubation of the reaction mixture under oxidative compared to reductive conditions did not affect enzyme activity. In contrast, when the enzyme was incubated under one of these conditions prior to addition of substrate a strong decrease in activity was observed (data not shown). From these findings it can be concluded that the oxidation state of the cysteine residues does not play any role in the activity of the enzyme. However, pre-incubation of the enzyme under assay conditions drastically decreased its activity, indicating a general low stability, which is in accordance to the instability at elevated temperature.

Enzyme kinetics

In our previous study NovO was found to be suitable for alkylation of coumarin- and naphthalene containing substrates [168]. One of the most promising, in terms of chemical structure and conversion rate, 2,7-dihydroxynaphthalene **5** (Figure 30) was analyzed in more detail concerning its kinetic parameters (Figure 33). The affinity for 2,7-dihydroxynaphthalene **5** was significantly lower than that for coumarinbenzamide **3**. In contrast, the turnover number for **5** was seven times higher than that for **3**. One possible reason is the acceptance of higher substrate concentrations. Whereas Vmax is already gained at 0.5 mM of **3**, up to 20 mM of **5** are needed for substrate saturation.

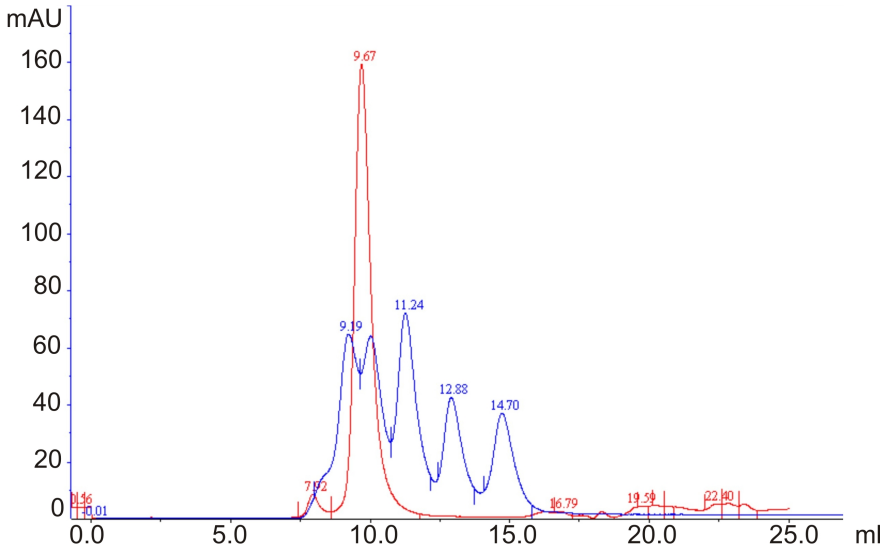

Figure 32: Gel-filtration chromatography of purified Strep-tagged NovO protein on a Superdex 75 HR 10/30 column. The peak at 9.67 ml corresponds to a dimeric state of Strep-tagged NovO (red line, 500 μg) compared to a molecular weight standard (blue line, GE Healthcare, 300 μg). 9.19 ml: 75 kDa conalbumin, 10.0 ml: 44 kDa ovalbumin, 11.24 ml: 29 kDa carbonic anhydrase, 12.88 ml: 13.7 kDa ribonuclease, 14.7 ml: 6.5 kDa aprotinin.

An enzyme going beyond methylation and is broadly capable of performing an enzymatic equivalent to the Friedel-Crafts-alkylation would be highly desirable. Previous results showed the ability of NovO to transfer other alkyl groups than methyl on selected substrates [168], (Figure 30). In order to learn about this ability in more detail, kinetic parameters of the SAM analogue allyl-SAH **b** were determined and compared to that obtained for SAM **a** (Figure 34). Not astonishingly the affinity to allyl-SAH **b** was four times lower than that observed for the natural co-substrate SAM **a**. However, the enzyme transferred allyl at much higher efficiency than methyl to coumarinbenzamide **3** in the same time duration (Figure 34).

Cofactor binding site

To gain more insights into the function of NovO a homology model was established (Figure 36). Despite the low sequence identity of related and structurally characterized methyltransferases the available information was useful to identify relevant residues. With the support from 3DM software (http://www.bioprodict.nl) (Figure 35), and the homology model created with Yasara software (Institute of Molecular Biosciences, University of

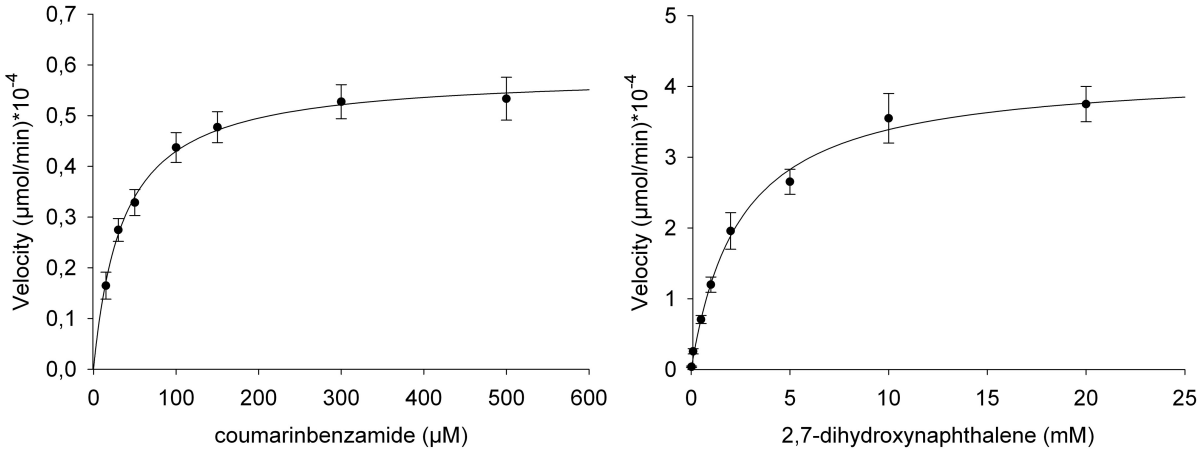

substrate [mM]	K_m [mM]	k_{cat} [s^{-1}]*10^{-4}	k_{cat}/K_m [$M^{-1} * s^{-1}$]
coumarinbenzamide **3**	0.036	5.2	14.4
2,7-dihydroxynaphthalene **5**	2.5	37	1.5

Figure 33: Determination of kinetic parameters for the substrates coumarinbenzamide 3 and 2,7-dihydroxynaphthalene 5. The SAM concentration was kept constant at 2 mM. Resultant K_m and k_{cat} values are listed in the table below the graphs.

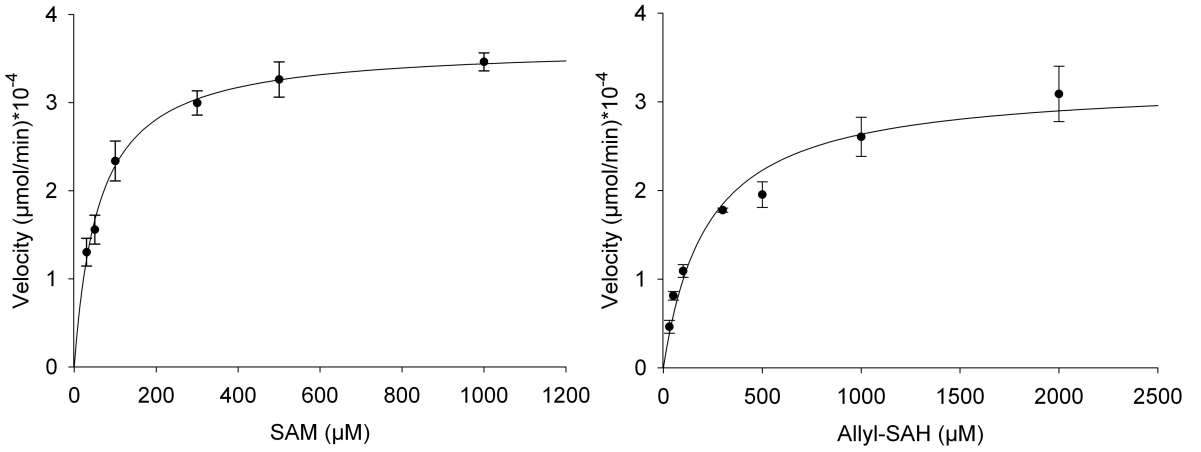

co-substrate [mM]	K_m [mM]	k_{cat} [s^{-1}]*10^{-3}	k_{cat}/K_m [$M^{-1} * s^{-1}$]
SAM **a**	0.06	3.2	53
allyl-SAH **b**	0.22	11	51

Figure 34: Determination of kinetic parameters for the co-substrates SAM a and allyl-SAH b. Concentrations of substrate coumarinbenzamide **3** were set four times higher than the respective co-substrate concentrations until 0.5 mM. Above that concentration 2 mM of substrate **3** were used. Resultant K_m and k_{cat} values are listed in the table below the graphs.

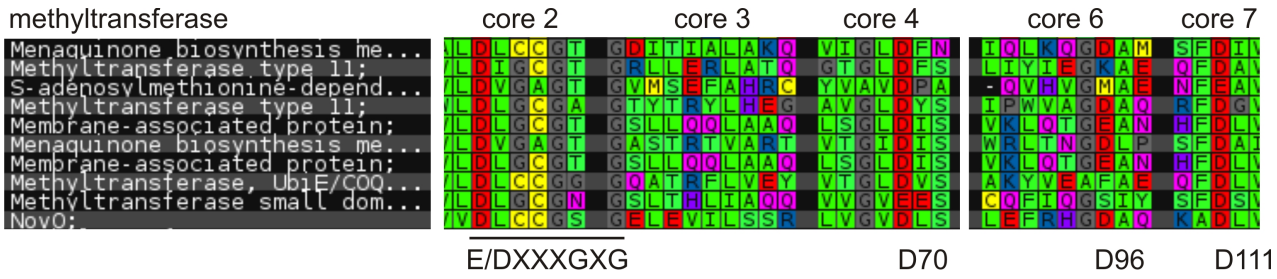

Figure 35: Representative part of the multiple sequence alignment in 3DM database including NovO. Only amino acids of conserved domains are listed in the alignment and ordered in cores. The sequence of NovO is located at the bottom line. The conserved domain E/DXXXGXG (motif I), which is present in NovO as D45 L46 C47 C48 G49 S50 G51, is located in core 2 and 3. The possible acidic loop residues (motif II) D70 and D96 are located in core 4 and 6, respectively. The invariant aspartate 111 is located in core 7. Core 5 is not shown because of any relevant residues.

Graz, http://www.yasara.org), the putative cofactor binding site and catalytic residues could be identified. The conserved sequence motif E/DXXXGXG can be found in NovO as D45 L46 C47 C48 G49 S50 G51. This sequence motif has been described several times as an indispensable part of all SAM-dependent methyltransferases and is associated with cofactor binding [85],[87]. Located close to the N-terminus of the protein this glycine-rich sequence has often been referred to as motif I. Another conserved domain, which is described as motif II and consists of acidic amino acids [85],[87] was identified in NovO too. Two aspartate residues, D70 and D96, are located within core 4 and 6 respectively (Figure 35). 3DM software links the aligned residues to literature that describes them to be involved in cofactor binding [170-174]. In addition, the homology model shows that these residues are in close proximity to bound SAH (demethylated SAM). This information suggests an involvement of these aspartates in cofactor binding. Although D111 is highly conserved in the aligned sequences, it is not dealing with ligand binding according to literature [175]. The homology model supports this data, because D111 is further away from SAH than D70 and D96. For a functional investigation of the respective residues, single or double mutations located within these sequence motifs were created. Enzyme activities of soluble protein fractions were determined as total conversion rates in a defined reaction time or as specific activities (Table 1). The conserved D45 was exchanged to leucine or asparagine. Whereas the D45L variant resulted in very small amounts of soluble and almost inactive enzyme, the exchange to an uncharged, but sterically similar residue, in this case asparagine resulted in a partially functional protein. The expression

of soluble protein was nearly as good as observed for the wild-type protein, but the activity towards methyltransfer on coumarinbenzamide **3** was significantly decreased. G49, when exchanged to alanine, showed similar results (Table 1). An exchange of G51 to alanine resulted in a strong decrease in soluble protein production and could only convert 3 % of coumarinbenzamide **3**. D70 and D96, which might match the acidic loop of motif II, were analyzed the same way. Exchanges to leucine resulted in insoluble and inactive protein in both cases. If asparagine was placed at position 70 again no soluble protein was produced. The variant D96N yielded the same amounts of soluble protein as the wild-type protein. No decrease of activity was detected. Due to these results, it is more likely that D70 represents the acidic loop, which is meant to be involved in the binding of the ribose hydroxyl groups of SAM [170-174]. Because of the fact that both variants D70L, and D70N could not be analyzed for their specific activities due to insolubility issues, a definitive proof remains open. To verify the possibility that also E52 could be involved in SAM binding, the variants E52L, and E52Q were constructed. This glutamate follows the conserved G51 of motif I and therefore could be involved in SAM binding. However, the multiple sequence alignment revealed that a glutamate at this position is very infrequent (Figure 35). Both variants gave similar results as exchanges of D96, indicating no direct involvement in the mechanism of cofactor binding.

Strep-tagged versions of some variants were purified and used for the determination of the specific conversion rates. The variants D45L and G51A did not convert any substrate. The variant G49A converted 16 % of coumarinbenzamide **3**. These results with purified enzymes supported the above described results of soluble protein fractions and verified the importance of the abovementioned residues for cofactor binding.

In addition, the cysteine residues C47 and C48, which are part of the conserved sequence motif, might be relevant for enzyme folding and activity. When C47 was replaced by glycine, the expression level was not affected, but the k_{cat} decreased. On the other hand a C48S exchange lowered the amount of soluble protein to 50 %, but resulted in an increase of specific activity. A double mutant consisting of both mutations reflected the effects of the mentioned single mutants. The variant C47G-C48S was slightly less active than C47G and the expression level was in between the ones observed for the variants C47G and C48S (Table 1). Furthermore, a glycine instead of C48, and a serine instead of

C47 completely destroyed the production of soluble protein. With the results of these experiments we concluded and experimentally verified that D45 and G49 are of great importance for enzymatic function whereas C47, C48, G51, and D70 are critical positions for correct folding of the protein.

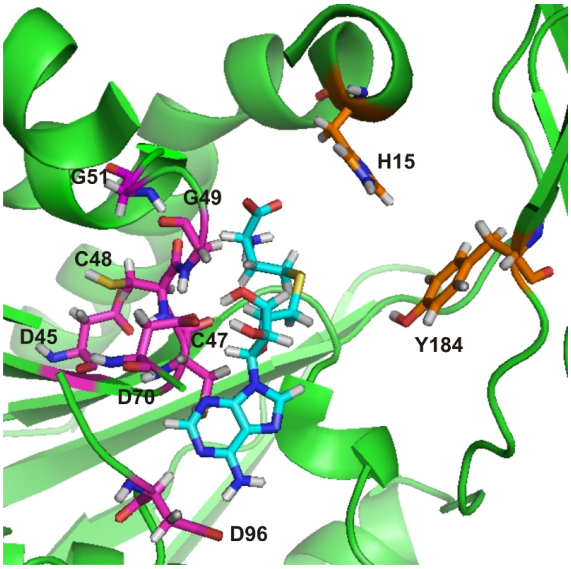

Figure 36: Homology model of NovO with bound SAH (demethylated SAM). For homology modeling the Yasara software was used. Figures were created with PyMOL software (www.pymol.org). The three-dimensional protein structure is shown in green cartoon with bound SAH, which is depicted as light blue sticks. Possible catalytic residues H15 and Y184 are illustrated as orange sticks. Residues which are involved in cofactor binding (D45, C47, C48, G49, G51, D70, D96) including the conserved sequence domain E/DXXXGXG are shown as magenta sticks.

Putative active site residues

The transfer of the methyl group has been described to depend on a histidine residue within the active site of the methyltransferases arginine-N-methyltransferase [176], calchone-O-methyltransferase [172], and sterol-C-methyltransferase [175]. The deprotonated imidazole group of histidine could act as a proton acceptor, and therefore be relevant for substrate activation. Another proposed mechanism combines the action of a tyrosine and a histidine residue [177]. In this particular mechanism the tyrosine is deprotonated, and the histidine would accept this proton, followed by a nucleophilic attack of the resulting oxyanion of tyrosine on the substrate. Correlated mutation analysis performed with the 3DM software [10] provided a link to the abovementioned work of Nes *et al* [175] and

Table 1: Kinetic parameters of NovO variants towards coumarinbenzamide 3. Specific activities of crude lysates were calculated as k_{cat} after quantitation of protein bands on SDS-polyacrylamide gels corresponding to NovO or NovO variants. Factor f indicates the increase or decrease of k_{cat} compared to the wild-type protein. Conversions of 0.5 mM coumarinbenzamide **3** after 16 hours incubation are shown in percentages. *n.d.*: not determined.

NovO variant	k_{cat} [s^{-1}]	f	16 h conversion [%]
wild-type	$2.5*10^{-2} \pm 2.5*10^{-3}$	1	100
D45N	$9.7*10^{-4} \pm 1.4*10^{-3}$	0.04	39
G49A	$1.2*10^{-3} \pm 1.2*10^{-3}$	0.05	9
G51A	n.d.	n.d.	3
D96N	$2.8*10^{-2} \pm 3.6*10^{-3}$	1.1	100
E52L	$2.3*10^{-2} \pm 1.0*10^{-2}$	0.9	100
C47G	$1.4*10^{-2} \pm 1.0*10^{-3}$	0.6	100
C48S	$3.*10^{-2} \pm 1.3*10^{-2}$	1.2	100
C47G-C48S	$1.0*10^{-2} \pm 1.5*10^{-3}$	0.4	n.d.

Wada *et al* [177]. Combined with the information obtained from the homology model a histidine (H15) and a tyrosine (Y184) could be identified, which are in spatial proximity to the methyl group of the cofactor (Figure 36). In NovO the exchange of H15 to glutamine or asparagine led to a drastic reduction of activity to only 6 % conversion compared to the wild-type enzyme. The activity could be rescued to higher levels (25 or 22 % conversion), if a lysine or an arginine was positioned at residue number 15, indicating the relevance of a basic amino acid for enzyme activity. The expression of soluble protein of these variants was not affected at all. On the other hand, NovO variants with exchanges of Y184 to serine, threonine, or phenylalanine did neither affect protein production nor enzyme activity. A combination of these exchanges, the variant H15Q-Y184F, gave the same results as the variant H15Q. These findings strongly suggest that the histidine residue at position 15 could act as the general base in the methyltransfer reaction.

2.2.5 Discussion

This study describes the characterization of a small molecule C-methyltransferase that is capable of performing an enzymatic equivalent to the classical chemical Friedel-Crafts alkylation. Cloning of the enzyme from its origin *Streptomyces spheroides* revealed a different sequence than the one of GenBank entry AAF67508.1. The available sequence information stated a serine at position 223, which turned out to be a sequencing artifact. Our data of three independent cloning and subsequent sequence determination experiments constitute a cysteine at the named position. The importance of this residue was emphasized by expression analysis of the putative (S223) in comparison to the genuine wild-type (C223). This alkyltransferase has been characterized in terms of biochemical data, enzyme kinetics and functional mutagenesis. Our observed data from gel-filtration chromatography of the purified enzyme show that the protein exhibits a dimeric conformation. This finding has recently been described for another small molecule C-methyltransferase of *Streptomyces chrysomallus* [117]. NovO is capable of effectively transferring allyl groups via the cofactor analogue allyl-SAH **b**. As expected, the affinity of the enzyme to this synthetic cofactor is smaller than that for the natural SAM **a**, indicating the evolutionary design of the protein towards the methyldonor, which is the second most frequently used cofactor in biological systems. Despite the lower affinity the enzyme transfers allyl groups faster than methyl groups, resulting in only a small difference in catalytic efficiency. This increased turnover rate can be explained by the fact that the reactivity of allyl is higher than that of methyl, due to the presence of the unsaturated carbon-carbon bond. Enzymatic methylation occurs via an S_N2 mechanism with inversion of the configuration at the transferred methyl group [16]. During enzymatic transition state formation a conjugative stabilization of the p orbital at the reactive carbon is built. Dalhoff and coworkers [22] proposed that in case of allyl transfer catalyzed by DNA-methyltransferases a conjugation of the transiently formed p orbital of the reactive carbon and the neighboring antibonding π orbital facilitates the reaction. Our findings are in agreement with this proposal and further experimentally verify the increased reactivity of an allyl group by lowering the activation energy for transition state formation. Moreover, the methyltransfer on the substrate 2,7-dihydroxynaphthalene **5** can be achieved with a turnover number that is seven times higher than that for the coumarin substrate coumarinbenzamide **3**. This

high turnover number is astonishing, considering the low affinity to this substrate. Altogether, these data favor the methyltransferase NovO as a biocatalyst for an enzymatic Friedel-Crafts alkylation.

Some insights into structural aspects of correct protein folding and protein-ligand interactions could be determined without the availability of a three-dimensional protein structure. The combination of multiple sequence alignment, homology modeling, and literature data led to the identification of putative residues relevant for catalytic function. Functional mutagenesis strongly supports the relevance of the amino acids D45 and G49 for cofactor binding. These residues are located within the conserved sequence domain E/DXXXGXG and their exchange to asparagine or leucine decreases the enzyme activity drastically. Proof for the involvement of D70 in cofactor binding is missing due to insolubility issues, but the described data strongly suggest its importance in SAM contact. The highly conserved G51, which is also part of this conserved sequence domain, seems to be of great importance for correct protein folding, because the exchange to alanine had a strong effect on the production of soluble and active enzyme. In terms of catalysis our data suggest H15 to be the catalytic base in NovO.

Knowledge about the position and function of certain amino acid residues are of great importance for the understanding of enzyme mechanisms. Our described data can be used for prospective engineering of the small molecule C-methyltransferase NovO towards effective alkylation of required substrates that could act as building blocks for e.g. pharmaceuticals.

Acknowledgements – We thank Horst Lechner for preparation of the homology model, Slaven Stekovic for technical support and Kerstin Steiner for critical reading the manuscript.

Footnotes

*This work has been supported by the Federal Ministry of Economy, Family and Youth (BMWFJ), the Federal Ministry of Traffic, Innovation and Technology (bmvit), the Styrian Business Promotion Agency SFG, the Standortagentur Tirol and ZIT - Technology

Agency of the City of Vienna through the COMET-Funding Program managed by the Austrian Research Promotion Agency FFG.

[1]To whom correspondence may be addressed: Mandana Gruber-Khadjawi, ACIB GmbH, Stremayrgasse 9, A-8010-Graz, Austria, Tel: +43 316 873 32410, Fax: +43 316 873 1032410, E-mail: mandana.gruber@acib.at

[2]Helmut Schwab, Institute of Molecular Biotechnology, Graz University of Technology, Petersgasse 14, Tel: +43 316 873 4070, Fax: +43 316 873 4071, E-mail: helmut.schwab@tugraz.at

[3]The abbreviations used are: SAM, S-adenosyl-L-methionine; SAH, S-adenosyl-L-homocysteine; coumarinbenzamide, *N*-(4,7-dihydroxy-2-oxo-2*H*-chromen-3-yl) benzamide

[4]The nucleotide sequence for the *novO* gene has been deposited in the GenBank database under GenBank Accession Number JN606326.

2.2.6 Supplemental data

Table 2: Oligonucleotides used for site-directed mutagenesis and gene amplification. Exchanged codon triplets (# 1 to # 24) are assigned in bold letters. Complementary oligonucleotides were used as reverse primers. Endonuclease recognition sites of primers # 25 to # 28 are assigned in bold letters.

primer #	primer name	sequence 5' to 3'
# 1	FnovC223S	GTTCCCACGGTCAAA**AGC**TTCGCCCGTCGGGCCGCT
# 2	FnovP5A	GAAGATTGAA**GCG**ATTACGGGATCCGAGGCCGA
# 3	FnovC48S	ACCGTGGTCGACCTGTGC**AGT**GGCTCGGGTGAGCTG
# 4	FnovC47S	ACCGTGGTCGACCTG**AGC**TGTGGCTCGGGTGAGCTG
# 5	FnovC47G	ACCGTGGTCGACCTG**GGC**TGTGGCTCGGGTGAGCTG
# 6	FnovC47G-C48G	ACCGTGGTCGACCTG**GGCGGT**GGCTCGGGTGAGCTG
# 7	FnovC47G-C48S	ACCGTGGTCGACCTG**GGCAGT**GGCTCGGGTGAGCTG
# 8	FnovG49A	ACCTGTGCTGT**GCC**TCGGGTGAGCTGGAAGTCATC
# 9	FnovG51A	ACCTGTGCTGTGGCTCG**GCG**GAGCTGGAAGTCATC
# 10	FnovD45L	ACGGCCAGACCGTGGTC**CTG**CTGTGCTGTGGCTC
# 11	FnovD45N	ACGGCCAGACCGTGGTC**AAC**CTGTGCTGTGGCTC
# 12	FnovE52L	GTGCTGTGGCTCGGGT**CTG**CTGGAAGTCATC
# 13	FnovE52Q	GTGCTGTGGCTCGGGT**CAG**CTGGAAGTCATC
# 14	FnovD70L	GAATCTGGTCGGTGTC**CTG**CTCTCGGAGGAC
# 15	FnovD70N	GAATCTGGTCGGTGTC**AAC**CTCTCGGAGGAC
# 16	FnovD96L	GAATTCCGGCACGGT**CTG**GCGCAACTCCTG
# 17	FnovD96N	GAATTCCGGCACGGT**AAC**GCGCAACTCCTG
# 18	FnovH15Q	AGGCCGAAGCATTT**CAG**CGGATGGGCTCCCAGGCGTC
# 19	FnovH15N	AGGCCGAAGCATTT**AAC**CGGATGGGCTCCCAGGCGTC
# 20	FnovH15K	GAGGCCGAAGCATTT**AAA**CGGATGGGCTCCCAG
# 21	FnovH15R	GAGGCCGAAGCATTT**CGC**CGGATGGGCTCCCAG
# 22	FnovY184F	TCTGGGCGCTGGCTCACCAT**TTC**GCGCCCCGGCTCGACG
# 23	FnovY184S	TCTGGGCGCTGGCTCACCAT**AGC**GCGCCCCGGCTCGACG
# 24	FnovY184T	TCTGGGCGCTGGCTCACCAT**ACC**GCGCCCCGGCTCGACG
# 25	Fnova1	ACGAGGGGCATC**CATATG**AAGATTGAAGCG
# 26	Rnova1	TCGGGTCCAG**AAGCTT**GTTTCAGACAATT
# 27	Fnova2	CAGG**CATATG**AAGATTGAAGCGATTACGG
# 28	Rnova2	TAGA**AAGCTT**TCAGGCGGCGGC

2.3 Additional Results and Discussion

2.3.1 Coumarin methylating enzymes

NovO The methyltransferase NovO of *Streptomyces spheroides* [104] was investigated as described by Stecher *et al.*, 2009 [168] and Tengg *et al.*, 2011 (Section 2.2). For clarity some additional comments will be addressed here. The high expression level of soluble protein is clearly visible on the SDS-PAGE analysis, and was quantified by the described gel quantitation methodology (Section 4.5), which could state the amount of the recombinant protein in the cleared lysate to approximately 30 to 35 %.

NovO constructs The described experiments were done with *E. coli* lysates containing recombinant NovO protein, or with purified Strep-tagged NovO. Although the tagged protein exhibits excellent activity, a pure preparation of an untagged protein is desirable in terms of structure determination experiments. In order to get a pure and unchanged protein, the gene *novO* was cloned into a plasmid which enables high value production of an N-terminally tagged protein with a Strep-binding-protein (SBP) and a TEV-protease cleavage site (TEV). After purification via streptactin columns, the eluted fraction can be incubated with TEV-protease (Tobacco Etch Virus protease) for cutting off the SBP and TEV peptide. After cleavage only one additional amino acid (serine) will be left on the NovO sequence. The resultant SBP-TEV peptide can be removed by additional purification via a streptactin column, and finally the hexa-histidine tagged TEV-protease is bound to a Ni^{2+} matrix leaving free NovO protein. For a possible support of soluble protein production a solubility enhancement tag (SET1) was attached to the SBP sequence. Another strategy was the insertion of the TEV cleavage site into the existing pET26b(+)-novO-Strep vector. The disadvantage of the latter method is, that after removal of the tag, the TEV-protease cleavage site remains at the protein. All three constructs were treated the same way by expression for 16 hours without addition of an inducer. The production of soluble NovO-TEV-Strep protein could be achieved at about the same high amounts as was observed for NovO and NovO-S (Figure 39 and Figure 37). Figure 39 shows that SET1-SBP-TEV-NovO (36.1 kDa) could not be produced without inducer (A), but strongly expressed with IPTG (B). SBP-TEV-NovO (31.5 kDa) was

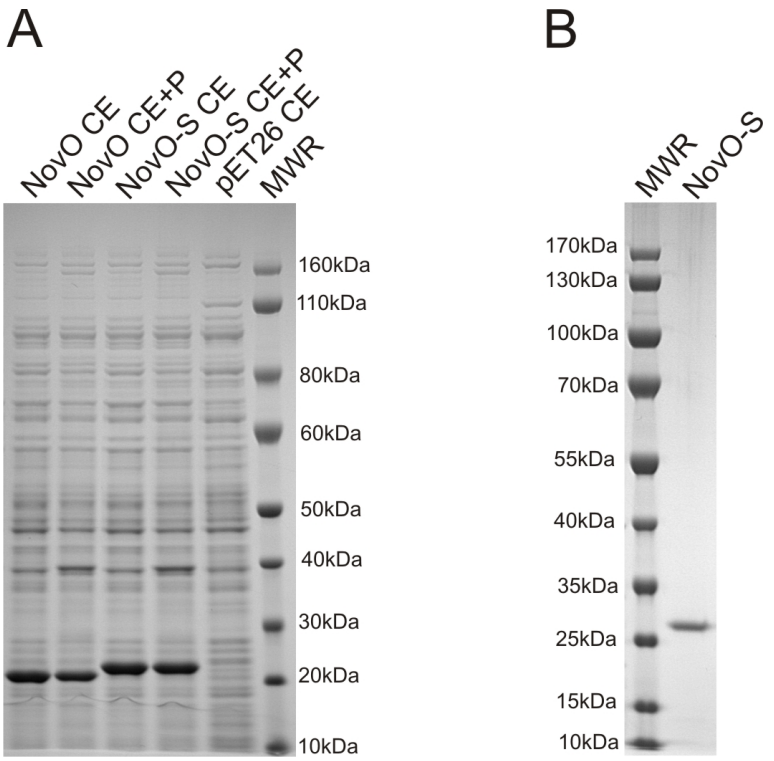

Figure 37: 4-12 % SDS-polyacrylamide gel of heterologous protein expression in *E. coli* BL21 Gold (DE3). **A**: NovO and NovO-Strep expression. NovO CE: cleared lysate of NovO (25.4 kDa), NovO CE+P: total crude extract of NovO, NovO-S CE: cleared lysate of NovO-Strep (26.6 kDa), NovO-S CE+P: total crude extract of NovO-Strep, pET26 CE: cleared lysate of the empty expression vector pET26b(+). The strong overexpression of soluble NovO and NovO-Strep proteins is clearly visible in lanes 1 and 3. The similar intensities of the respective protein bands in lanes 2 and 4 indicate no insoluble protein production. Total soluble protein pattern of the empty vector in lane 5 highlights the overexpression level of NovO and NovO-Strep. **B**: NovO-Strep purification. The high purity of the eluted fraction is clearly visible in lane 2 at the expected size of 26.6 kDa, where 500 ng protein was loaded.

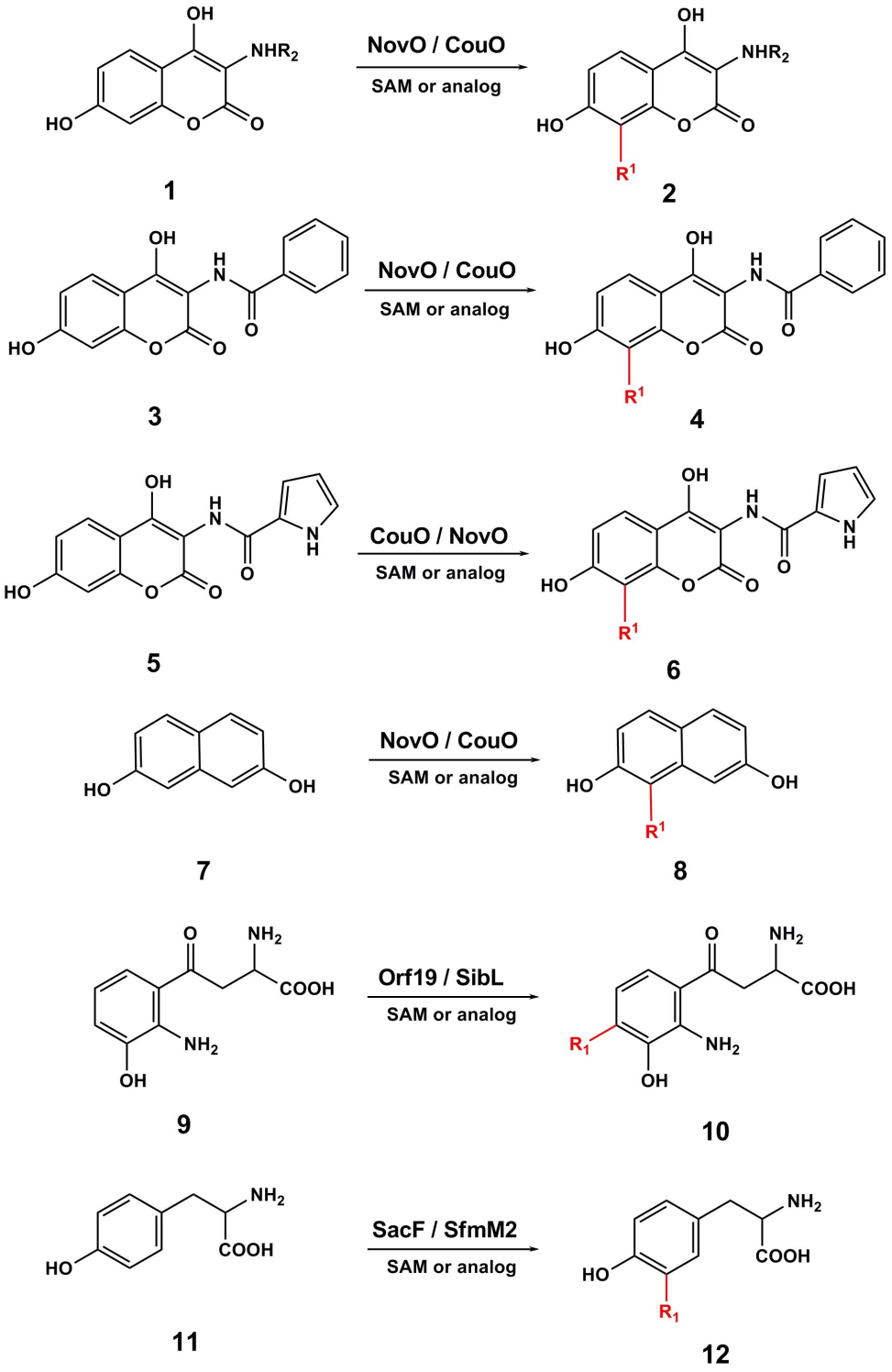

Figure 38: Alkyltransfer catalyzed by investigated methyltransferases. 1: coumarin derivative, 2: 8-alkylated coumarin derivative, 3: coumarinbenzamide, 4: 8-alkylcoumarinbenzamide, 5: coumarinpyrrolamide, 6: 8-alkylcoumarinpyrrolamide, 7: 2,7-dihydroxynaphthalene, 8: 1-alkyl-2,7-dihydroxynaphthalene, 9: 3-hydroxykynurenine, 10: 4-alkyl-3-hydroxykynurenine, 11: tyrosine, 12: 3'-alkyltyrosine.

slightly produced without inducer (A), and also strongly overexpressed with IPGT (B). Different concentrations of IPTG (0.5, 0.1, 0.02 mM) did only show marginal effects. The SET1 domain did not effect the amount of soluble protein. Overall, the amount of soluble protein is impressive. For purification the lysate SBP-TEV-NovO derived from expression with 0.02 mM IPTG was used.

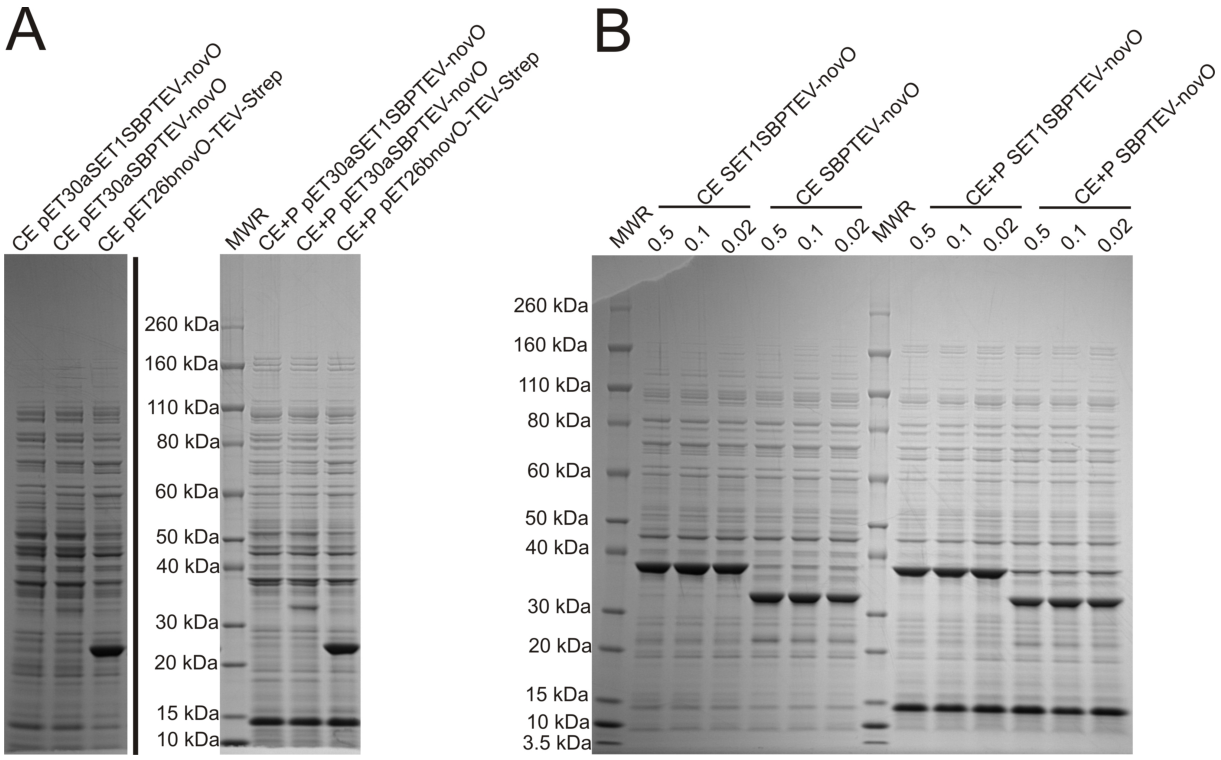

Figure 39: 4-12 % SDS-polyacrylamide gel of heterologous protein expression in *E. coli* BL21 Gold (DE3). **A**: Cleared lysate (CE, lane 1 - 3) and total crude extracts (CE+P, lane 5 -7) of SET1-SBP-TEV-NovO, SBP-TEV-NovO, and NovO-TEV-Strep. A strong overexpression of soluble NovO-TEV-Strep (26.6 kDa) protein compared to little expression of soluble and insoluble SBP-TEV-NovO (31.5 kDa) is obvious. No band according to SET1-SBP-TEV-NovO (36.1 kDa) is visible neither in the soluble nor in the insoluble fraction. **B**: Cleared lysates (CE, lane 2 - 7) and total crude extracts (CE+P, lane 9 -14) of SET1-SBP-TEV-NovO and SBP-TEV-NovO prepared after expression with different inducer concentrations (0.02, 0.1, and 0.5 mM IPTG). All three conditions lead to the production of huge amounts of soluble protein. In all (A and B) total crude extracts a strong band at 14 kDa is visible, which derives from lysozyme.

NovO purification The SBP-TEV-NovO protein could be successfully purified and subsequently separated from TEV-protease protein to yield almost pure NovO protein (Figure

40). Unfortunately the SBP-TEV peptide could not be separated, because desthiobiotin would have had to be removed by buffer exchange methodology prior loading this fraction on a streptactin column. Gel-filtration chromatography revealed the same picture as was observed for the tagged protein (data not shown). 50 μg of the pure enzyme revealed a moderate conversion rate of coumarinbenzamide **3** of 12 to 16 % after 90 minutes at standard assay conditions, which is comparable to that obtain for purified Strep tagged NovO. For comparison the purified SBP-TEV-NovO showed 29 % conversion, the fraction after TEV cleavage 31 %, and the lysate 93 %, indicating a strong decline of activity during purification procedure.

In a scale-up experiment about 45 mg of untagged NovO could be purified out of a one liter culture.

Isotopic labeling and purification of NovO In order to determine a protein structure by nuclear magnetic resonance spectroscopy (NMR) the protein has to be incorporated with stable isotopes of nitrogen or carbon. For this purpose it was decided to label NovO with ^{15}N.

Figure 41 shows the successful expression (lane 2), purification (lane5) and further processing of SBP-TEV-NovO to yield pure NovO protein (lane 8). The purification procedure yielded a total of 1.4 mg ^{15}N labeled NovO derived from one liter culture, which is far below the yield of unlabeled NovO.

50 µg of the pure NovO protein revealed a moderate conversion rate of 0.5 mM coumarinbenzamide **3** of 30 % after 90 minutes incubation time, which is similar to that obtain for purified C-terminally Strep-tagged NovO (26 %). The increased conversion rate compared to the one obtained for unlabeled purified NovO could be due to assay conditions and HPLC analysis, because the conversion rate of the C-terminally Strep-tagged NovO was higher too.

Interestingly little amount of a protein of about 25 kDa was present in the cleared lysate (lane 2) and in the eluate fraction (lane 5). This could be due to TEV-cleavage by *E. coli* enzymes, or to the production of untagged NovO by internal translation initiation. In order to prove the two possibilities, the band at 25 kDa of the eluate fraction (lane 5)

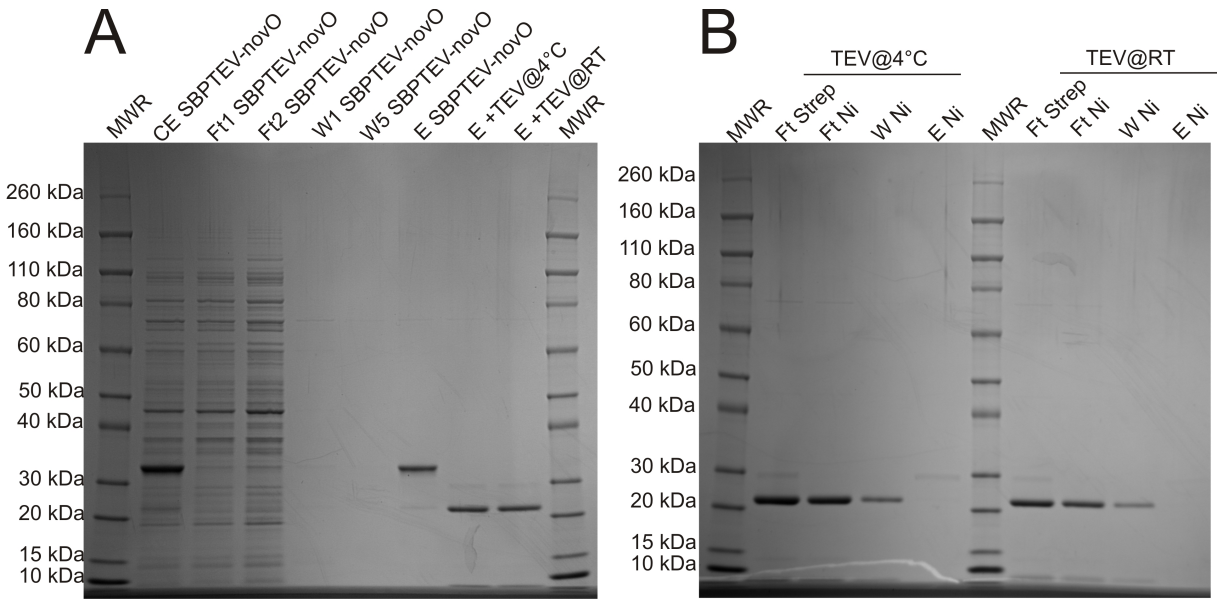

Figure 40: 4-12 % SDS-polyacrylamide gel of purification procedure for SBP-TEV-NovO. A: Purification of SBP-TEV- NovO (E SBPTEV-novO) and subsequent TEV-protease cleavage (E+TEV@4°C, and E+TEV@RT), including intermediates flowthrough- (Ft1, Ft2) and wash (W1, W5) fractions. No band according to the size of SBP-TEV-NovO is visible in the flowthrough- and wash fractions indicating that all of the protein bound to the streptactin column. The eluate fraction (E SBPTEV-NovO) shows that the protein was purified to a high degree. A faint band is visible at the size of untagged NovO protein. Total cleavage could be achieved under both used conditions (E+TEV@4°C, and E+TEV@RT) showing only one band at the size of the untagged NovO. TEV-protease is visible at the size of $\sim$ 30 kDa. **B**: Removal of SBP-TEV peptide (Ft Strep) and of TEV-protease (Ft Ni, W Ni), and elution of bound TEV-protease (E Ni) of both fractions (4°C and RT). SBP-TEV peptide did not bind to streptactin matrix and is still present in the flowthrough (Ft Strep). TEV-protease was removed successfully by Ni^{2+} affinity chromatography (Ft Ni, W Ni). Remaining TEV-protease was removed (E Ni) showing no contaminations.

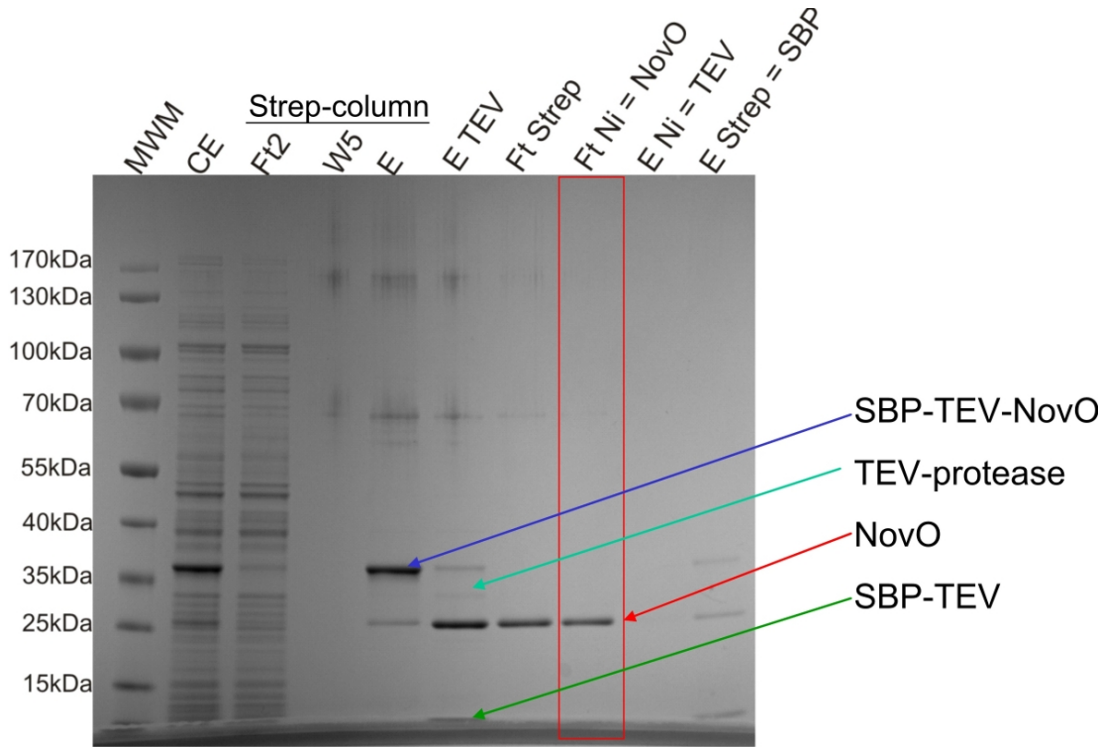

Figure 41: 4-12 % SDS-polyacrylamide gel of Strep Tag purification followed by TEV-protease cleavage, His Tag purification and second Strep Tag purification of ^{15}N labeled NovO. The overexpression of SBP-TEV-NovO is clearly visible in lane 2 (CE), but also a band at the size of the untagged NovO is visible at 25 kDa. SBP-TEV-NovO was purified to homogeneity (lane 5, E), cut off the SBP-TEV peptide by TEV-protease incubation (lane 6, E TEV), removal of the SBP-TEV peptide (lane 7, Ft Strep), and removal of His-tagged TEV-protease (lane 8, Ft Ni = NovO). Lane 9 (E Ni = TEV) should contain TEV-protease, but is not detectable due to the low concentration. Lane 10 (E Strep = SBP) should only contain the SBP-TEV peptide, but also NovO (at 25 kDa) and SBP-TEV-NovO (at 36 kDa) are present in this fraction.

and the band at 25 kDa of the final NovO (lane 8) were analyzed by nanoLC-tandem MS spectroscopy (Ruth Birner-Grünberger, ZMF, Medical University of Graz).

Gel slices were digested with two enzymes, chymotrypsin and subtilisin, and afterwards analyzed by nanoLC-tandem MS. The final NovO (figure 41, lane 8) contains mainly the TEV-protease cleaved product with an N-terminal peptide of SMKIEP. The 25 kDa band of the eluate fraction (figure 41, lane 5) contains three different species of proteins with N-termini of FQSMKIEP, SMKIEP, and MKIEP. The species MKIEP could derive from an internal translation initiation, but could also derive from proteolytic cleavage. The other two species could only derive from proteolytic cleavage at two distinct sites. It is impossible that the species SMKIEP is due to TEV protease cleavage, because there was no addition of this enzyme at this stage of procedure, and *E. coli* lysates do not contain TEV protease. Nevertheless, the final NovO predominantly consists of one species, which derived from TEV protease cleavage.

NMR spectroscopy was performed by Klaus Zangger at the KFU Graz. Unfortunately a structure determination was not possible due to heterogeneous conformations, which might derive from alternating mono- and multimer conformation of the protein. However, the analysis revealed a structured protein with little flexible residues. Nevertheless, it should be possible to use the protein for determination of ligand-protein interaction, including binding affinity and conformation of binding.

CouO CouO, the methyltransferase of *Streptomyces rishiriensis* [103] that shows high sequence identity (85 % on protein sequence) to the described NovO protein, was also successfully expressed in *E. coli* cells. The amount of soluble protein was comparable to the high level production of soluble protein achieved for the described NovO (Figure 42 A). Activity analysis revealed a similar picture compared to NovO. Highest conversion rates can be achieved at 37 °C and pH 7 in sodium phosphate buffer. The enzyme is totally inactivated at temperatures above 44 °C, and precipitates below pH 5. In addition the use of Tris-HCl buffer exhibits a less favorable environment than sodium phosphate buffer. These findings are not surprising, because of the high similarity of the enzymes, which has already been described by Pacholec *et al.*, 2005 [105]. The used substrate coumarinpyrrolamide **5** is closely related to the natural substrate. The only difference is a lack

of a carboxy and a methyl group on the pyrrol scaffold. Substrate **5** could be converted beyond 99 %. The 'natural' substrate of NovO, **3** could be converted by 96%. This again indicates the high similarity of both enzymes. Biochemical characterization of CouO was done with the purified enzyme (Figure 42 D). Therefore, analogue to the purification of NovO (Section 4.6), a C-terminally Strep tagged version was constructed and purified. The Strep tagged CouO protein could not be produced at the same high amount as was observed for the untagged version. Several attempts were made to increase the production rate by varying the expression temperature, time, and addition of inducer. These experiments did not lead to a better protein production. The use of an autoinduction medium came up to our expectations by a recognizable increase of the soluble protein production (Section 4.4.1, Figure 42 B and C). As expected the protein revealed a dimeric state in gel-filtration chromatography (Figure 43). The 'natural' substrate coumarinpyrrolamide **5** had a K_m value of 0.064 mM and a k_{cat} value of $2.7*10^{-3}$ s^{-1}, whereas the non-natural substrate 2,7-dihydroxynaphthalene **7** showed a much lower affinity with a K_m value of 0.26 mM. The k_{cat} value of $6.2*10^{-3}$ s^{-1} is much higher due to the acceptance of higher substrate concentrations (Figures 44, and 45). The kinetic data for CouO correlate with the ones obtained for NovO, showing higher affinities for their 'natural' substrates **5** and **3** compared to the unusual **7**. Also the turnover numbers towards 2,7-dihydroxynaphthalene **7** were higher for both enzymes (Table 3). The remarkable differences in K_m values of 2,7-dihydroxynaphthalene **7** of NovO and CouO could be due to different assay conditions concerning DMSO concentration. It was observed that higher DMSO concentrations shift the Michaelis-Menten graph to the right, yielding higher K_m values. This is obvious concerning the K_m of 2.5 mM for NovO and **7** obtained with constant 5 % of DMSO and the K_m of 0.26 mM for CouO and **7** obtained with DMSO concentrations from 0.02 % (at 0.02 mM substrate) to 1.5 % (at 1.5 mM substrate).

Table 3: Kinetic parameters for selected substrates of NovO and CouO.

enzyme	substrate	K_m [mM]	k_{cat} [s^{-1}]	k_{cat} / K_M [$M^{-1}*s^{-1}$]
NovO	coumarinbenzamide **3**	0.036	$5.2*10^{-4}$	14
NovO	2,7-dihydroxynaphthalene **7**	2.5	$3.7*10^{-3}$	1.5
CouO	coumarinpyrrolamide **5**	0.064	$2.7*10^{-3}$	42
CouO	2,7-dihydroxynaphthalene **7**	0.26	$6.2*10^{-3}$	24

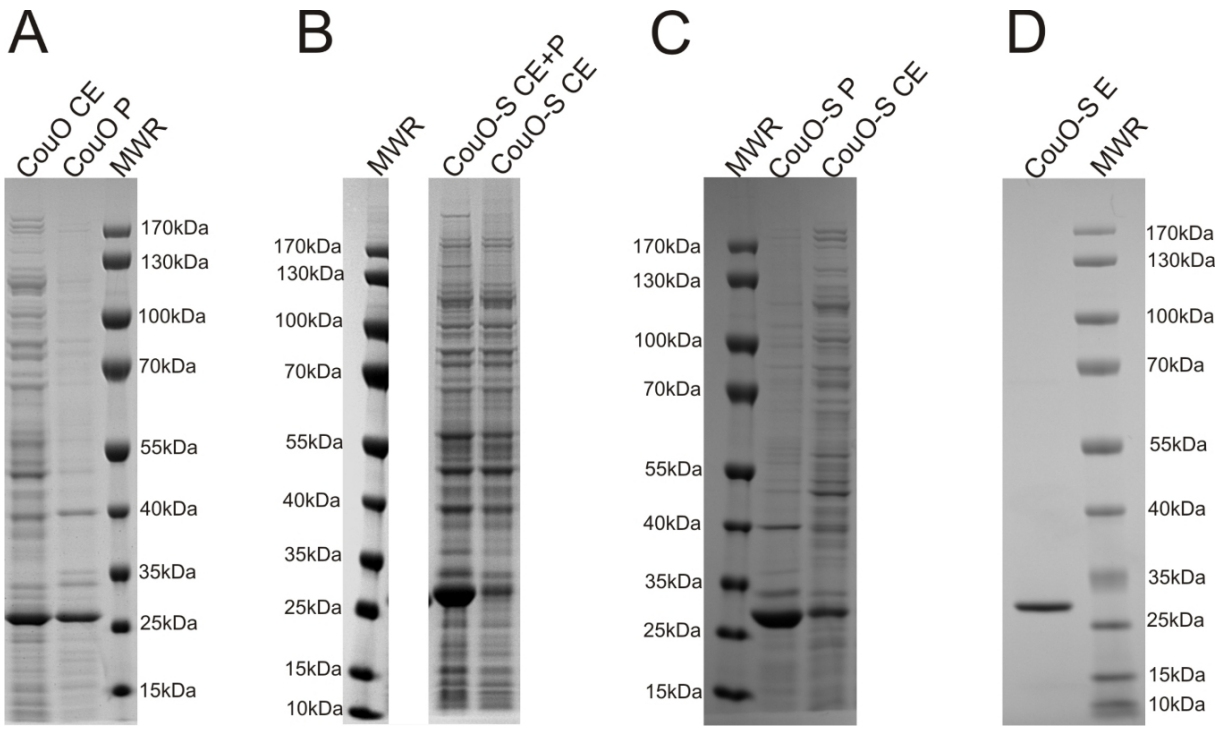

Figure 42: 4-12 % SDS-polyacrylamide gel of heterologous protein expression in *E. coli* BL21 Gold (DE3). CE: cleared lysate, P: resuspended pellet, CE+P: total crude extract, E: purified protein, CouO: CouO expression, CouO-S: Strep-tagged CouO expression. **A**: The strong overexpression of soluble CouO (25.7 kDa) is clearly visible in lanes 1. **B**: CouO-S expression in LB-Lennox medium. Only small amounts of soluble CouO-S (26.8 kDa) were produced compared to a strong formation of insoluble proteins. **C**: CouO-S expression in autoinduction medium. A considerable increase of soluble CouO-S is shown in lane 3. **D**: Purified CouO-S. The high purity of the eluted fraction is clearly visible in lane 1 at the expected size of 26.8 kDa, where 500 ng protein was loaded.

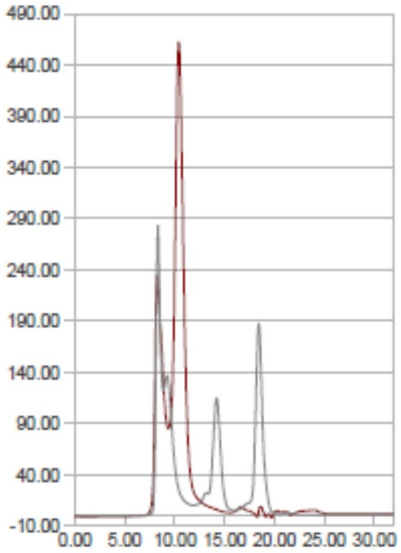

Figure 43: Gel-filtration chromatography of purified CouO-S protein on a Superdex 75 HR 10/30 column. The peak at approximately 10 ml corresponds to a dimeric state of CouO-S (red line) compared to a molecular weight marker (black line).

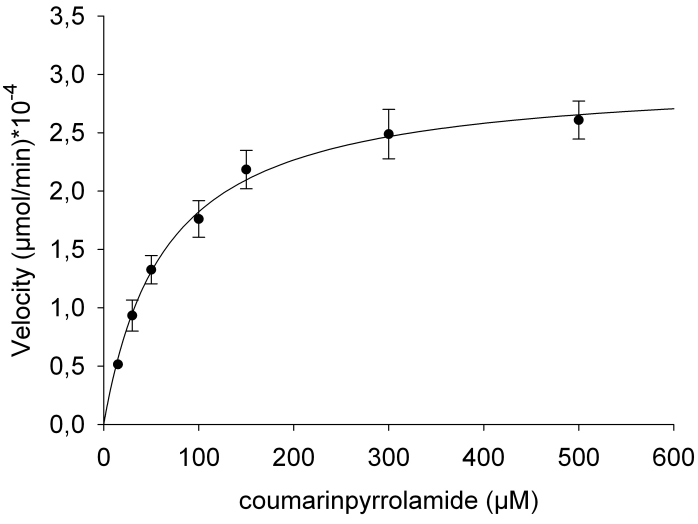

Figure 44: Michaelis-Menten graph of CouO-Strep methylation of substrate coumarinpyrrolamide at constant SAM concentration. Determined parameters K_{m} value of 0.064 mM and V_{max} value of $3*10^{-4}$ μmol/min.

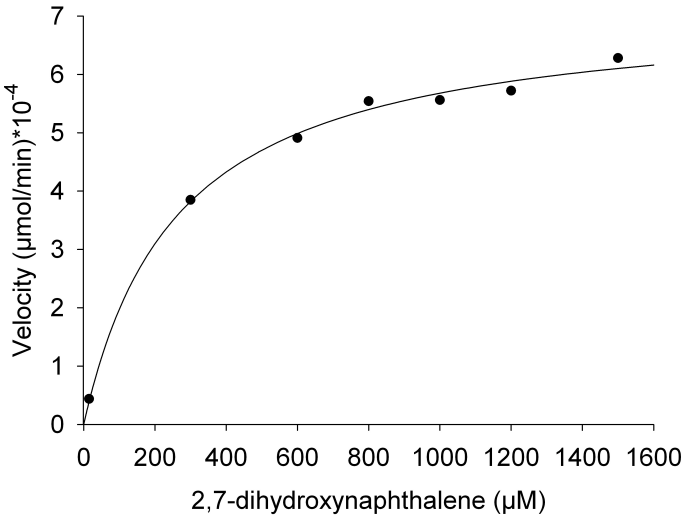

Figure 45: Michaelis-Menten graph of CouO-Strep methylation of substrate 2,7-dihydroxynaphthalene at constant SAM concentration. Determined parameters K_{m} value of 0.263 mM and $V_{\max}$ value of 7*10^{-4} μmol/min.

The stability of CouO turned out to be a critical point in terms of storage and temperature conditions, in about the same manner as described for NovO in Tengg *et al.*, 2011 (Section 2.2). As mentioned above it was observed that CouO was totally inactivated above 44 °C. Freezing and subsequent thawing of crude lysates decreased enzyme activity drastically, leading to precipitation and inactivation. Due to the fact that NovO consists of four, and CouO of three cystein residues, and the observation of a dimeric state in gel-filtration chromatography (Figure 43) the possibility of disulfide bond formation or oxidation of cysteins had to be investigated. NovO has one additional cystein at position 145. The incubation of the reaction mixtures under oxidative compared to reductive conditions did not affect enzyme activities (Figure 46). Rather, a strong decrease in activity could be observed if the enzymes were incubated under the same conditions prior to addition of substrates (Figure 46). From these data it can be concluded that the state of the cystein residues does not play any role in the activity of the enzymes. Pre-incubation of the enzymes under assay conditions drastically decreases their activities, which support the mentioned instability at elevated temperature.

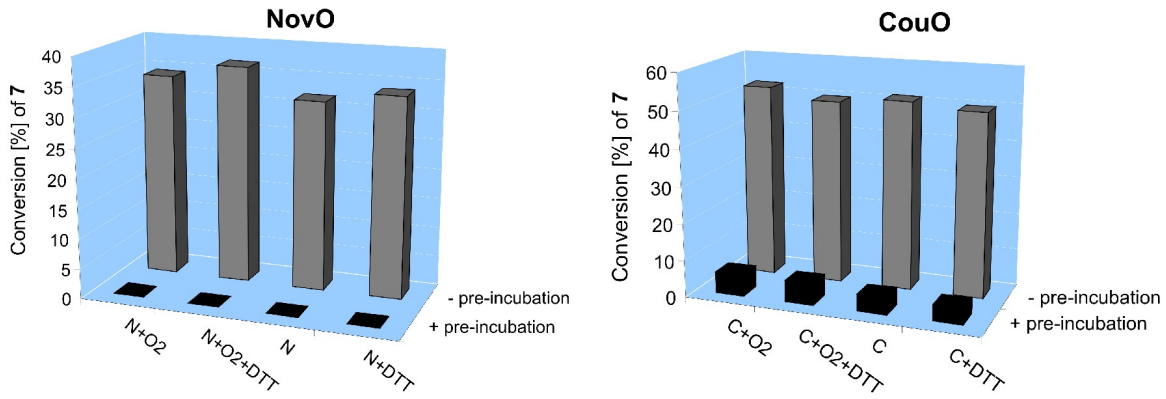

Figure 46: Influence of oxidative and reductive conditions on the activity of NovO (N) and CouO (C). Gray bars represent enzyme activities without pre-incubation under assay conditions. Black bars show enzyme activities after pre-incubation prior to substrate addition. N/C + O_2: great oxygen supply; N/C + O_2 + DTT: great oxygen supply, addition of reducing agent; N/C: low oxygen supply; N/C + DTT: low oxygen supply, addition of reducing agent; y-axes: conversionrate of 2,7-dihydroxynaphthalene **7**.

2.3.2 Tyrosine methylating enzymes

SacF The codon optimized and synthesized gene *sacF* of *Pseudomonas fluorescence A1* [44] was heterologously expressed in *E. coli* cells (Figure 50). The amount of soluble SacF was in the range of constitutively expressed *E. coli* proteins and was quantified to 6 % of total soluble protein amount. The small amount was not due to the formation of inclusion bodies, because there was no increased amount present in the insoluble fraction. In order to improve the production of SacF protein the mRNA secondary structure was analyzed in detail concerning the formation of long stem structures. It was found that a long stem formation occurs with a free energy of -28.5 kcal/mol which could effect translation efficiency negatively. An optimal translation reaction can only be achieved if the energy of stems is beyond -20 kcal/mol. In order to solve this problem mutants were created with base exchanges in selected regions of the coding sequence, which lead to a more relaxed secondary structure of the mRNA. There were two regions found, one located close to the start codon (base 87 to base 100), and the other one close to the stop codon of *sacF* (base 1043 to base 1056). On one hand the sequence 5'-GCCATGCGGCGT-3' was exchanged to 5'-GTCACGCTGCAT-3' (*sacFXN*), and on the other hand the sequence 5'-ACGCCGCATGGC-3' was exchanged to 5'-ACTCCGCACGGT-3' (*sacFXC*). The re-

sultant *sacF-variants* were analyzed for improved protein production. Another attempt, to increase the production of SacF, was the use of other *E. coli* strains.

Unfortunately, neither the improvement of the mRNA secondary structure, nor the use of other strains could increase the protein production (Figure 47, 48, 49). When Figure 50 is compared to Figure 47 one can see that the amount of soluble SacFXN is less than that of SacFXC and SacF, which were produced to approximately the same amount. This observation is supported by Figure 48 where lysates of *E. coli* BL21 Gold (DE3) were analyzed for comparison to other strains. The decreased amount of soluble SacFXN can be observed in all analyzed strains. Moreover transformation of pET26b(+)-sacFXN into *E. coli* BL21 Star (DE3) resulted in the formation of unequal colony size. There were two morphologies obvious, one of normal size and the other of small size. The fermentation of a normal size colony resulted in no protein formation. In contrast when a small size colony was picked, SacFXN could be produced to about the same amount as SacF and SacFXC (Figure 48 and 49). The same phenomenon was observed if *E. coli* K12 HMS174 (DE) was used as expression host, but with the result of even less protein production (Figure 49). The formation of smaller colonies could be a result of heterologous protein production, because in general the overexpression of heterologous genes leads to impaired cell division. This hypothesis is supported by the fact that in case of *E. coli* BL21 plysS (DE3) only normal size colonies were formed after transformation, which led to no SacF production (Figure 49). This strain has the advantage of a strong promoter repression under non induced conditions. *E. coli* Rosetta (DE3) could not enhance *sacF* expression, indicating that certain tRNA does not support the production of SacF. Again SacFXN was not produced at all (Figure 48). The use of the exotic *E. coli* Arctic Express (DE3) led to no detectable SacF production (Figure 49). The chaperon Cpn60, which enables protein folding at low temperatures, is clearly visible on the SDS-PAGE.

Nevertheless the enzyme was highly active on several substrates. L-tyrosine **11** was converted to yield 87 % 3'-methyl-L-tyrosine **12** (Figure 38). The enantiomer D-tyrosine was methylated to 64 %. It was also possible to methylate the racemate DL-tyrosine, and even L-DOPA.

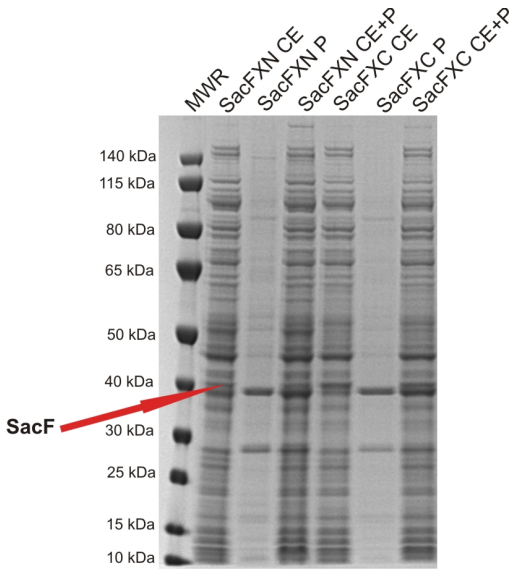

Figure 47: 4-12 % SDS-polyacrylamide gel of SacF-variants expression in *E. coli* BL21 Gold (DE3). CE: cleared lysate, P: resuspended pellet, CE+P: total crude extract. SacFXN: variant with exchanges near the N-terminus. SacFXC: variant with exchanges near the C-terminus. The band representing SacF is indicated with a red arrow for lysate of SacFXN. In the other lanes the band of SacF appears at the same position.

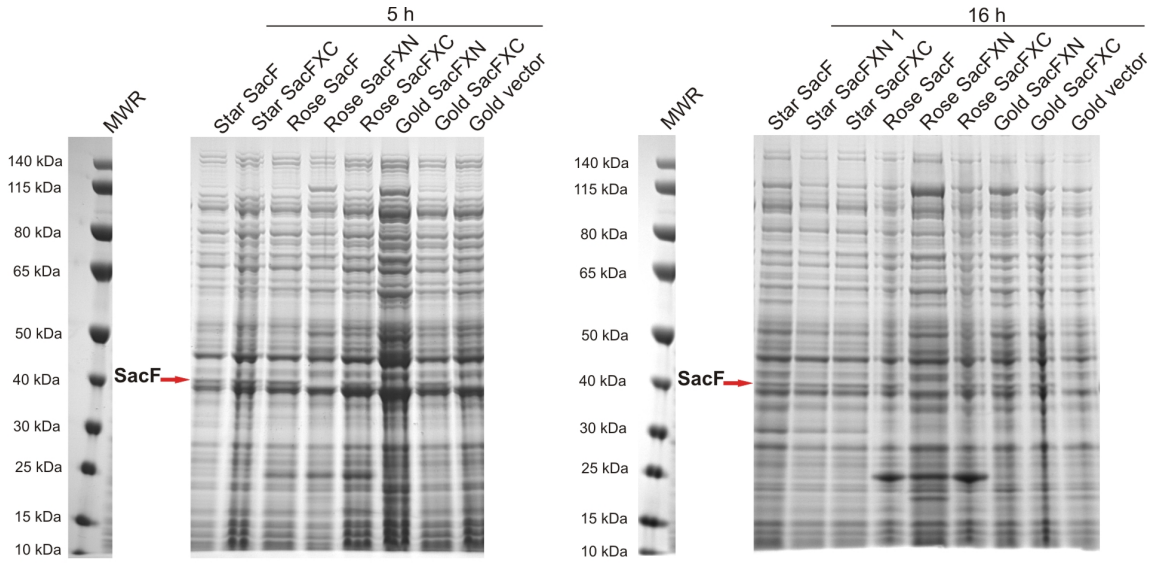

Figure 48: 4-12 % SDS-polyacrylamide gel of SacF-variants expression in different *E. coli* strains. Total crude extracts of SacF, SacFXN, SacFXC, and empty expression vector pET26b(+) were loaded. Star: *E. coli* BL21 Star (DE3), Rose: *E. coli* Rosetta (DE3), Gold: *E. coli* BL21 Gold (DE3), 1: normal size colony. The position of the band corresponding to SacF is indicated with a red arrow.

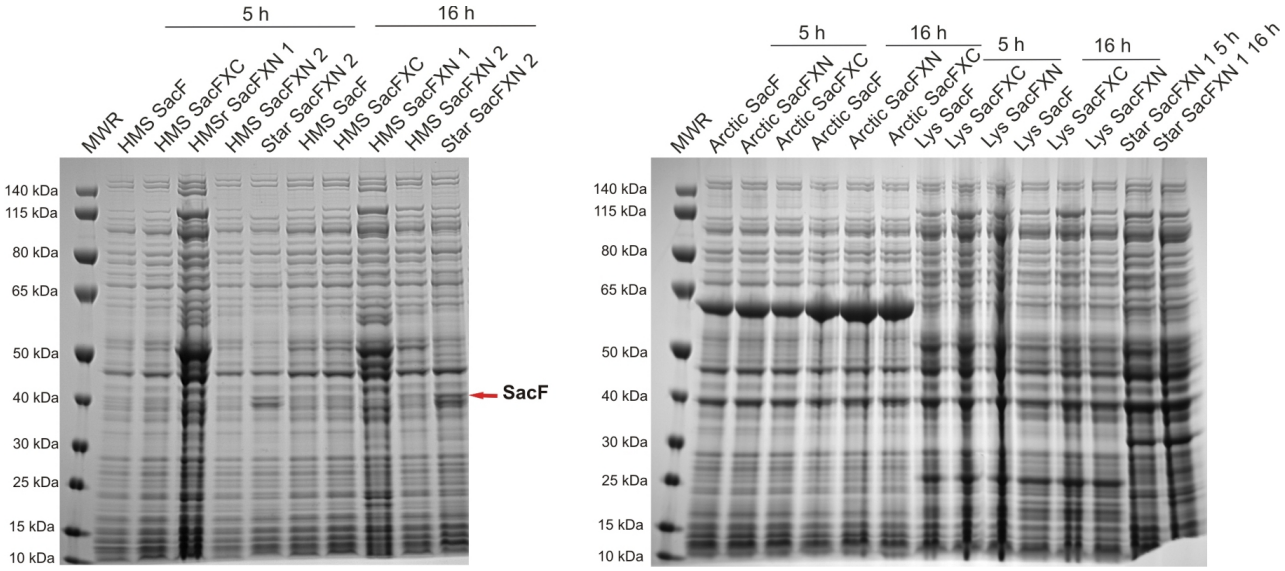

Figure 49: 4-12 % SDS-polyacrylamide gel of SacF-variants expression in different *E. coli* strains. Total crude extracts of SacF, SacFXN, and SacFXC were loaded. Extracts were prepared after 5 or 16 hours. HMS: *E. coli* K12 HMS174 (DE3), Star: *E. coli* BL21 Star (DE3), Arctic: *E. coli* Arctic Express (DE3), Lys: *E. coli* BL21 plysS (DE3), 1: normal size colony, 2: small size colony. The position of the band corresponding to SacF is indicated with a red arrow. The prominent band at about 60 kDa corresponds to Cpn60.

SfmM2 The expression of the codon optimized and synthesized *sfmM2*, the methyltransferase of *Streptomyces lavendulae* [45], resulted in a strong overproduction of soluble protein (Figure 50). Hence, it was not problematic that great amounts of insoluble protein were produced as well. The protein was tagged on its C-terminus with the Strep Tag II to facilitate fast and clean protein purification. The purification yielded great amounts of highly pure enzyme (Figure 50). SDS-PAGE analysis under non reductive conditions suggests a dimeric state of the protein (data not shown). SfmM2 accepted the same substrates as SacF, but with lower conversion rate. 65 % of L-tyrosine and 24 % of D-tyrosine were methylated. As SacF is only present in small amounts in the analyzed lysate (6 %) compared to big amounts of SfmM2 (29 %), the turnover number of SacF is higher.

2.3.3 Hydroxykynurenine methylating enzymes

Orf19 The codon optimized version of *orf19* was successfully overexpressed in *E. coli*, resulting in an impressive amount (60 % of the cleared lysate, Figure 50) of soluble protein. The enzyme did not accept 3-hydroxyanthranilic acid, but was able to convert up to 51 %

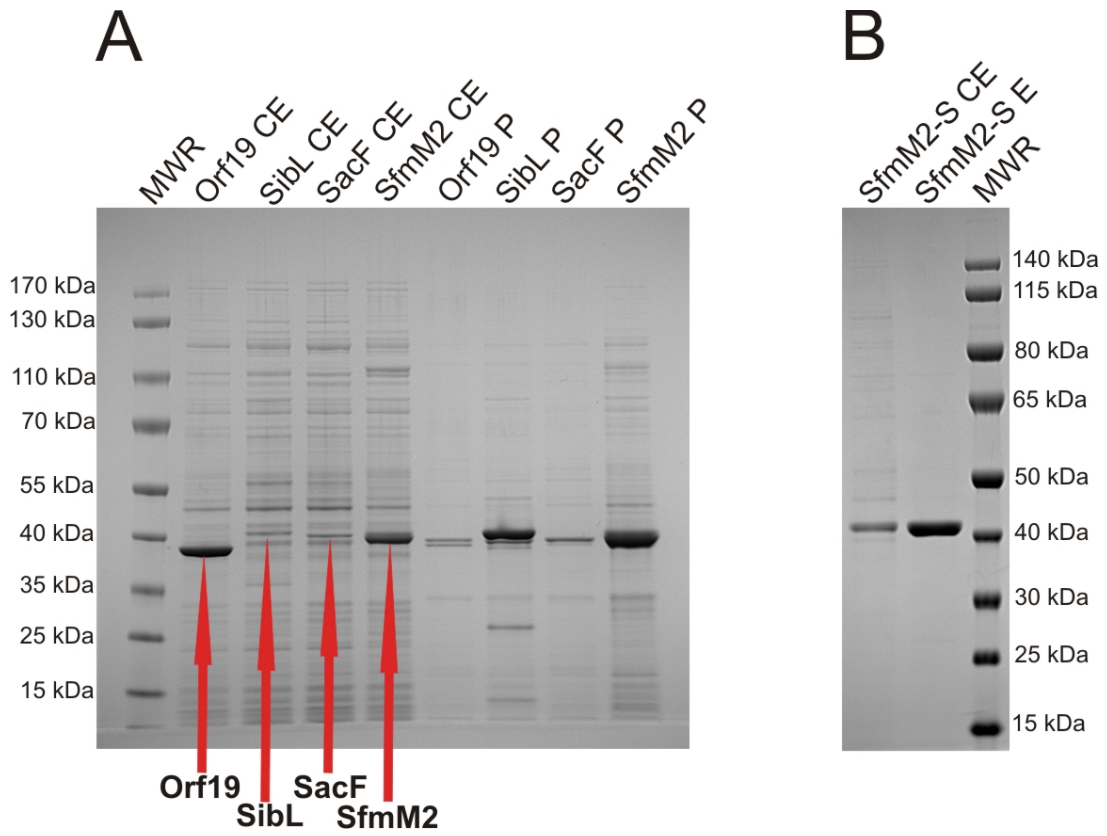

Figure 50: 4-12 % SDS-polyacrylamide gel of heterologous protein expression in *E. coli* BL21 Gold (DE3). **A:** CE: cleared lysate of Orf19 (38.4 kDa), SibL (38.8 kDa), SacF (39.8 kDa), SfmM2 (39.9 kDa), P: resuspended pellet of Orf19, SibL, SacF, SfmM2. **B:** CE: cleared lysate of SfmM2-Strep, E: purified fraction of SfmM2-Strep (41.2 kDa). The high purity is clearly visible in lane 2, compared to crude lysate in lane 1. One μg of the 41.2 kDa protein was loaded on the gel.

of a racemic mixture of 3-hydroxykynurenine **9** (Figure 38). The fact that more than 50 % of the racemate could be converted, demonstrates the ability of the enzyme to accept both enantiomers as substrates. Little activity was observed for L-tyrosine **11** (3 %), D-tyrosine (1 %), and L-DOPA (1 %). The acceptance of both enantiomers of 3-hydroxykynurenine and tyrosine is striking, considering the findings of of Crnovčić *et al.*, 2010 [117] obtained with similar enzymes.

SibL The biosynthesis of sibiromycin shares several enzymatic steps with the biosynthesis of anthramycin, involving a methylation step of 3-hydroxyanthranilic acid or 3-hydroxykynurenine [121],[122]. The putative methyltransferase encoding gene *sibL* was codon optimized and synthesized. The cloned gene could be expressed in *E. coli*, but the amount of soluble protein was in the range of constitutively expressed *E. coli* proteins (6 % of the total lysate, Figure 50). Much more of the protein can be found in the insoluble fraction. SibL shows the same result as Orf19 in methylation of 3-hydroxykynurenine **9** (Figure 38), and no acceptance of 3-hydroxyanthranilic acid. The conversionrate of 10 % was significantly lower than that observed with Orf19.

The high sequence identity of described tyrosine-, and hydroxykynurenine methylating enzymes allows the guess of some functional similarities. The results describe the acceptance of tyrosine by the 3-hydroxykynurenine methylating enzyme Orf19. On the contrary, the tyrosine methylating enzymes could not convert 3-hydroxykynurenine. The structural difference of these compounds gives an explanation, meaning that 3-hydroxykynurenine consists of one more carbon and additional functional groups. SacF and SfmM2 are evolutionary designed for the acceptance of tyrosine, and therefore could exhibit too little space for the acceptance of 3-hydroxykynurenine.

Putative methyltransferases Early studies within this project dealed with a methyltransferase of *Streptomyces antibioticus*. The methylation of 3-hydroxyanthranilic acid reveals a step in the biosynthesis of actinomycins that has been described for *Streptomyces antibioticus* and *Streptomyces chrysomallus* [178],[179],[167],[118]. Although the activity of a methyltransferase that acts on 3-hydroxyanthranilic acid has been described in the mentioned literature, it was not possible to detect product formation with total

crude extracts of four different *Streptomyces antibioticus* strains (Table 10). Motivated by the described results obtained with the cloned methyltransferase Orf19 (Section 2.3.3), the genome of *Streptomyces antibioticus* and *Streptomyces chrysomallus* should be investigated towards a similar protein.

PCR search One approach was a direct PCR amplification of similar DNA fragments. In order to isolate this methyltransferase, a conserved domain of the protein sequence of Orf19 from *Streptomyces refuineus* was found. This domain refers to the cofactor binding motif I with the sequence D V G G G. Primer were designed to amplify the region of 150 bp upstream and downstream (Table 17 #17 and #18). A PCR fragment isolated by the

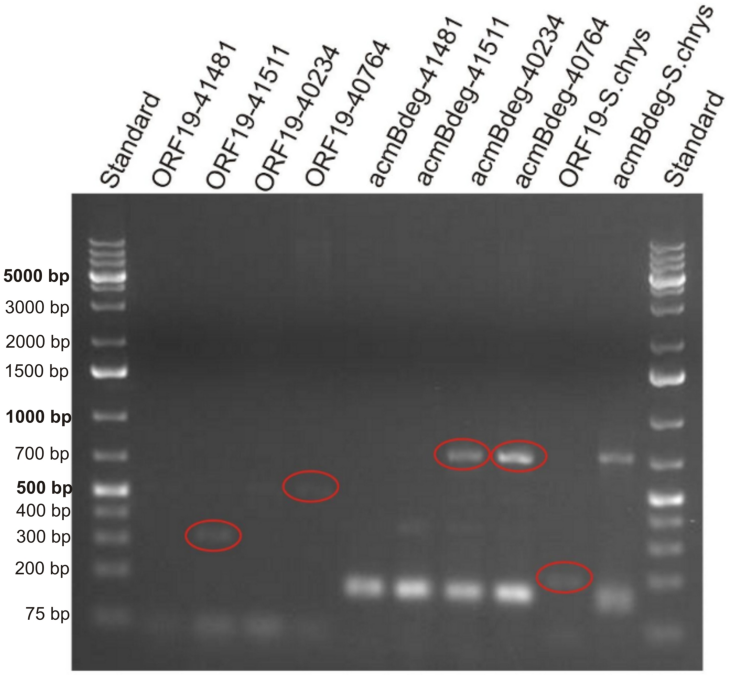

Figure 51: 1 % agarose gel for analysis of PCR to isolate a putative 3-hydroxyanthranilic acid methyltransferase encoding gene. Sequenced fragments are marked in red ellipses. ORF19 refers to the primer pair that bind 150 bp upstream and downstream of the conserved sequence domain of Orf19 (Table 17 #17 and #18). AcmBdeg refers to the degenerated primer pair that binds between two conserved sequence domains of AcmB (Table 17 #19 and #20). Numbers indicate the strain designation of *Streptomyces antibioticus*. S.chrys: *Streptomyces chrysomallus*.

use of genomic DNA from *Streptomyces antibioticus* 41511 showed 78 % sequence identity on DNA level and 100 % sequence identity on protein level with Orf19 from *Streptomyces*

refuineus (Figure 51, lane 3). This finding motivated us to use a genome walking strategy for isolation of the whole open reading frame. Beforehand another try was made for isolation of a larger fragment with a combinatorial use of primers that bind to the 5' and 3' regions of *orf19*. Unfortunately none of the used combinations resulted in the isolation of a fragment corresponding to a similar methyltransferase encoding gene. Another approach was to use the information that was available about the biosynthetic gene cluster of *Streptomyces chrysomallus* [108],[181] for isolation of similar genes in *Streptomyces antibioticus*. Two conserved domains were found in the *acmB* encoded actinomycin synthetase II (741-V V F G G E A L and 966-N G K L D R A A L). This enzyme is meant to act two steps after the methylation step in the biosynthesis of actinomycin. Degenerated primers were designed to amplify the region between these two domains (Table 17 #19 and #20). Two fragments, one obtained from *Streptomyces antibioticus* 40234 and one from *Streptomyces antibioticus* 40764 showed 80 % identity on DNA level and 75 % identity on protein level with AcmB of *Streptomyces chrysomallus* (Figure 51). Earlier attempts with the use of non-degenerated primers to isolate DNA fragments that share homology to *acmB*, *acmA*, or *acmD* did not bring promising results. Although several fragments could be isolated, none of them shared homology to the described genes.

Southern blot In order to continue the search of the methyltransferase from *Streptomyces antibioticus* southern hybridization experiments were performed. Therefore the conserved regions 178-D V G G G of Orf19, 144-S G S T G R P K of AcmA, and 618-S G S T G V P K of AcmB were used for the construction of Digoxigenin (DIG) labeled DNA-probes. On one hand the Orf19-probe was produced by the use of the obtained fragment from *Streptomyces antibioticus* 41511 (Figure 51) and designated probe-SaHAA. On the other hand the synthetic DNA of *orf19* was used as template for the construction of probe-Orf19. Probe-AcmA and probe-AcmB were constructed with the use of genomic DNA from *Streptomyces chrysomallus*. Hybridization was done with genomic DNA of the four *Streptomyces antibioticus* strains and *Streptomyces chrysomallus*. As a positive control the synthetic DNA of *orf19* was used. In order to determine the sensitivity of the chromogenic detection, dilutions of *orf19* DNA were blotted, and could be detected with probe-Orf19. The lowest detectable amount was 30 pg of digested pGA4-ORF19 DNA. As the detected *orf19* represents one fourth of the whole vector DNA, the limit

has to be designated to 7.5 pg DNA of a 1 kb DNA fragment (Figure 52). Hybridization of this probe with DNA of *Streptomyces chrysomallus* or *Streptomyces antibioticus* did not lead to a detectable signal. This indicates that the coding sequence of Orf19 does not share high similarity with DNA of the analyzed strains. In contrast, the use of probe-SaHAA led to one (41481) or two (41511, 40234, 40764) specific signals with blotted DNA of all *Streptomyces antibioticus* strains, but no hybridization with DNA of *Streptomyces chrysomallus*. As expected *orf19* gave a clear signal (Figure 53, panel B). These findings support the results of the above described isolation of a DNA fragment of *Streptomyces antibioticus* 41511 (Figure 51). Probe-AcmA and probe-AcmB led to specific signals with genomic DNA of *Streptomyces chrysomallus*, but no signal with *Streptomyces antibioticus* DNA (Figure 53, panel C, D). DNA of *orf19* gave signals at about the same intensity, but they were much weaker than the ones observed with the specific probes probe-Orf19 and probe-SaHAA. As no bands could be detected in other lanes, and the fact that probe-AcmA, and probe-AcmB detected different fragments, the reliability of a specific detection is proven. These data indicate limited sequence similarity of respective strains. The fact that specific signals could be obtained with probe-AcmA and probe-AcmB on digested DNA of *Streptomyces chrysomallus* shows that the digestion of the analyzed DNA was done in a proper way and that hybridization of related fragments leads to specific signals.

Genome walking The results of the PCR search prompted us to use the obtained information for a genome walking strategy. The principle of this method is to use a known coding sequence for further identification of neighboring regions. In our case the fragment obtained from the PCR of genomic *Streptomyces antibioticus* 41511 DNA, that shares high sequence identity with *orf19* (Figure 51), was used as sequence template. Nested PCR of genome libraries yielded several fragments, which were sequenced (Figure 54). Unfortunately BLAST analysis showed no homology to methyltransferases. Not even the sequence of the gene specific primers (GSP) were part of the cloned fragments. This indicates that the GSP did bind to unspecific regions of the genome library, and therefore led to the amplification of fragments, which are not located next to the template fragment. Another third PCR with further nested primers could not increase specificity, and therefore was not analyzed for sequence determination. Control PCR reaction resulted in

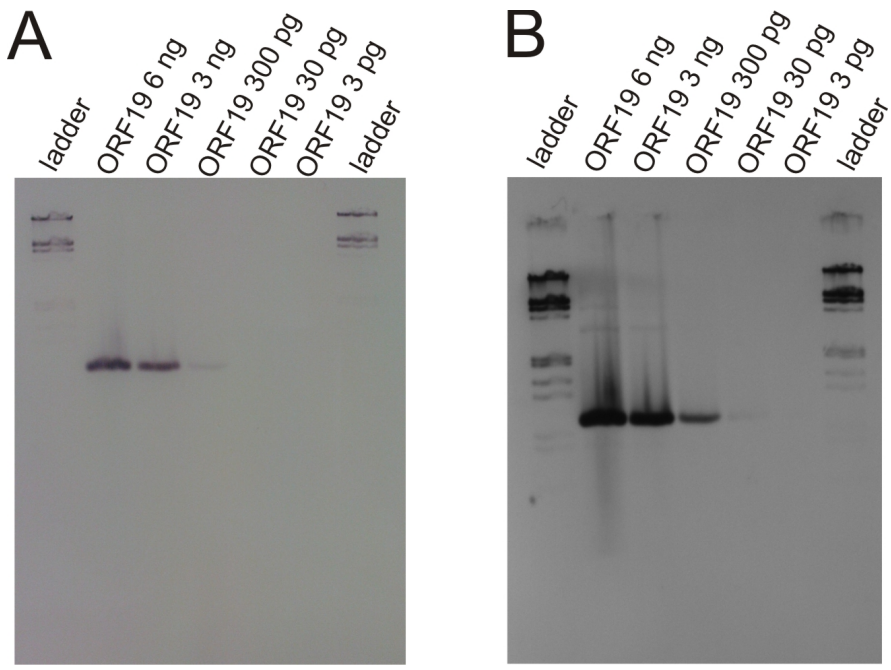

Figure 52: Southern blot for determination of the detection limit. Five dilutions of pGA4-ORF19, digested with *NdeI* and *HindIII* to yield *orf19* and vector backbone, were blotted. Ladder: molecular weight marker of DIG-labeled fragments. Photographs taken after 10 minutes **A** and 16 hours **B** of incubation with the chromogenic substrate.

an expected fragment at 1.5 kb, which proves the used PCR conditions and the adapter primers.

In summary, the results obtained from the described experimental setups, show that *Streptomyces chrysomallus* and *Streptomyces antibioticus* do not share very high sequence similarity concerning their biosynthetic gene cluster for actinomycin production. The PCR search with the use of degenerated primers for amplification of a region between highly conserved domains 741-V V F G G E A L and 966-N G K L D R A A L was successful, but in contrast the hybridization with the use of probes that involve the conserved domains 144-S G S T G R P K (AcmA) or 618-S G S T G V P K (AcmB) did not lead to a detection. It seems that there is some, but limited similarity between the two species. This finding is somewhat surprising due to the production of the same antibiotic. Although the CDS of a methyltransferase could not be identified, the similarity of Orf19 to a putative methyltransferase of *Streptomyces antibioticus* is undeniable.

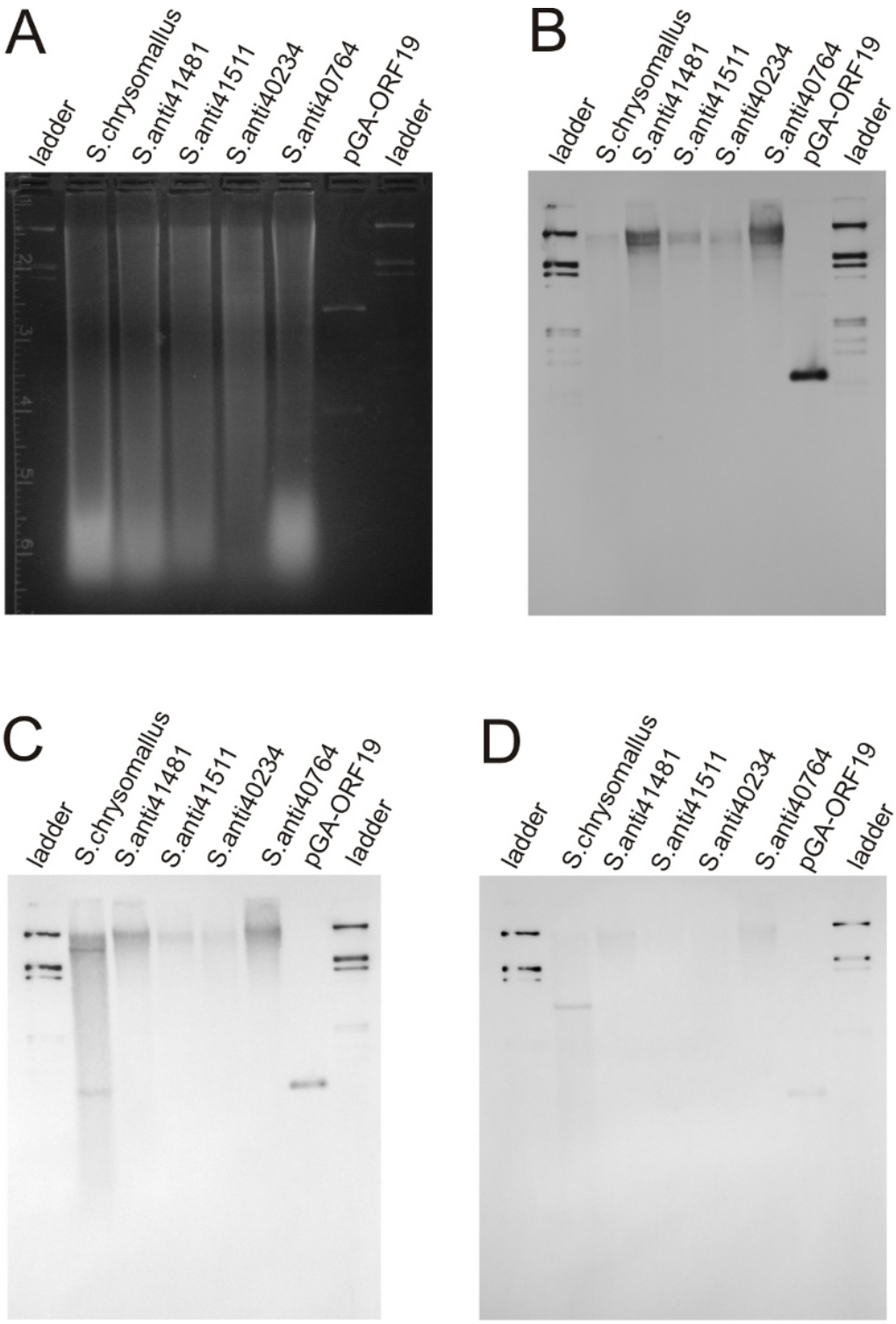

Figure 53: Southern blot for identification of similarities between *Streptomyces chrysomallus* and *Streptomyces antibioticus* 41481, 41511, 40234, 40764. Digested pGA4-ORF19 served as control. Ladder: molecular weight marker of DIG-labeled fragments. **A**: 1 % agarose gel for separation of digested genomic DNA and vector DNA. **B**: Hybridization with probe-SaHAA. **C**: Hybridization with probe-AcmA. **D**: Hybridization with probe-AcmB.

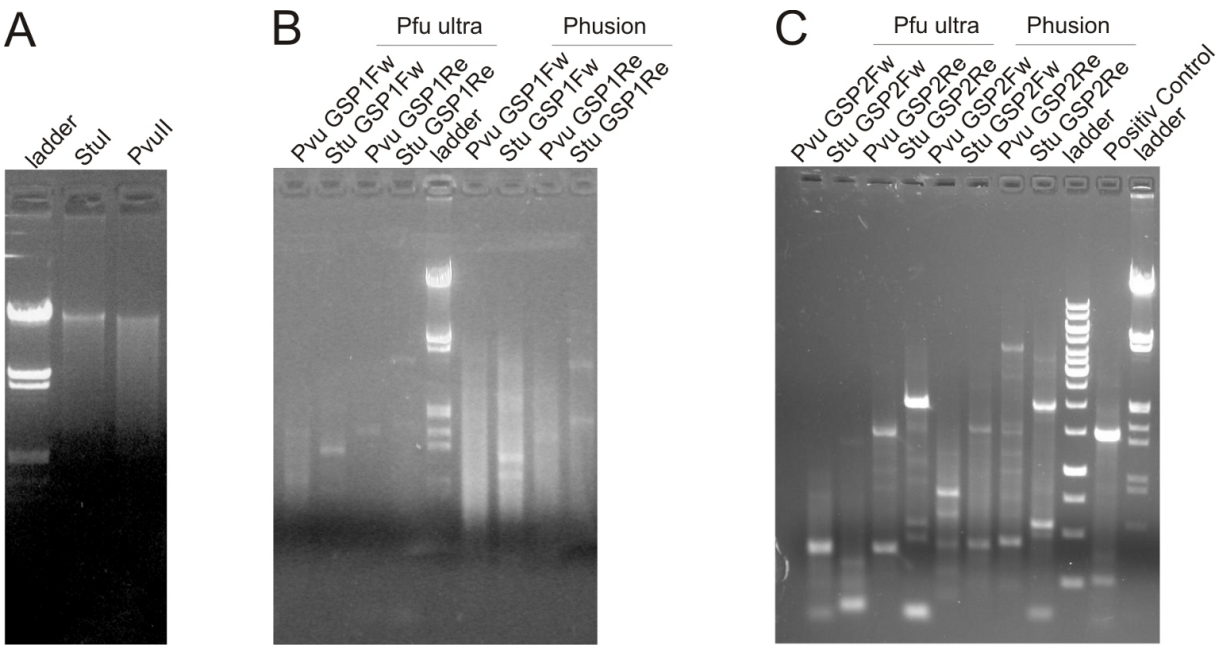

Figure 54: Genome walking procedure of *Streptomyces antibioticus* 41511 analyzed on 1% agarose gels. **A**: Digested genomic DNA of *Streptomyces antibioticus* 41511 with blunt end cutters *PvuII* and *StuI*. Ladder: λ-DNA digested with *EcoR1* and *HindIII*. **B**: Primary PCR of *PvuII*- and *StuI*-libraries with forward (Fw) or reverse (Re) gene specific primers 1 (GSP1), and adapter primer 1. Ladder: λ-DNA digested with *EcoR1* and *HindIII*. **C**: Secondary (Nested) PCR of corresponding products of the primary PCR with forward (Fw) or reverse (Re) gene specific primers 2 (GSP2), and adapter primer 2. Ladder: λ-DNA digested with *EcoR1* and *HindIII*; 1 kb DNA ladder. All PCRs were done with the DNA polymerases Pfu Ultra Hotstart or Phusion. Positive control proves the PCR conditions, yielding the expected fragment at 1.5 kb.

2.3.4 Tryptophan methylating enzymes

Heterologous expression of the cloned genes *tsrM*, *trsP*, and *sioF* yielded different amounts of soluble and insoluble protein (Figure 55). TsrM was only present in the insoluble fraction, but to a high extend. TsrP could be produced soluble to a moderate quantity. No band could be identified, which corresponds to SioF, neither in the soluble and nor in the insoluble fraction. Furthermore, no difference was observed concerning induced (+ IPTG) or leaky expression. Unfortunately none of the enzyme preparations (crude extracts, cleared lysates, resuspended pellets) showed any activity towards methyl transfer reaction on tryptophan.

In contrast, 2-methyltryptophan could be detected by using whole cells and crude extracts of disrupted cells of the natural host organisms *Streptomyces azureus*, *Streptomyces laurentii*, *Streptomyces hawaiiensis*, and *Streptomyces sioyaensis*. Among these preparations whole cells of *Streptomyces azureus* showed the highest activity [182].

In order to obtain specific activity of the putative tryptophan methyltransferase, the enzyme should be detected and purified from its host *Streptomyces azureus*. As the results obtained with disrupted cells were below the ones obtained with whole cells, and no activity could be detected with cleared lysates, the preparation of lysates had to be optimized. Therefore a lysis buffer described by Frenzel *et al.*, 1990 [132], which includes glycerol, EDTA, β-mercaptoethanol, and protease inhibitor was used for sonication. Another strategy was the use of lysozyme treatment, and the addition of detergents in order to stabilize the membrane associated enzyme.

Some activity could be detected in the cleared lysate after sonication (LS) using the lysis buffer described by Frenzel *et al.*, 1990 [132], but anyway the activity was below the conversion rate of whole cells (C) (Figure 56). Lysozyme cell disruption led to no active methyltransferase in the cleared lysate (LL), but moderate activity in the crude extract (EL). The addition of a detergent led to inactivation of the enzyme (LLD, ELD).

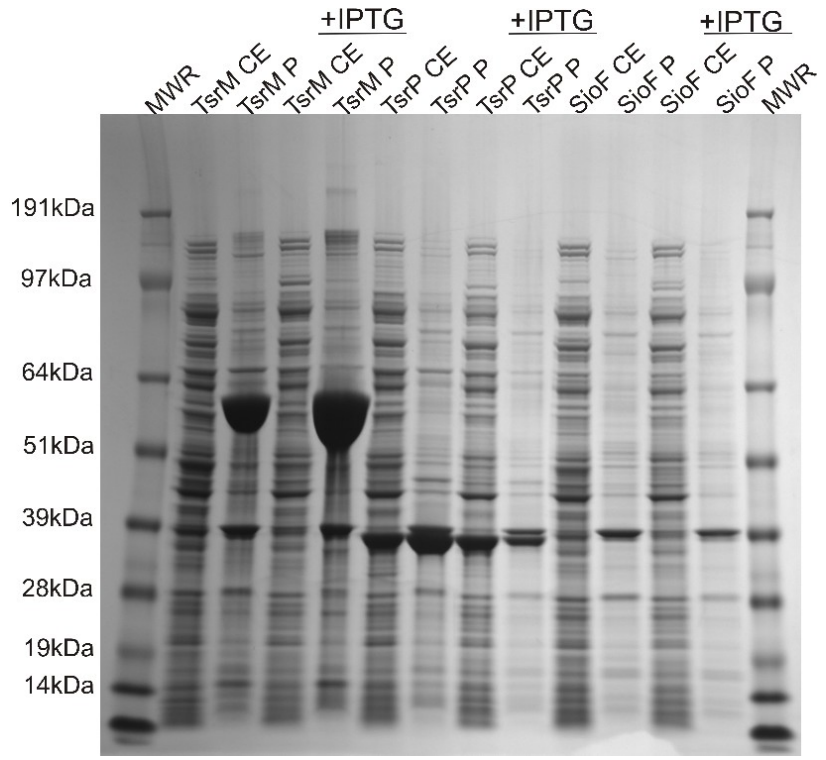

Figure 55: 4-12 % SDS-polyacrylamide gel of heterologous tryptophan methyltransferase expression in *E. coli* BL21 Gold (DE3). CE cleared lysate; P resuspended pellet; TsrM 67.3 kDa; TsrP 35.1 kDa; SioF 32.2 kDa; +IPTG indicates the induction of expression with 0.1 mM IPTG.

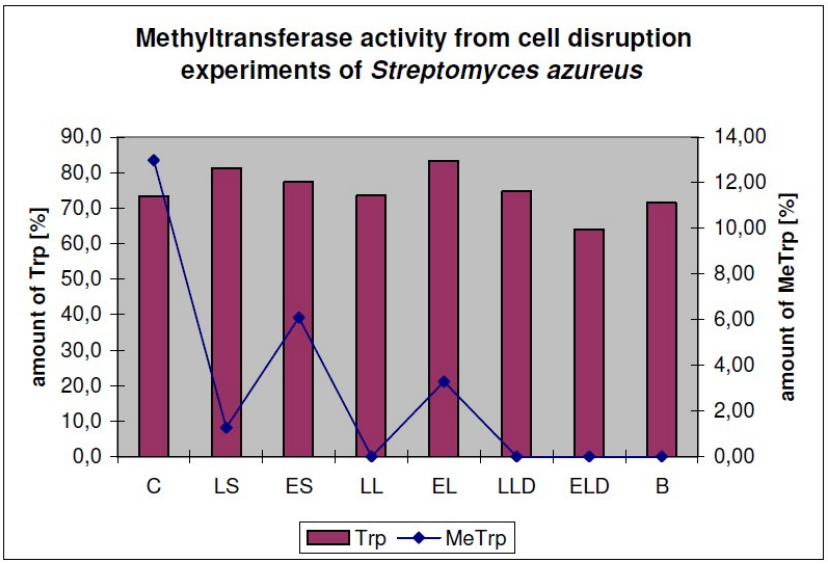

Figure 56: Methyltransferase activity on tryptophan using different cell disruption methods of *Streptomyces azureus*. Red bars represent the substrate-, and blue lines the product concentration after enzyme assay of 24 hours. C: whole cells; LS: cleared lysate of sonication; ES: crude extract of sonication; LL: cleared lysate of lysozyme treatment; EL: crude extract of lysozyme treatment; LLD: cleared lysate of lysozyme treatment including detergent; ELD: crude extract of lysozyme treatment including detergent; B: blank reaction.

2.3.5 Alkyltransferase activity

The described methyltransferases were investigated towards their activities to transfer other groups than methyl. The transfer of alkyl groups by NovO and CouO on various coumarin- **1** and naphthalene **7** substrates has been described previously [168]. The idea of an enzymatic equivalent to the Friedel-Crafts alkylation prompted us to test a possible alkyltransfer on described substrates 3-hydroxykynurenine **9** and tyrosine **10** by the enzymes Orf19, SibL, SacF, and SfmM2. Despite SibL all enzymes were able to transfer allyl-, butynyl-, and benzyl groups on selected substrates (Table 4).

These results show that the transfer of other alkyl groups than methyl is not restricted to the coumarin methylating enzymes NovO and CouO, but can also be performed by the methyltransferases SacF, SfmM2, and Orf19. It is noteworthy that these tyrosine- and 3-hydroxykynurenine methylating enzymes seem to contain a different structural organization. An indication for this hypothesis is the different localization of the conserved sequence motif I. Furthermore the 3DM software classifies SacF, SfmM2, and Orf19 in different subfamilies.

Table 4: Alkyltransfer catalyzed by selected methyltransferases. Activities are shown as conversion of substrates in percentages.

enzyme, substrate #	methyl	allyl	crotyl	propynyl	butynyl	benzyl
NovO, # **3**	>99	>99	42	99	41	40
NovO, # **5**	>99	96	30	35	28	24
CouO, # **3**	>99	>99	38	99	77	45
CouO, # **5**	96	42	11	11	-	21
Orf19, # **9**	51	17	-	-	13	3
SibL, # **9**	10	-	-	-	-	-
SacF, # **11**	87	73	-	-	31	19
SfmM2, # **11**	65	56	-	-	31	14

2.3.6 Whole-cell biotransformation

The disadvantage of SAM-dependent methyltransferases in terms of industrial application are the high costs. This is due to the complex production of SAM by the use of recombinant *Pichia pastoris* and *Saccharomyces cerevisiae* fermentation [183-185]. An approach which would not need the supply of costly SAM is desirable. Therefore the SAM production of the host cell, in our case *E. coli* should be used to supply the recombinant methyltransferase NovO with sufficient methyl-donor. This goal can be achieved by addition of substrate to a suspension of living cells. Results are presented in Table 5. Fermented *E. coli* cells harboring pET26b(+)-novO could methylate 67 % of 1 mM coumarinbenzamide **3** after 16 hours incubation, compared to a total conversion if two equivalents SAM were added. This high conversion rate prompted us to test for a time dependent conversion (Figure 57). The time course of methylation shows that in the first 30 minutes the substrate is methylated to the same extend, yielding 7 % product. Longer incubation leads to a higher degree of conversion in case of additional SAM, and a resulting steeper slope. Relative activity could be addressed to 0.4 μM/min compared to 1.1 μM/min if SAM was added. On the other hand, the conversion of the unusual 2,7-dihydroxynaphthalene **7** was only possible to 5 %, compared to 50 % when SAM was added. This low conversion of 2,7-dihydroxynahpthalene **7** without SAM supply could be due to a lower rate of cellular uptake. In contrast to the assay conditions with coumarinbenzamide **3**, which contained 10 % DMSO, the reactions with 2,7-dihydroxynaphthalene **7** did not contain any solvent, which could enhance influx of the substrate into the cells. In addition the lipophilic nature of coumarin compounds enables a rapid passage through the cell membrane. Positive controls of purified NovO-S yielded 48.6 % of 1-methyl-2,7-dihydroxynaphthalene **8** or 95.3 % of 8-methylcoumarinbenzamide **4**. All negative controls, cells with empty plasmid and incubation of substrate without any cells, led to no detectable product.

The ability of viable recombinant *E. coli* cells to methylate the substrate coumarinbenzamide **3** to a high degree is striking. A methylation without the need of costly cofactor is possible. Of course limitations are the efficiency of cellular uptake, which have been observed for 2,7-dihydroxynaphthalene. Nevertheless this can be overcome by simple addition of organic solvents. Another restriction is the limitation to transfer methyl-, but no

Table 5: Methyltransferase activity by whole-cell catalysis. Viable *E. coli* cells harboring the empty expression plasmid pET26b(+), or the methyltransferase expression plasmid pET26b(+)-novO were analyzed towards their enzymatic activities on 2,7-dihydroxynaphthalene **7** and coumarinbenzamide **3**.

substrate #	plasmid	cofactor	conversion %
7	pET26b(+)-novO	2 mM SAM	49.2
7	pET26b(+)-novO	1 mM SAM	34.9
7	pET26b(+)-novO	-	4.9
7	pET26b(+)	2 mM SAM	0.0
7	pET26b(+)	1 mM SAM	0.0
7	pET26b(+)	-	0.0
3	pET26b(+)-novO	2 mM SAM	100
3	pET26b(+)-novO	1 mM SAM	100
3	pET26b(+)-novO	-	67.3
3	pET26b(+)	2 mM SAM	0.0
3	pET26b(+)	1 mM SAM	0.0
3	pET26b(+)	-	0.0

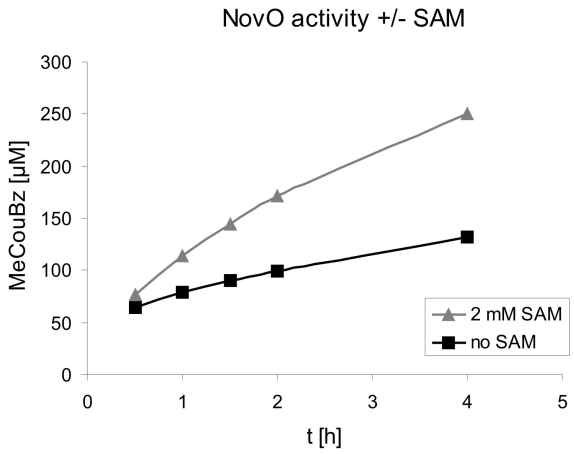

Figure 57: Time course of methylation reaction of coumarinbenzamide 3 by incubation with viable cells. Product formation of methylated coumarinbenzamide **3** (MeCouBz) is plotted against incubation time. 2 mM of SAM supply yields a relative activity of $11*10^{-5}$ μmol/min compared to $4*10^{-5}$ μmol/min if no methyldonor was added.

other alkyl groups. Cell engineering with focus on the adjustment of the SAM pathway towards the biosynthesis of SAM analogues could pave the way for a cellular alkylation.

2.3.7 Alternative Cofactors for methyltransferases

NovO and CouO Another approach to overcome the dependence on costly SAM would be the use of cheap and commercially available alkyl donors. Trimethylsulfonium (Me3S) (Figure 8), trimethylsulfoxonium (Me3S=O) and S-methyl-L-methionine (SMM) halides were used for enzymatic methylation of coumarin derivatives. Total cell extracts of *E. coli* cells expressing Strep-tagged NovO or Strep-tagged CouO showed a methylation activity with the use of these alternative cofactors [182]. Therefore it should be tested if this can also be observed by the use of purified enzymes. Also the influence of additional SAH should be investigated. This was done to clarify a possible transmethylation reaction of SAH by the used sulfonium salts. Therefore 0.5 or 0.1 substrate equivalents of SAH were added to the reactions. The results presented in Table 6 compare the conversion

Table 6: Conversion rates of coumarinbenzamide 3 by Strep-tagged NovO with the use of different cofactors. Three different conditions were tested in order to clarify the influence of SAH.

	conversion %		
cofactor	no SAH	0.5 eq. SAH	0.1 eq. SAH
SAM	52.5 ± 11.5	20	35
SMM	0.5 ± 0.1	0	0.3
Me3S	0.5 ± 0.1	0	0.3
Me3S=O	0.4 ± 0.1	0	0.3
none	0.45 ± 0.15	0	0.3
control	0	0	0

rates obtained at different SAH concentrations. Very little activity of Strep-tagged NovO can be detected by the use of an alternative or even no cofactor. No increase of activity was detected, if alternative cofactors were used instead of water. The addition of 0.5 equivalents SAH decreased the activity observed with SAM from 64 to 20 %. No product

formation was measured in the presence of 0.5 equivalents SAH together with an alternative cofactor, not even if no donor was present. This finding verifed that SAM is not bound to the enzyme, but more likely in solution or bound non-covalentely, because SAH displaced SAM. The addition of 0.1 equivalents of SAH decreased the activity observed with SAM from 41 to 35 %, which was less inhibition compared to the addition of 0.5 equivalents SAH. The same conversion rates were measured in the presence of 0.1 equivalents SAH together with an alternative cofactor or no cofactor, indicating that SAM was not displaced by SAH molecules. Concerning Strep-tagged CouO the use of an alternative or no cofactor did not lead to product formation. It could be possible that NovO binds SAM more strongly than CouO. After purification procedure only bound cofactor remains in the final protein solution. The inhibition rate of SAH is at about the same level as measured for Strep-tagged NovO. The addition of 0.5 equivalents SAH decreased the conversion rate from 49.6 ± 0.2 % to 23.6 %. If 0.1 equivalents SAH were present, still 45.3 % of coumarinpyrrolamide **5** could be methylated.

It can be concluded that higher amounts of SAH can displace SAM from the enzyme, and that SAM is not bound covalently. The addition of alternative cofactors did not stimulate the methylation reaction. The used concentrations of SAH did not lead to transmethylation. Moreover background activity without addition of cofactor was not due to bound SAM in the enzyme, but to SAM that is present in the environment. The activity of Strep-tagged NovO without additional SAM in contrast to no activity of Strep-tagged CouO under the same conditions could be due to different binding efficiencies to SAM. But this could also be due to fermentation conditions and cellular SAM concentrations.

DNA-methyltransferases As an alternative to the investigated methyltransferases NovO and CouO, which use small molecules as substrates, DNA-methyltransferases should be investigated. Stimulated by the experiments done in the lab of Saulius Klimašauskas [186],[187],[23] it should be shown that the activity of these enzymes can easily be detected by successive restriction analysis with a DNA endonuclease, e.g. the activity of endonuclease *EcoR1* is inhibited by a prior methylation done with the methyltransferase M.EcoR1. This system should be used to investigate a possible methylation with the alternative cofactors SMM, Me3S, and Me3S=O. A DNA molecule which contains one or more *EcoR1* recognition sites was chosen as substrate for DNA-methyltransferase M.EcoR1, which

methylates the N6 position of the internal adenine in the sequence GAATTC. Therefore DNA of bacteriophage λ with 5 recognition sites was chosen. First results showed, that the analyzed DNA was also protected from digestion even if no methyl donor was added (Figure 58 A). Purification of the DNA prior to digestion did not solve this problem, indicating that the methyltransferase does not inhibit digestion by binding to the DNA (Figure 58 B). In addition it could be shown that 100 mM Me3S and 100 m Me3S=O did partially inhibit the digestion of λ-DNA without the action of methyltransferase activity. Therefore all successive experiments were done with 25 mM of each alternative cofactor (Figure 59).

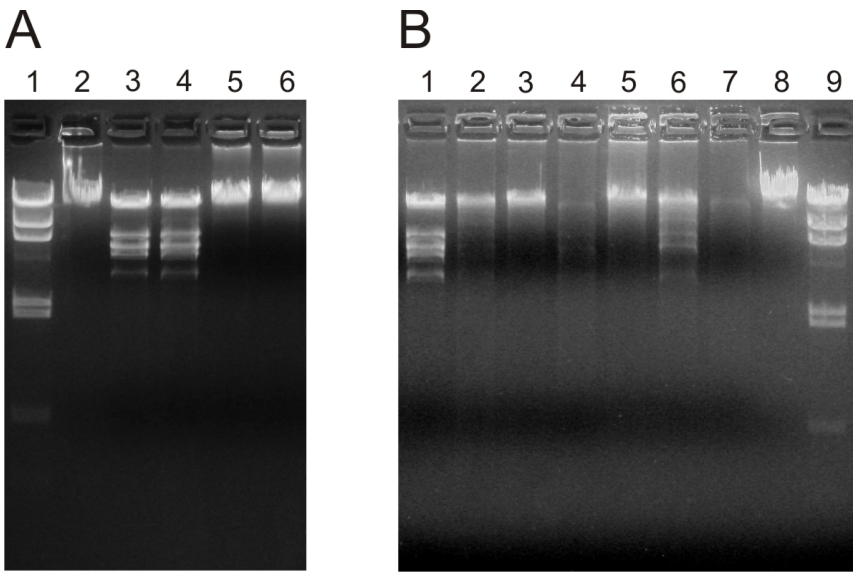

Figure 58: 1 % agarose gel for analyzing the methylation of λ-DNA. A: Slot 1: 500 ng λ-DNA digested with *HindIII*; slot 2: 500 ng λ-DNA; slot 3: λ-DNA digested with *EcoR1*; slot 4: control without M.EcoR1, with SAM; slot 5: control methylation without SAM; slot 6: control methylation with SAM. **B**: 500 ng λ-DNA digested with *EcoR1* ; slot 2 -4: phenol – chloroform purification; slot 5 – 7: column purification; slot 2, 5: methylation with SAM; slot 3, 6: methylation without SAM; slot 4, 7: control without M.EcoR1; slot 8: 500 ng λ-DNA uncut; slot 9: 500 ng λ-DNA digested with *HindIII*.

It was concluded that bound SAM in the supplied methyltransferase M.EcoR1 is sufficient for methylation and therefore blocking of successive digestion. This proposal is supported by the results obtained with Strep-tagged NovO and no addition of a methyl donor. In order to get rid of the bound SAM, the methyltransferase had to be incubated with a different DNA substrate to spend all its SAM, and thereafter would necessarily need new SAM for another methylation reaction. A short 23 bp DNA fragment with an

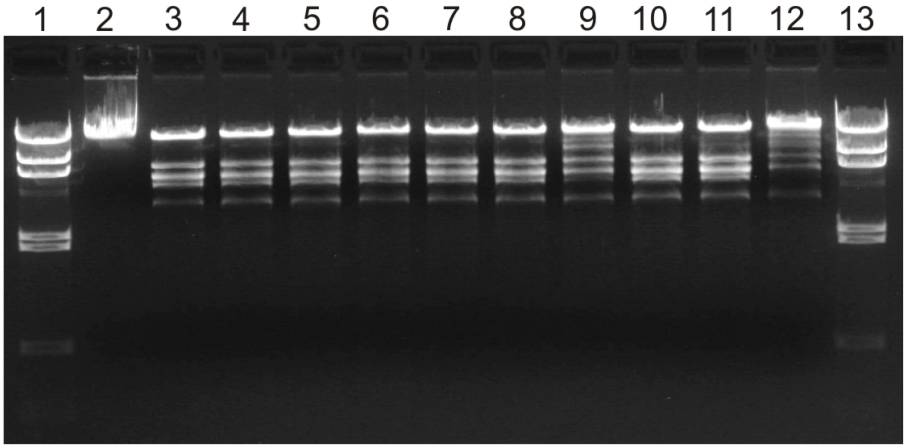

Figure 59: 1 % agarose gel for analyzing the influence of sulfonium salts on λ- DNA. Slot 1: 500 ng λ- DNA digested with *HindIII*; slot 2: 500 ng λ- DNA; slot 3: λ- DNA digested with *EcoR1*; slot 4 – slot 12: λ- DNA incubated with alternative cofactor; slot 4: 2 mM SMM; slot 5: 25 mM SMM; slot 6: 100 mM SMM; slot 7: 2 mM Me3S; slot 8 : 25 mM Me3S; slot 9: 100 mM Me3S; slot 10: 2 mM Me3S=O, slot 11: 25 mM Me3S=O; slot 12: 100 mM Me3S=O; slot 13: 500 ng λ- DNA digested with *HindIII*.

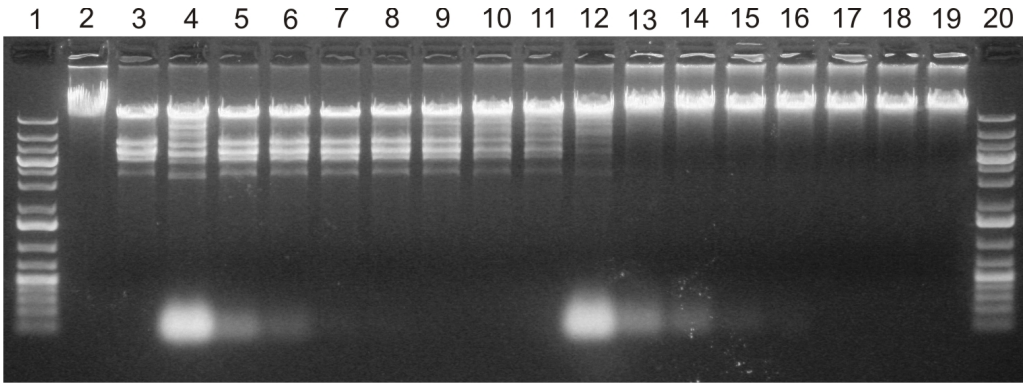

Figure 60: 1 % agarose gel for analyzing the amount of pre-substrate concentration. Slot 1: 500 ng 1kb ladder mix; slot 2: 500 ng λ-DNA; slot 3: λ-DNA digested with *EcoRI*, slot 4 – 11: methylation without SAM with decreasing amounts of pre-substrate from 100 µM to 20 nM; slot 12 – 19: methylation with SAM with decreasing amounts of pre-substrate from 100 µM to 20 nM; slot 20: 500 ng 1kb ladder mix.

EcoR1 recognition site was chosen as pre-substrate, and used for incubation with the methyltransferase M.EcoR1. Before starting the experiment, the optimal concentration of the pre-substrate had to be found. This has to be done, because if too much of the pre-substrate is added, the bound SAM would not be sufficient for a total methylation and therefore would leave unmethylated pre-substrate behind. The follow-up reaction with λ-DNA would be interrupted by the availability of the unmethylated pre-substrate, which must be methylated more efficiently than λ-DNA. On the other hand, if not enough pre-substrate is present, the bound SAM will not be consumed. The optimal concentrations were found by titration. They were in the range of 20 to 1 µM. At these concentrations digestion of unmethylated DNA was not inhibited, whereas methylated DNA was inhibited from digestion with *EcoR1* (Figure 60). Figure 61 shows that the methylation of λ-

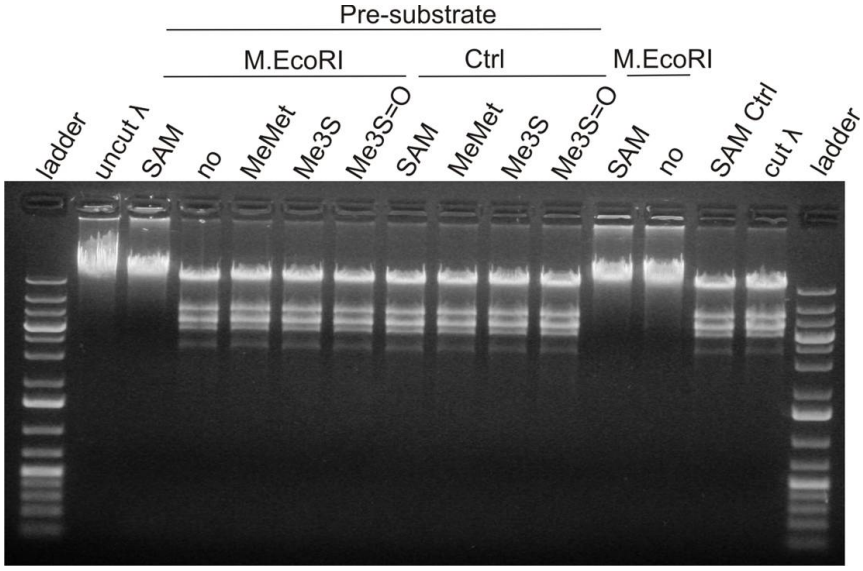

Figure 61: 1 % agarose gel for analyzing the methylation of λ- DNA. Slot 1: 500 ng 1kb ladder mix; slot 2: 500 ng λ-DNA; slot 3 - 12: incubation with pre-substrate; slot 3 -7: addition of M.EcoR1; slot 8 - 11: no M.EcoR1; slot 3, 8: SAM; slot 4: no donor; slot 5, 9: SMM; slot 6, 10: Me3S; slot 7, 11: Me3S=O, slot 12: M.EcoR1, SAM, no pre-incubation, slot 13: M.EcoR1, no donor, no pre-incubation, slot 14: no M.EcoR1, SAM, no pre-incubation, slot 15: digestion of λ-DNA , slot 16: 1kb ladder mix.

DNA could only be sufficient to protect from *EcoR1* digestion if SAM was added to the reaction. No inhibition of digestion could be observed if no, or an alternative cofactor was added. The difference between methylation (slot 3) and no methylation (slot 4 – 11) is clearly visible. The positive effect of a pre-incubation of the used methyltransferase is also obvious, if the reactions of slot 3 and 4 are compared to the reactions of slot 12 and

13. Summing up a possible methylation with the use of alternative cofactors could not be detected with EcoRI-methyltransferase and λ-DNA.

For a more sensitive analysis of possible DNA methylation via alternative cofactors, a short DNA fragment should be digested to nucleosides after methyltransfer and the methylated products analyzed by HPLC-MS. This method has been successfully used for analyzing the transfer of aldehydes to DNA by methyltransferases [23]. The cytosin-C5-methyltransferase M.HhaI was analyzed towards its action on a 23 bp DNA fragment with an *HhaI* recognition site. M.HhaI methylates the C5 position of an internal cytosin in the sequence GCGC. The incubation with SAM gave 19 % conversion, whereas all other reactions showed no product formation. These results support the findings of the above described experiments, where none of the alternative cofactors led to detectable methylated product.

3 Conclusion

With this study a break through in biocatalysis could be achieved. For the first time an enzymatic equivalent to the Friedel-Crafts alkylation is described. Mainly the aminocoumarin methylating enzymes CouO and NovO were investigated. As described in section 2.1 these two enzymes were the first biocatalysts of performing the named reaction. The publication of the results obtained with CouO and NovO underlines the importance and the topicality of the achievements. Two striking results were achieved. First, the acceptance of SAM analogues with extended carbon chains of allyl, crotyl, propynyl, butynyl, and even benzyl. Second, the broad substrate scope including several coumarin- and also naphthalene derivatives. In terms of regioselectivity and monoalkylation preference has to be given to the now possible enzymatic variant of the Friedel-Crafts alkylation.

Characterization towards optimal reaction conditions and stability of the enzymes, in particular NovO, revealed important information for the establishment of a new biocatalyst.

Detailed analyses of biochemical properties showed that NovO can methylate increased amounts of 2,7-dihydroxynaphthalene, and transfers allyl groups faster than methyl groups to the coumarin derivative substrate.

Information about the three-dimensional conformation of NovO was gathered from homology modeling an multiple sequence alignments. The use of both tools and the link to literature led to the identification of putative relevant residues in terms of cofactor binding and active site. As it is common for C-methyltransferases to depend on an active deprotonation mechanism, in contrast to the passive mechanism of some N-methyltransferases, the activation of the attacked substrate carbon atom is realized by a histidine located within the substrate binding pocket.

The homology model and the conserved cofactor binding motif classify NovO to the class I SAM-dependent methyltransferases. Information obtained from gel-filtration chromatography and NMR spectroscopy revealed that NovO, like a recently described

aromatic C-methyltransferase, takes up a dimeric conformation [117].

The extension to other enzymes, which are able to perform an enzymatic equivalent to the Friedel-Crafts alkylation, led to the identification of tyrosine- and 3-hydroxykynurenine alkylating enzymes. In contrast to CouO and NovO, the substrate scope of SacF, SfmM2 (tyrosine-C-methyltransferases) and Orf19, SibL (3-hydroxykynurenine-C-methyltransferases) was limited.

The identification of 3-hydroxykynurenine as the natural substrate of Orf19 and SibL goes in hand with the recent characterization of a similar methyltransferase of *Streptomyces chrysomallus* [117]. This result disproves a list of published data nominating 3-hydroxyanthranilic acid as the natural substrate for these enzymes.

The utilization of alternative methyl donors (SMM, Me3S, Me3S=O) by purified CouO and NovO did not lead to detectable methylated products. A proof of principle by an similar approach with DNA-methyltransferases (M.HhaI, M.EcoRI) gave the same results, indicating a conserved structural conformation of cofactor binding.

An alternative route to overcome highly costs of SAM supply, the biotransformation with viable cells yielded promising results, but is restricted to methyl group transfer so far.

4 Materials and Methods

4.1 Media and growth conditions

E. coli strains were grown in LB-Lennox or 2xTY medium and incubated at 37 °C or lower temperature if heterologous expression was achieved [188]. If a plasmid was transformed into bacteria, the corresponding antibiotic was added to appropriate concentrations (Table 8). After mixing of the components with double distilled water, the media were sterilized for 25 minutes at 121 °C and a pressure of 1.3 bar. Heat unstable substances like antibiotics were added sterile after the media had cooled to about 60 °C. In order to prevent glucose from caramelizing it was sterilized separately. For preparation of solid media agar was added to a final concentration of 15 g/l. The components of the media were supplied from Roth or Oxoid.

Streptomyces strains were grown on M65 agar medium according to Kieser *et al.*, 2000 [160] for 2 to 4 days at 28 °C. If the cell mass had to be used for genomic DNA isolation, a dialysis membrane was put on the agar dishes before streaking out the spores.

4.2 Bacterial strains and plasmids

Bacterial strains and plasmids which were used and or constructed in this work are listed with relevant information in Table 9, 10, 11, 12, 13, 14 and 15.

4.3 DNA manipulation techniques

4.3.1 Isolation of genomic DNA of gram-positive bacteria

The genomic DNA from *Streptomyces* species was isolated according to the CTAB procedure of Kieser *et al.*, 2000 [160]. Mycelium was prepared from cultures grown on agar dishes supplied with dialysis membranes. Cell lysis was done in 10 mM sodium phosphate buffer pH 7 and 20 % saccharose. Proteinase K (Fermentas, St.Leon-Rot, Germany) treatment was done in TE buffer (10 mM Tris-HCl, 1 mM EDTA pH 7.5). Before precipitation

Table 7: Components and concentrations of used media.

medium	component	concentration
2 x TY	tryptone	16 g/L
	yeast extract	10 g/L
	NaCl	5 g/L
LB-Lennox	tryptone	10 g/L
	yeast extract	5 g/L
	sodium chloride	5 g/L
auto-induction	LB-Lennox	20 g/L
	glucose	0.05 g/L
	glycerol	0.5 g/L
	lactose	0.2 g/L
	$MgSO_4$	1 mM
M65	glucose	4 g/L
	yeast extract	4 g/L
	malt extract	10 g/L
	$CaCO_3$	2 g/L
SOC	tryptone	20 g/L
	yeast extract	5 g/L
	NaCl	0.5 g/L
	$MgCl_2$	10 mM
	$MgSO_4$	10 mM
	glucose	4 g/L
^{15}N minimal media	KH_2PO_4	3 g/L
	Na_2HPO_4	6 g/L
	NaCl	0.5 g/L
	$(^{15}NH_4)_2SO_4$	1 g/L
	$MgSO_4$	1 mM
	thiamine	20 mg/L

Table 8: Concentrations of used antibiotics.

antibiotic	concentration
kanamycin	40 mg/L
ampicillin	100 mg/L
chloramphenicol	34 mg/L
tetracyclin	12 mg/L
gentamycin	20 mg/L

Table 9: E. coli strains used in this work.

bacteria	genotype	source
E. coli Top10	F^-, *mcr*A, D(*mrr-hsd*RMS-*mcr*BC), f80*lac*ZDM15, D*lac*X74, *deo*R, *rec*A1, *ara*D139,D(*ara-leu*)7697, *gal*K, *rps*L(StrR), *end*A1, *nup*G	BT # 1461 Invitrogen #C4040
E. coli BL21 Gold (DE3)	*E. coli* B, F^-, *dcm*, *ompT*, *hsd*S_B($r_B^-m_B^-$), *gal*(DE3)	Invitrogen # V420-20
E. coli BL21 Star (DE3)	*E. coli* B, F^-, *dcm*, *ompT*, *hsd*S_B($r_B^-m_B^-$), *gal*(DE3), *rne*131	Invitrogen # C6010 BT # 5060
E. coli BL21 plysS (DE3)	*E. coli* B, F^-, *dcm*, *ompT*, *hsd*S_B($r_B^-m_B^-$), *gal*(DE3) pLysS (Cm^r)	Invitrogen # C6020 BT # 1584
E. coli Rosetta (DE3)	*E. coli* B, F^-, *dcm*, *ompT*, *hsd*S_B($r_B^-m_B^-$), *gal*(DE3) pRARE^2 (Cm^r)	Novagen # 71209 BT # 4839
E. coli Arctic Express (DE3)	*E. coli* B, F^-, *ompT*, *hsd*S_B($r_B^-m_B^-$) dcm^+ Tet^R, *gal*(DE3), *end*A Hte [*cpn10*, *cpn60*, $Gent^r$]	Stratagene # 230192 BT # 5902
E. coli K12 HMS174 (DE3)	F^-, , *rec*A1, *hsdR*($r_{K12}^-m_{K12}^+$)(DE3)(Rif^R)	Novagen # 69453

Table 10: Streptomyces strains used in this work. BT: culture collection at IMBT, TUG.

bacteria	genotype	source
Streptomyces rishiriensis	wild-type	DSMZ # 40489
		BT # 3058
Streptomyces spheroides	wild-type	DSMZ # 40292
		BT # 877
Streptomyces antibioticus	wild-type	DSMZ # 41481
		BT # 5235
Streptomyces antibioticus	wild-type	DSMZ # 41511
		BT # 2000
Streptomyces antibioticus	wild-type	DSMZ # 40234
		BT # 3059
Streptomyces antibioticus	wild-type	DSMZ # 40764
		BT # 3000
Streptomyces chrysomallus	wild-type	DSMZ # 40128
= *Streptomyces anulatus*		BT # 3056
Streptomyces sioyaensis	wild-type	DSMZ # 40032
Streptomyces azureus	wild-type	DSMZ # 40106
		BT # 3057

Table 11: Plasmids used in this work.

plasmid	description	source
pET26b(+)	colE1 pBR322 origin, lac-operator, T7-promotor, kan^R	Novagen # 69862
pET30a-SBP-TEV	colE1 pBR322 origin, lac-operator, T7-promotor, kan^R, SBP = strep binding protein, TEV = TEV-protease cleavage site	K.Steiner
pET30a-SET1-SBP-TEV	colE1 pBR322 origin, lac-operator, T7-promotor, kan^R, SET1 = solubility enhancement tag, SBP = strep binding protein, TEV = TEV-protease cleavage site	K.Steiner

of DNA an additional extraction with CIP (Phenol:Chloroform:Isoamylalkohol = 25:24:1) was done. DNA was dissolved in aqua dest. and further purified with an gel and PCR purification column from Promega (Madison, USA). Therefore DNA was bound to the column by mixing with membrane binding solution, subsequent washing with buffer BP (Quiagen, Hilden, Germany),(miniprep kit, contains isopropanol) and membrane wash solution (Promega, Madison, USA). Finally DNA was eluted with aqua dest. at 60 °C.

4.3.2 Site-directed mutagenesis

For construction of tag fusion proteins and variants of cloned genes site-directed mutagenesis was performed [169]. PCR were done with Phusion or Pfu Ultra Hot Start polymerase (Section 4.3.7). *DpnI* digested DNA was transformed into electrocompetent *E. coli* Top10 cells.

Table 12: Constructed and deposited *E. coli* strains of this study I.

E. coli	plasmid	culture collection IMBT
BL21 Gold (DE3)	pET26b(+)-novO	# 3730
BL21 Gold (DE3)	pET26b(+)-novO-Strep	#3720
BL21 Gold (DE3)	pET26b(+)-couO	# 3728
BL21 Gold (DE3)	pET26b(+)-couO-Strep	# 3729
BL21 Gold (DE3)	pET26b(+)-sacF	# 3727
BL21 Gold (DE3)	pET26b(+)-sfmM2	# 3710
BL21 Gold (DE3)	pET26b(+)-sfmM2-Strep	# 3711
BL21 Gold (DE3)	pET26b(+)-ORF19	# 3726
BL21 Gold (DE3)	pET26b(+)-sibL	# 3712
BL21 Gold (DE3)	pET26b(+)-sioF	# 3713
BL21 Gold (DE3)	pET26b(+)-tsrM	# 3714
BL21 Gold (DE3)	pET26b(+)-tsrP	# 3715
BL21 Gold (DE3)	pET26b(+)-Cr-smt1	# 3723
BL21 Gold (DE3)	pET26b(+)-At-tmt	# 3722
BL21 Gold (DE3)	pET26b(+)-Bo-tmt1	# 3721
BL21 Gold (DE3)	pET26b(+)-ubiE	# 3716
BL21 Gold (DE3)	pET30a-cmcJ	# 3725
BL21 Gold (DE3)	pET14-cmcI	# 3705
BL21 Gold (DE3)	pETD-cmcI-cmcJ	# 3709
Top10	pMA-At-tmt	#3704
Top10	pMA-Bo-tmt1	#3707
Top10	pMA-sibL	#3708
Top10	pMA-tsrP	#3703
Top10	pMK-RQ-tsrM	#3719
Top10	pMK-RQ-Cr-smt1	#3724
Top10 F'	pGA4-ORF19	#3706
Top10 F'	pGA15-sfmM2	#3718
Top10 F'	pGA15-sacF	#3717

Table 13: Constructed and deposited *E. coli* strains of this study II.

E. coli	plasmid	culture collection IMBT
BL21 Gold (DE3)	pET26b(+)-novO-Strep-D70N	# 3932
BL21 Gold (DE3)	pET26b(+)-novO-Strep-D96N	#3936
BL21 Gold (DE3)	pET26b(+)-novO-Strep-P5A	# 3935
BL21 Gold (DE3)	pET26b(+)-novO-Strep-D70L	# 3930
BL21 Gold (DE3)	pET26b(+)-novO-Strep-E52L	# 3934
BL21 Gold (DE3)	pET26b(+)-novO-Strep-D96L	# 3933
BL21 Gold (DE3)	pET26b(+)-novO-Strep-P5A-C223S	# 3928
BL21 Gold (DE3)	pET26b(+)-novO-Strep-C223S	# 3929
BL21 Gold (DE3)	pET26b(+)-novO-Strep-D45N	# 3937
BL21 Gold (DE3)	pET26b(+)-novO-Strep-E52Q	# 3931
BL21 Gold (DE3)	pET26b(+)-novO-Strep-H15Q	# 3947
BL21 Gold (DE3)	pET26b(+)-novO-Strep-Y184S	# 3946
BL21 Gold (DE3)	pET26b(+)-novO-Strep-Y184T	# 3945
BL21 Gold (DE3)	pET26b(+)-novO-Strep-H15N	# 3944
BL21 Gold (DE3)	pET26b(+)-novO-Strep-Y184F	# 3943
BL21 Gold (DE3)	pET26b(+)-novO-Strep-G49A	# 3942
BL21 Gold (DE3)	pET26b(+)-novO-Strep-G51A	# 3941
BL21 Gold (DE3)	pET26b(+)-novO-Strep-H15R	# 3940
BL21 Gold (DE3)	pET26b(+)-novO-Strep-H15K	# 3939
BL21 Gold (DE3)	pET26b(+)-novO-Strep-H15Q-Y184F	# 3938
BL21 Gold (DE3)	pET26b(+)-novO-Strep-D45L	# 3967
BL21 Gold (DE3)	pET26b(+)-novO-Strep-C145S	# 3966
BL21 Gold (DE3)	pET26b(+)-novO-Strep-C48S	# 3965
BL21 Gold (DE3)	pET26b(+)-novO-Strep-C47S	# 3958
BL21 Gold (DE3)	pET26b(+)-novO-Strep-C47S-C48S-C145S	# 3957
BL21 Gold (DE3)	pET26b(+)-novO-Strep-C47G-C48S	# 3956
BL21 Gold (DE3)	pET26b(+)-novO-Strep-C47G-C48G	# 3955
BL21 Gold (DE3)	pET26b(+)-novO-Strep-C47G	# 3954

Table 14: Constructed and deposited *E. coli* strains of this study III.

E. coli	plasmid	culture collection IMBT
BL21 Gold (DE3)	pET30a-SBP-TEV-novO	# 3949
BL21 Gold (DE3)	pET30a-SET1-SBP-TEV-novO	# 3951
BL21 Gold (DE3)	pET26b(+)-novO-TEV-Strep	# 3953
BL21 Gold (DE3)	pETD-novO-novN	# 3955
Rosetta (DE3)	pHIS2-SsSAHH	# 3948

Table 15: Constructed *E. coli* strains of this study IV. Internal glycerol stocks of M.Tengg located in the -80 °C freezer, tower number 30, Petersgasse 14/2.

E. coli	plasmid	internal glycerol stock
Top10 F'	pKS470-couO	# 09
Top10 F'	pKS470-novO	# 14
Top10 F'	pKS470-sfmM2	# 06
Top10 F'	pKS470-sacF	# 07
Top10 F'	pKS470-ORF19	# 12
BL21 Gold (DE3)	pET26b(+)-sacFXN	# 10
BL21 Gold (DE3)	pET26b(+)-sacFXC	# 30
BL21 Gold (DE3)	pET26b(+)-couO-His	# 31
BL21 Gold (DE3)	pET26b(+)-novO-His	# 32
BL21 Gold (DE3)	pET26b(+)-couO-Strep-H120A	# 33
BL21 Gold (DE3)	pET26b(+)-novO-Strep-H120A	# 35
BL21 Gold (DE3)	pET26b(+)-Cr-smt1kurz	# 49
Top10	pET26b(+)-novO	# 50
Top10	pET26b(+)-novO-Strep	# 51
BL21 Gold (DE3)	pET26b(+)-novO-Strep-dC47	# 73
BL21 Gold (DE3)	pET26b(+)-novO-Strep-dC47-dC48	# 75
BL21 Gold (DE3)	pET26b(+)-novO-Strep-novN	# 120
BL21 Gold (DE3)	pET26b(+)-couO-novN	# 121
BL21 Gold (DE3)	pET26b(+)-couO-Strep-novN	# 121
Top10	pHIS2-SsSAHH	#110

4.3.3 Transformation

The first step of a successful transformation was the preparation of electro-competent *E. coli* strains. Therefore bacteria were incubated at 37 °C until they had reached an OD_{600} between 0.5 and 0.7. Then cells were harvested by centrifugation at 3000 x g for 10 minutes at 4 °C. After several washing steps with ice cold aqua dest. and 10 % glycerol, to remove residual salt and media, the cells were frozen in liquid nitrogen. During electroporation the cell wall becomes temporarily porous because of the impressed voltage. Therefore 40 to 80 μl of the prepared competent cells were mixed with an appropriate volume of plasmid DNA, and put into a electroporation-vessel. Then a voltage of 2.5 kV was impressed by the electroporator from BioRad. After the pulse was released, the cells were mixed with 1 ml of SOC media and incubated for 45 minutes at 37 °C. Finally 100 μl of various dilutions were plated on selective LB agar medium and incubated over night at 37 °C.

4.3.4 Plasmid isolation

Plasmid DNA was isolated by the use of miniprep isolation kits of Fermentas (St.Leon-Rot, Germany), Promega (Madison, USA), or Quiagen (Hilden, Germany) following the protocol of the supplier. The isolated DNA was dissolved in sterile water from Fresenius.

4.3.5 DNA endonucleases

DNA endonucleases and the referring buffers were supplied by New England Biolabs (Ipswich, UK) and Fermentas (St.Leon-Rot, Germany). They were used following the instruction of the supplier.

4.3.6 Agarose gel electrophoresis

Dependent on expected fragments, 0.8 % to 1.5 % TAE-agarose gels were used. In order to separate the DNA fragments, a voltage of 6-12V/cm was impressed. As running buffer

served 1 x TAE [189]. To visualize the DNA under UV-light, 1 μl of Ethidiumbromid (10 mg/ml) was added to 100 ml of agarose solution.

4.3.7 Polymerase chain reaction

For the amplification of DNA fragments from genomic DNA Phusion DNA polymerase from Finnzymes (Thermo Fischer, Waltham, USA) was used. In order to provide the optimal conditions for its activity on GC-rich DNA, the appropriate buffer (GC-buffer) was used. Site-directed mutagenesis of plasmid-DNA and amplification of genome walker libraries were done with Phusion DNA polymerase, or with Pfu Ultra Hotstart DNA polymerase from Stratagene (Agilent Technologies, Santa Clara, USA). A-tailing of blunt fragments was done with Dream Taq polymerase from Fermentas (St.Leon-Rot, Germany). In Table 16 and 17 the used oligonucleotides are listed. A general PCR preparation contained 0.2 - 2 ng/μl template DNA, 2.5 mM dNTPs, 400 nM forward and reverse primer, 1 x reaction buffer, and 0.01 to 0.02 U/μl polymerase. The amplification was carried out in a thermocycler of Applied Biosystems using the recommended program of the supplier of the polymerase.

4.3.8 Southern blot

For preparation of southern blot the DIG system of Roche (Basel, Switzerland) was used. Experimentals were done according to the protocol of the supplier and to Ausubel *et al.*, 1987 [189], with the following exceptions. DNA-probes were prepared by incorporation of DIG-11-dUTP into DNA by PCR using primers listed in Table 17. Probe-Orf19 was constructed with pGA-ORF19 as template and primers # 17 and # 18. For probe-SaHAA, the fragment that was obtained from PCR of genomic DNA of *Streptomyces antibioticus* 41511 and primers # 17 and # 18 (Table 17), was used as template and amplified with the same primers. If PCR yielded specific bands the solution was directly used for hybridization. In case of unspecific bands, respective bands were gel-purified prior to hybridization (Wizard SV Gel- and PCR clean-up system, Promega, Madison, USA). 5 µg genomic DNA of *Streptomyces* species were partially digested with *XhoI*. For positive control 100 ng of vector DNA pGA4-ORF19 were digested with *NdeI* and

HindIII to yield fragments of *orf19* and vector backbone. For determination of the detection limit, dilutions of digested pGA-ORF19 were loaded on an agarose gel. Digested DNA was separated by agarose gel electrophoresis. A DIG-labeled molecular weight marker was loaded which included fragments of 21226, 5148, 4973, 4268, 3530, 2027, 1904, 1584, 1375, 947, 831, 564, 125 bp. Afterwards gels were stained in ethidiumbromid solution, and finally transferred on a nylon membrane by capillary transfer. Optimal hybridization temperature was identified as 50 °C (calculated 55 °C according to GC-content of *Streptomyces* genomic DNA), and washing was done in 0.2 x SSC (30 mM sodium chloride, 3 mM sodium citrate pH 7), 0.1 % SDS at 55 °C.

4.3.9 Genome Walking

The GenomeWalker™ kit of Clontech (Mountain View, USA) was used for genome walking experiments. Therefore the genomic DNA of *Streptomyces antibioticus* 41511, isolated as described (4.3.1), was digested with *StuI* or *PvuII* in separate reactions to yield two types of libraries, which were achieved by ligation of the *StuI*- or *PvuII*-fragments with supplied adapter fragments. Prior to ligation, DNA was precipitated with 1 vol. isopropanol and 1/10 vol. 3 M sodium acetate and dissolved in sterile aqua dest. Libraries were used as templates for a primary PCR that was achieved with supplied adapter primer (AP1) and gene specific primers (FwGSP1, ReGSP1, FwGSP1n, ReGSP1n), which bind to both ends of the PCR-fragment obtained from *Streptomyces antibioticus* 41511 and primers Orf19son (Table 17, Figure 51). Binding of the gene specific primers occurs at a distance of 64 bp (GSP1) or 100 bp (GSP1n) to one end of the PCR fragment. Secondary (nested) PCR was done with 1/50 of the primary PCR product as templates with nested adapter primer (AP2) and nested gene specific primers (FwGSP2, ReGSP2, FwGSP2n, ReGSP2n). GSP2 overlap at 2 bp with the respective GSP1 and bind closer to the end of the fragment obtained from *Streptomyces antibioticus* 41511. GSP2n do not overlap with respective GSP1n. A control reaction was done with supplied control library and control primers (PCP1 and AP1). Agarose gel electrophoresis of digested genomic DNA and PCR products were performed under standard conditions (Section 4.3.6) using the following DNA ladders (Fermentas, St.Leon-Rot, Germany). λ-DNA digested with *EcoR1* and *HindIII*: 21226, 5148, 4973, 4268, 3530, 2027, 1904, 1584, 1375, 947,

831, 564 bp. 1 kb ladder mix: 20000, 10000, 7000, 5000, 4000, 3000, 2000, 1500, 1000, 700, 500, 400, 300, 200, 75 bp. Selected fragments were cloned into pCR4-TOPO vector (Life Technologies, Paisley, UK) via TA ligation, followed by transformation into *E. coli* Top10 electrocompetent cells. PCR were done with Phusion (Finnzymes of Thermo Fischer, Waltham, USA) or Pfu Ultra Hotstart (Stratagene of Agilent Technologies, Santa Clara, USA) polymerase. Before the fragments were cloned into the sequencing vector, A-tailing had to be done. Therefore PCR fragments were incubated with 0.3 mM dATP and Dream Taq (Fermentas, St.Leon-Rot, Germany) polymerase: 3 minutes at 95 °C, 20 minutes at 72 °C. Respective plasmids, isolated from two clones of each transformation, were sequenced by AGOWA. In total two rounds of the whole setup were performed with two individually prepared libraries of separately isolated genomic DNA. First 'walk' was done with oligonucleotides FwGSP1, ReGSP1, FwGSP2, ReGSP2, and the second with FwGSP1n, ReGSP1n, FwGSP2n, ReGSP2n. Additionally a third PCR was done with secondary PCR product as template and with nested adapter primer (AP2) and further nested gene specific primers (FwGSP3, ReGSP3). GSP3 primers have an overlapping region of 3 bp with respective GSP2 primers and bind even closer to the end of the sequence template.

4.4 Cloning and Expression

4.4.1 Coumarin methylating enzymes

Cloning For cloning and heterologous expression of the methyltransferase encoding genes *novO*, and *couO*, the genomic DNA of *Streptomyces spheroides* (DSMZ 40292) [104], and *Streptomyces rishiriensis* (DSMZ 40489) [103], were isolated with an adaption of the CTAB procedure of Kieser *et al.*, 2000 [160], respectively. Both genes were amplified by standard PCR conditions using the forward primer # 1 and the reverse primer # 2 (Table 16). These primers introduced the respective *NdeI* and *HindIII* restriction sites for subsequent cloning into the expression vector pET26b(+) and led to two amino-acid exchanges (A5P and S223C) in case of NovO compared to protein ID AAF67508.1. The PCR products were gel-purified, digested with *NdeI* and *HindIII*, and ligated into

the linearized pET26b(+) vector backbone. For an efficient purification procedure, C-terminal Strep Tag II was introduced into *novO* and *couO* by site-directed mutagenesis of the plasmids pET26b(+)-novO and pET26b(+)-couO using the forward primer # 3 and the reverse primer # 4 (Table 16) [169]. The same protocol was used for insertion of a TEV-protease cleavage site between the sequence of novO and the Strep tag using primers # 11 and # 12. For cloning of *novO* into the vector pET30a-SET1-SBP-TEV and pET30a-SBP-TEV the gene was amplified by standard PCR conditions using the primers # 13 and # 14, which introduce the respective *PagI* and *HindIII* restriction sites, and the plasmid pET26b(+)-novO as template. Gel-purified fragments were digested with *PagI* and *HindIII*, and ligated into the *NcoI* and *HindIII* linearized pET30a-SET1-SBP-TEV and pET30a-SBP-TEV vector backbone.

Expression The expression plasmids pET26b(+)-novO, pET26b(+)-novO-Strep, pET26b(+)-couO, pET26b(+)-couO-Strep, pET26b(+)-TEV-novO, pET30a-SET1-SBP-TEV-novO, and pET30a-SBP-TEV-novO were transformed into *E. coli* BL21 Gold (DE3) electrocompetent cells for protein expression. Transformants harboring the desired plasmids were grown over night at 37 °C in LB-Lennox medium supplemented with 40 mg/l kanamycin. A pre-culture was inoculated to an OD_{600} of 0.1, grown at 30 °C to an OD_{600} of 1.0. The main culture was inoculated to an OD_{600} of 0.1 and grown at 30°C for 2 hours, followed by decreasing the temperature to 25 °C and incubation for further 16 hours. Cells harboring pET30a-SET1-SBP-TEV-novO and pET30a-SBP-TEV-novO were induced at an OD_{600} of 0.8 - 1.0 with 0.02, 0.1, or 0.5 mM isopropyl-D-thiogalactopyranoside (IPTG). In order to increase the amount of soluble Strep-tagged CouO protein, the autoinduction medium was used for the mainculture, which consists of LB-Lennox supplemented with 1 mM $MgSO_4$, 0.5 % glycerol, 0.05 % glucose, and 0.2 % lactose. The cells were harvested by centrifugation (10 min at 5000 x g), resuspended in buffer A (50 mM Na-phosphate pH 6.5 or pH 7 for CouO), or buffer W (100 mM Tris-HCl pH 8, 150 mM NaCl, 1 mM EDTA) in case of Strep-tagged proteins. Therefore 5 to 10 ml of buffer was used per gram wet cell paste. Cells of pET26b(+)-novO, pET26b(+)-novO-Strep, pET26b(+)-couO, and pET26b(+)-couO-Strep were lysed by sonication for 6 minutes of discontinuous pulsing. Lysis of cells harboring pET26b(+)-TEV-novO, pET30a-SET1-SBP-TEV-novO, and pET30a-SBP-TEV-novO was achieved by incubation with 6 mg

lysozyme (Roth, Karlsruhe, Germany) per gram wet cell paste at room temperature for 20 minutes and subsequent incubation with 250 U Benzonase® (Merck, Darmstadt, Germany) per gram wet cell paste at room temperature for another 20 minutes. Aliquots of total crude extracts were analyzed on SDS-PAGE. The resultant cell debris was removed by centrifugation (60 min at 50000 x g). The supernatant was analyzed by SDS-PAGE and kept at 4 °C for enzymatic reactions and further affinity chromatography.

^{15}N labeling of NovO Best expression of soluble SBP-TEV-NovO in minimal media was achieved by auto-induction, via the availability of distinct concentrations of glycerol (0,5 %), glucose (0,05 %), and lactose (0,2 %) as carbon sources in the media. For labeling the media contained 98 % of the isotope ^{15}N. The overnight culture was prepared in 2xTY medium, and the pre-cultures were prepared in the same minimal media, but including $(^{14}NH_4)_2SO_4$. Protein expression was done in 2 x 500 ml media for 17 hours at 25°C yielding 0,67 g wet cell paste (OD_{600} = 1,0). Lysis was done by sonication for 6 minutes of discontinuous pulsing. The resultant cell debris was removed by centrifugation (60 min at 50000 x g). The supernatant was analyzed by SDS-PAGE and kept at 4 °C for enzymatic reactions and further affinity chromatography.

4.4.2 Tyrosine methylating enzymes

For cloning and heterologous expression of the methyltransferase encoding genes *sacF* of *Pseudomonas fluorescence* [44], and *sfmM2* of *Streptomyces lavendulae* [45] published coding sequences were used as templates for codon optimization and chemical synthesis by Geneart. Codon optimization was done for heterologous expression in *E. coli* K12. The delivered cloning plasmids pGA15-sacF and pGA15-sfmM2 were used for subsequent cloning into the expression vector pET26b(+) via the restriction sites *NdeI* and *HindIII*. Gel-purified fragments of *sacF* or *sfmM2* were ligated into the linearized pET26b(+) vector backbone. C-terminal Strep Tag II was introduced into *sfmM2* as described for coumarin methylating enzymes with the use of primers # 5 and # 6 (Table 16). Heterologous expression and purification was achieved as described for *couO* and *novO* with the difference that protein production was induced with 0.1 mM isopropyl-D-thiogalactopyranoside (IPTG). Wildtype or Strep-tagged cells were lysed by sonication in buffer A pH 7 or

Table 16: Oligonucleotides used in this study, supplied by Life Technologies (Paisley, UK) or IDT (Coralville, USA). Endonuclease recognition sites are assigned in bold letters.

primer #	primer name	sequence 5' to 3'
# 1	FWcouO	AATCTG**CATATG**AAGATTGAACCGATTAC
# 2	REcouO	TAGGTA**AAGCTT**TCAGGCAGCGGCCCGACGGG
# 3	FwEcouStr	GCCCGTCGGGCCGCTGCCAGCGCTTGGAGCCA CCCGCAGTTCGAAAAATGAAAGCTTGCGGCCG CACTCGAGC
# 4	ReEcouStr	GCTCGAGTG CGGCCGCAAGCTTTCATTTTTCG AACTGCGGGTGGCTCCAAGCGCTGGCAG CGGC CCGACGGGC
# 5	FwM2Str	TGATTATTGCGACCAAAAGCGCTTGGAGCCACC CGCAGTTCGAAAAATAATAAAAGCTTGCG GCCGCACTCG
# 6	ReM2Str	AGTGCGGCCGCAAGCTTTTATTATTTTTCGAAC TGCGGGTGGCTCCAAGCGCTTTTGGTCG CAATAATCACGC
# 7	FwMsF1	TGAGCGGCATTCTGTTTGGTCACGCTGCATTT CAGTATCTGCGTGCGAGC
# 8	ReMsF1	TCGCACGCAGATACTGAAATGCAGCGTGACCA AACAGAATGCCGCTCAGG
# 9	FwMsF2	ACCGCGATTCCGGGTTGGACTCCGCACGGTAT CATTGTGGCGTATAAATAATAAAAGC
# 10	ReMsF2	TATTATTTATACGCCACAATGATACCGTGCGG AGTCCAACCCGGAATCGCGGTACGC
# 11	FnovTEV	TCGCCCGTCGGGCCGCTGCCGAGAACCTGT ACTTCCAAAGCGCTTGGAGCCACCCGCAG
# 12	RnovTEV	CTGCGGGTGGCTCCAAGCGCTTTGGAAGTA CAGGTTCTCGGCAGCGGCCCGACGGGCGA

Table 17: Oligonucleotides used in this study, supplied by Life Technologies (Paisley, UK) or IDT (Coralville, USA). Endonuclease recognition sites are assigned in bold letters.

primer #	primer name	sequence 5' to 3'
# 13	FnovSNSBP	TCG**TCATGA**AGATTGAACCGATTACG
# 14	RnovSNSBP	TATA**AAGCTT**TCAGGCAGCGGCC
# 15	Forf19	CCTAAACATATGGTGACGAAACCGGTCGACCTCA
# 16	Rorf19	ATACGGAAGCTTTCACGCATCGGGCTTGCGCCCC
# 17	Forf19son	AGGCTGGCAGCGATCTGTATAGCCGTCTGGA
# 18	Rorf19son	AATCTGAACATATCGCCCGCCACCACACGAA
# 19	FacmBdeg	AGCTTGGTGGTCTTCGGCGGCGAGGCSCTS
# 20	RacmBdeg	AGCTTGCAGGGCCGCTCGGTCCAGTTTSCCRTT
# 21	FacmBson	AATCTGAGCTCCCCGACAGGCACACCGCGCC
# 22	RacmBson	AATCTGGCCGCCGTGCAGCAGGGCTCCCCAC
# 23	FacmAson	AATCGAGCAGTACCTGGTCGTGGCTGCGGGT
# 24	RacmAson	GACCGAATCAGGCCCATGTTGTGCATGACCG
# 25	EcoRI	GCCGCCGGAATTCGCCGCCGCCG
# 26	HhaI	TAATAATGCGTAATAATAATAAT
# 27	FwGSP1	ATAGGAAGGTGCGGCGGAAGTGGCGCGTG
# 28	ReGSP1	CGAGAGTTCAGACCAGCTGTTCATGCCAC
# 29	FwGSP2	ATAGAACATTGCGGATGCGGGCCTGGGCGATC
# 30	ReGSP2	CGAGAAAACAGGTTTTCCAGATCCAGCGCCTG
# 31	FwGSP3	CGAGTATTCGTGTGGTGGCGGGCGATATGTTC
# 32	ReGSP3	CGAGTTCCAGACGGCTATACAGATCGCTG
# 33	FwGSP1n	TGCGCATCCGCATCTGCGTGTGACC
# 34	ReGSP1n	GCACATCACGATAATCCACCTGATGCAGCAGC
# 35	FwGSP2n	AGGTGCGGCGGAAGTGGCGCGTGATAAC
# 36	ReGSP2n	GCTCAGTTCAGACCAGCTGTTCATGCCACG
# 37	AP1	GTAATACGACTCACTATAGGGC
# 38	AP2	ACTATAGGGCACGCGTGGT
# 39	FwsioF	TCGA**CATATG**CCGGGCGCGCCACCGCCCGGCTC
# 40	ResioF	TCAG**AAGCTT**TCACCCGGAGGGTGCCGGGTCCGCGAG
# 41	FubiE	GCCT**CATATG**GTGGATAAGTCAC
# 42	RubiE	GCCT**AAGCTT**TCAGAACTTATAACC

buffer W, respectively (Section 4.4.1). Site-directed mutagenesis of *sacF* was done as described for Strep tagging procedure of coumarin methylating enzymes. In order to overcome the production of mRNA secondary structures that consist of strong stem formation, the sequence at position 87 - 100, 5'-GCCATGCGGCGT- 3' was exchanged to 5'-GTCACGCTGCAT-3' using primers # 7 and # 8. The resulting plasmid was designated to pET26b(+)-sacFXN. The primers # 9 and # 10 were used for mutation of the sequence at position 1043 - 1056, 5'-ACGCCGCATGGC-3' to 5'-ACTCCGCACGGT-3'. The resulting plasmid was designated to pET26b(+)-sacFXC.

The SacF plasmids pET26b(+)-sacF, pET26b(+)-sacFXN, and pET26b(+)-sacFXC were transformed into several electrocompetent *E. coli* strains: BL21 Gold (DE3), BL21 Star (DE3), BL21 plysS (DE3), Rosetta (DE3), K12 HMS174 (DE3), Arctic Express (DE3) (Table 9). Over night cultures were incubated at 37 °C in LB-Lennox medium supplemented with the appropriate antibiotic (Table 8). The main culture was inoculated to an OD_{600} of 0.1 and grown at 37 °C until an OD_{600} of 0.8. Then isopropyl-D-thiogalactopyranoside (IPTG) was added to a final concentration of 1 mM, and cells were further incubated at 37 °C for 5 to 18 hours. *E. coli* Arctic Express was incubated at 30 °C to an OD_{600} of 0.8, then IPTG was added and temperature was decreased to 11 °C. One ml samples were centrifuged at 16.000 x g, the resultant cell paste was lyzed by resuspension in final sample buffer (loading dye and reducing agent) and heating to 95 °C for 10 minutes. After centrifugation at 16.000 x g for 10 minutes the supernatants were analyzed on SDS-PAGE.

4.4.3 Hydroxykynurenine methylating enzymes

Cloning and heterologous expression of the methyltransferase encoding genes *orf19* of *Streptomyces refuineus* [121], and *sibL* of *Streptosporangium sibiricum* [122] was done as described in 4.4.2. Synthesized genes were delivered in the cloning plasmids pGA4-ORF19 and pMA-sibL.

4.4.4 Tryptophan methylating enzymes

Cloning and heterologous expression of the methyltransferase encoding gene *sioF* of *Streptomyces sioyaensis* [133] was done similar to section 4.4.1. Genomic DNA was isolated from *Streptomyces sioyaensis* (DSMZ 40032), primers # 39 and # 40 introduced the respective *NdeI* and *HindIII* restriction sites for subsequent cloning into the expression vector pET26b(+). The genes *tsrP* and *tsrM* were codon optimized and synthesized by Geneart, and cloned as described in section 4.4.2. Synthesized genes were delivered in the cloning plasmids pMA-tsrP and pMK-RQ-tsrM. Heterologous expression in *E. coli* BL21 Gold (DE3) was done as described in section 4.4.2 with or without addition of IPTG. Cell lysis was done by sonication in buffer A at pH 7.8 (Section 4.4.1). In terms of enzyme preparations of *Streptomyces azureus* the following methods and buffers were used: *Sonication*: 5 g wet cell paste were sonicated in 10 ml of buffer A: 50 mM sodium phosphate pH 7.8, 15 % (v/v) glycerol, 5 mM β-mercaptoethanol, 1 mM EDTA, 1 x complete (1 tablet per 10 ml, Roche, Basel, Switzerland) for 10 minutes of discontinuous pulsing. *Lysozyme*: 5 g wet cell paste were incubated in 7.5 ml of buffer B1: 50 mM sodium phosphate pH 8, 5 mM EDTA, 10 % (w/v) saccharose, 500 mg/l lysozyme (Roth, Karlsruhe, Germany) for 30 minutes at room temperature, subsequently 7.5 ml buffer C: 10 mM sodium phosphate pH 8, 1 mM EDTA, 500 units Benzonase® (Merck, Darmstadt, Germany) were added and further incubated for 10 minutes at room temperature. *lysozyme and detergent*: Same procedure as *lysozyme*, but with the use of buffer B2: buffer B1 plus 0.5 % (v/v) Triton X-100 (Sigma-Aldrich, St. Louis, USA).

4.4.5 Ubiquinone methylating enzymes

Cloning of the methyltransferase encoding gene *ubiE* of *E. coli* BL21 Gold (DE3) was done similar to section 4.4.1. Gene amplification with primers # 41 and # 42 was done using a colony-PCR approach of an over-night culture of the respective strain grown on solid LB-agar medium. Cloning was done with respective *NdeI* and *HindIII* restriction sites into the expression vector pET26b(+).

4.5 Expression analysis

Total protein concentrations were determined by Bradford assay using the reagent of BioRad® (Hercules, USA). Calibration curve was achieved by triplicate measurement of 7 different concentrations of BSA (bovine serum albumin) supplied by Thermo Fisher® (Waltham, USA). Gel quantitation was done with the *GeneTools* software from SynGene® (Cambrigde, UK). This program identifies all protein bands on photographs of respective protein gels, and calculates volumes for each band by multiplication of the area and the intensity of the band. The sum of volumes of all bands of one lysate is set to 100%. Afterwards the amount of the band of interest can be calculated.

4.5.1 SDS-polyacrylamide gel electrophoresis

Proteins were separated on NuPAGE 4 -12 % (w/v), Bis-Tris polyacrylamide gels according to the protocol of the supplier Life Technologies (Paisley, UK). Samples were prepared in final sample buffer (loading dye, reducing agent: 50 mM DTT), denatured at 95°C for 5 minutes and then applied to the SDS gel for separation. Electrophoresis was performed in MOPS running buffer at 100 mA. PageRuler Prestained Protein Ladder (SM0671) from Fermentas (St.Leon-Rot, Germany), Novex-sharp pre-stained protein standard (LC5800) and SeeBlue Plus2 pre-stained standard (LC5925) from Life Technologies (Paisley, UK) served as molecular weight standard.

4.5.2 Coomassie staining

SDS-gels were stained according to Ausubel *et al.*, 1987 [189], with Coomassie solution: 0.25 % (w/v) Coomassie Brilliant Blue, 10 % (v/v) acetic acid, 45 % (v/v) ethanol and destained with destain solution: 10 % (v/v) acetic acid, 40 % (v/v) ethanol.

4.6 Purification

The cleared lysates of Strep-tagged NovO, CouO, and SfmM2 were immediately used for affinity purification using a Streptactin Superflow High-Capacity column from IBA

(Göttingen, Germany) following the manual of the supplier. The eluted fractions in buffer E (100 mM Tris-Cl pH 8, 150 mM NaCl, 1 mM EDTA, 2.5 mM D-desthiobiotin) were pooled and concentrated with ultrafiltration spin columns (cut-off 10.000 Da) from Vivaspin (Sartorius, Aubagne Cedex, France) to a final concentration of 5 to 10 mg/ml. For storage at -20 °C glycerol was added to a final concentration of 40 %. Aliquots were analyzed by SDS-PAGE. The cleared lysate containing SBP-TEV-NovO (Figure 39, lane 7) was used for a small scale purification procedure (Figure 40). 2 ml lysate [2 mg/ml] were loaded on a 1 ml 'Streptactin Superflow' column. 3 ml of the eluted fraction [0.5 mg/ml] were incubated with 1/10 of TEV-protease (w/w) [1 mg/ml] which was kindly provided by Kerstin Steiner (ACIB, Graz). Therefore DTT was added to the elution buffer E (100 mM TrisCl, 150 mM NaCl, 1 mM EDTA, 2.5 mM Desthiobiotin, pH 8) to a final concentration of 1 mM. One half of the volume was incubated at 4°C for 16 hours, the other half at RT for 3 hours and afterwards stored at -20 °C. Both protease digested fractions were loaded, one after the other, on the same Streptactin Superflow column for removal of the SBP-TEV peptide. The flowthrough was loaded on 0.5 ml settled Ni^{2+}-sepharose 6 Fast Flow (GE Healthcare, Uppsala, Sweden) for removal of the hexa-histidine tagged TEV-protease. The flowthrough was collected and used for determination of methyltransferase activity, and for SDS-PAGE analysis.

^{15}N labeled NovO purification The cleared lysate derived form sonication of 0,67 g in 20 ml buffer [1 mg/ml] was applied for Strep Tag purification, followed by TEV-protease incubation, removal of SBP-TEV peptide by Strep Tag purification, and final removal of TEV-protease by His Tag purification. The lysate SBP-TEV-NovO was used for purification procedure. 20 ml of the lysate [1 mg/ml] were loaded on a 10 ml Streptactin Superflow High Capacity column. 30 ml of the eluted fraction [0.1 mg/ml] were incubated with 1/15 of TEV-protease (w/w) (provided by Kerstin Steiner, ACIB, Graz). Therefore DTT was added to the elution buffer E (100 mM TrisCL, 150 mM NaCl, 1 mM EDTA, 2.5 mM Desthiobiotin, pH 8) to a final concentration of 1 mM. Cleavage was done at 4 °C for 16 hours. The fraction was concentrated from 30 to 10 ml by ultra filtration centrifugation at 10 °C. Buffer exchange to buffer W was done with PD-10 columns (GE healthcare, Uppsala, Sweden). The resulting 14 ml were loaded on the same Streptactin Superflwo High Capacity column for removal of the SBP-TEV peptide. The flowthrough

(14 ml) plus 10 ml of buffer W was loaded on 0.5 ml settled Ni^{2+}-sepharose 6 Fast Flow (GE Healthcare, Uppsala, Sweden) for removal of the hexa-histidine tagged TEV protease. The flowthrough (27 ml) was concentrated to 1 ml, buffer exchanged to 50 mM Na- Pi pH 6.5 yielding 3.5 ml, and again concentrated to 1.2 ml with a concentration of 1.2 mg/ml.

4.6.1 Gel-filtration chromatography

Gel-filtration chromatography of Strep-tagged CouO was performed by Andrzej Lyskowski (ACIB, Graz).

4.7 Methyltransferase assay

NovO and CouO Cleared lysates of NovO, Strep-tagged NovO, CouO, or Strep-tagged CouO were incubated in 0.1 ml scale in a thermomixer at 35 °C and 1000 rpm (revolutions per minute) for 16 hours containing 0.5 mM or 1 mM substrate from a 10 mM stock solution prepared in DMSO, 2 mM SAM (Sigma-Aldrich, St. Louis, USA)(or analogue) from a 20 mM stock solution prepared in 50 mM sodium phosphate buffer (pH 6.5 for NovO and pH 7 for CouO), and 0.1 mg/ml BSA from a 2 mg/ml stock solution prepared in 50 mM sodium phosphate buffer (pH 6.5 for NovO and pH 7 for CouO). The amount of lysates was set to 80 % of total reaction volume. The assay was stopped by heating the vials for 10 minutes at 80 °C, followed by maintaining the vials in the refrigerator for 15 minutes. Subsequently the mixtures were centrifugated at 16.000 x g for 15 minutes. Two to 20 μl of the aqueous solution was analyzed with HPLC.

SacF, SfmM2, Orf19, and SibL Cleared lysates of SacF, SfmM2, Orf19, or SibL were incubated in 0.5 ml scale in a thermomixer at 30 °C and 1000 rpm (revolutions per minute) for 24 h containing 1 mM substrate from a 10 mM stock solution (in 30 mM NaOH in Aqua dest. to obtain full solubility), 2 mM SAM (Sigma-Aldrich, St. Louis, USA) (or analogue) from a 20 mM stock solution (in 1 mg/ml BSA in Aqua dest.). The amount of lysates was set to 80 % of total reaction volume. The assay was stopped by heating the vials for 10 minutes at 85 °C, followed by maintaining the vials in the refrigerator for

15 minutes. Subsequently the mixtures were centrifugated at 16.000 x g for 15 minutes. Five μl of the aqueous solution was analyzed with HPLC.

TsrM, TsrP, SioF, Streptomyces azureus Preparations of heterologous expressed TsrM, TsrP, SioF, and cultivated mycelia of *Streptomyces azureus* were incubated in 0.5 ml scale in a thermomixer at 45 °C and 1000 rpm (revolutions per minute) for 24 h containing 1 mM substrate from a 10mM stock solution (in 10 mM sodium phosphate buffer), 2 mM SAM (Sigma-Aldrich, St. Louis, USA) from a 20 mM stock solution (in 1 mg/ml BSA in Aqua dest.). The amount of lysates was set to 80 % of total reaction volume. The reactions were stopped via acidic precipitation of the enzyme by addition of 0.3 times the reaction volume of 0.33 M HCl. Subsequently the mixtures were centrifugated at 16.000 x g for 15 minutes. Five μl of the aqueous solution was analyzed with HPLC.

4.7.1 HPLC methods

UV detection HPLC analyses were performed on an Agilent 1100 instrument composed of vacuum degasser G1379A, quaternary pump G1311A, autosampler G1367A, thermostat column compartment G1330B, and diode array detector (DAD) G1315B. Reactions of NovO and CouO were analyzed with a Merck Chromolith® Performance 4.6 mm column and eluent 10 mM ammonium acetate (NH_4OAc) pH 5.5 and acetonitrile (CH_3CN). Coumarinbenzamide **1** was separated with 93 % NH_4OAc and 7 % CH_3CN, flow 2 ml/min, 40°C. Coumarinpyrrolamide **5** was separated with 95 % NH_4OAc and 5 % CH_3CN, flow 1 ml/min, 40°C. 2,7-dihydroxynahpthalene **3** was separated with 90 % NH_4OAc and 10 % CH_3CN, flow 2.5 ml/min, 40°C. Analyses of methyltransfer reactions other than NovO or CouO were done by Harald Stecher [182].

MS detection HPLC-MS analyses were performed on an Agilent 1200 instrument composed of vacuum degasser G1379B, binary pump G1312B, autosampler G1367C with thermostat G1330B, thermostatted column compartment G1316B, and multi wavelength detector (MWD) G1365C connected to an Agilent quadrupole-MS 6120 with electrospray ionization (ESI) unit. Reactions of nucleosides were analyzed with an Agilent Poroshell® column (rp18e, 100*3 mm, 2.7 μm diameter) and eluent 10 mM NH_4OAc pH 6.7 (95

%) and CH_3CN (5 %), flow 0.4 ml/min, 40°C. All analyses were done by Harald Stecher [182].

4.7.2 Determination of temperature and pH optimum

Cleared lysates of NovO or CouO were incubated as described (Section 4.7) containing 1 mM coumarinbenzamide **3** or coumarinpyrrolamide **5** as substrate, respectively. For determination of the optimal reaction temperature 12 different temperatures were chosen between 27 and 48 °C. Reactions were initiated with 0.23 mg total protein of cleared lysates and incubated for 4 or 24 hours. To find the optimal buffer and pH conditions crude lysates containing NovO or CouO were prepared in 50 mM sodium phosphate buffer with pH values of 5, 5.5, 6, 6.5, 7, 7.5, and 8, or in 50 mM Tris-HCl buffer with pH values of 7.5, 8, 8.5, and 9. Reactions were set up in these buffers and initiated with 0.23 mg total protein of the corresponding cleared lysates and incubated for 24 hours.

4.7.3 Determination of K_M, V_{max} and k_{cat}

For determination of kinetic parameters the reactions were performed as described (Section 4.7). The reactions were carried out in a 0.1 ml scale of triplicate measurements using substrate stock solutions of 10 mM coumarinbenzamide **3** (prepared in DMSO), 10 mM coumarinpyrrolamide **5** (prepared in DMSO), 40 mM 2,7-dihydroxynaphthalene **7** (prepared in 10 % DMSO, 90 % 50 mM sodium phosphate buffer pH 6.5 for NovO), or 20 mM 2,7-dihydroxynaphthalene **7** (prepared in 20 % DMSO, 80 % 50 mM sodium phosphate buffer pH 7 for CouO). The SAM concentration was kept constant at 2 mM. Substrate concentrations were varied from 0.015 to 0.5 mM for coumarinbenzamide **3** or coumarinpyrrolamide **53**, and 0.02 mM to 20 mM in case of 2,7-dihydroxynahpthalene **7**, keeping the DMSO concentration at 5 %. In case of CouO the DMSO concentration of both substrates was varied depending on the dilution of the substrate stock solution, e.g. 1 mM coumarinpyrrolamide **5** or 10 mM 2,7-dihydroxynaphthalene **7** had a DMSO concentration of 10 %. If kinetic parameters of co-substrates were investigated the concentration of coumarinbenzamide **3** was set 4 times higher than the respective co-substrate concentration with a maximum of 2 mM leading to a DMSO concentration of 20 %. The

SAM concentrations were varied from 0.03 to 1 mM, and the allyl-SAH concentration from 0.03 to 2 mM. Reactions were initiated with 0.05 mg Strep-tagged NovO, 0.05 mg Strep-tagged CouO, or with 0.0125 mg Strep-tagged NovO for allyl-SAH parameters, and stopped after 2.5, 5, 10, 20, 30, and 60 minutes.

4.7.4 Stability assay

The state of the cystein residues of NovO and CouO was analyzed by incubation of the enzymes under oxidative or reductive conditions. Reactions were prepared as described (Section 4.7) containing 0.5 mM 2,7-dihydroxynaphthalene **7**, with or without the addition of DTT (1,4-dithiothreitol from Roth) and incubation in an oxygen rich or poor environment. Therefore DTT was added to a final concentration of 1 mM. Reactions of 100 μl scale were incubated in 15 ml or 200 μl reaction tubes. Reactions were initiated with 0.05 mg of purified Strep-tagged NovO or Strep-tagged CouO and incubated for 16 hours. In another experiment the enzymes were pre-incubated for 4 hours under the described conditions before substrate and cofactor were added and further incubated for 16 hours.

4.8 Whole cell biotransformation

E. coli cells harboring pET26b(+)-novO or the empty pET26b(+) were grown under standard expression condition over night (Section 4.4.1). Centrifuged cell pellets were washed once with buffer A: 50 mM sodium phosphate buffer pH 6.5, and directly used for enzyme activity assay. The cell pellet of a 50 ml culture was resuspended in 5 ml buffer A. 0.1 ml scale reactions contained 70 % resuspended cells, 1 mM substrate (10 mM stock solution coumarinbenzamide **3** prepared in DMSO or 5 mM stock solution 2,7-dihydroxynaphthalene **7** prepared in buffer A), 2 mM or 1 mM SAM from a 20 mM phosphate buffer stock, or no cofactor. The control reaction was initiated with 0.1 mg purified Strep-tagged NovO. Reactions were incubated and analyzed as described in Section 4.7. For determination of relative activity the reactions were stopped after 0.5, 1, 1.5, 2, and 4 hours.

4.9 Alternative Cofactors

NovO and CouO 0.1 ml scale reactions were incubated with 1 mM coumarinbenzamide **3**, 0.1 mg/ml BSA, and one of the cofactors: 2 mM SAM, 100 mM S-methyl-L-methionine (SMM), 25 mM trimethylsulfonium iodide (Me3S), 25 mM trimethylsulfoxonium iodide (MeS=O). As a control no cofactor was added, or no Strep-tagged NovO was added to a reaction with SAM. The same reactions were set up with the addition of 0.5 mM or 0.1 mM SAH. Purified Strep-tagged CouO was analyzed the same way, but coumarinpyrrolamide **5** was used as substrate. Reactions were initiated with 0.14 mg Strep-tagged NovOvor 0.19 mg Strep-tagged CouO.

DNA methyltransferases Generally, 500 ng of λ-DNA were incubated with 40 U of adenine-N6-methyltransferase M.EcoR1 (New England Biolabs, Ipswich, UK), with or without 80 µM SAM, or alternative cofactor for 60 minutes at 37°C followed by inactivation for 15 minutes at 65 °C. The λ-DNA is Dam-, Dcm-, and EcoK1 methylated, which do not interfere with the methylations carried out in these experiments, because of different recognition sites. Dam methylates the N6 position of the adenine residues in the sequence GATC. Dcm methylates the internal cytosine residues in the sequences CCAGG and CCTGG at the C5 position. The EcoKI methylase modifies adenine residues in the sequences AAC(N6)GTGC and GCAC(N6)GTT. Basically, λ-DNA is not methylated to 100 % in *E. coli* strains. All reactions were performed in the supplied reaction buffer of NEB. Concentrations of the alternative cofactors SMM, Me3S, Me3S=O were adjusted to 2 mM, 25 mM, or 100 mM. Afterwards 1 U *EcoR1* endonuclease was added and samples were incubated for another 60 minutes at 37 °C. Reactions were stopped by adding gel-loading dye. Agarose-gel-electrophoresis was performed under standard conditions (Section 4.3.6) using the following DNA ladders (Fermentas, St.Leon-Rot, Germany). λ-DNA digested with *HindIII*: 23130, 9416, 6557, 4361, 2322, 2027, 564, 125 bp. 1 kb ladder mix: 20000, 10000, 7000, 5000, 4000, 3000, 2000, 1500, 1000, 700, 500, 400, 300, 200, 75 bp. Purification of potentially methylated λ-DNA was done with 'Wizard SV Gel and PCR purification columns' (Promega, Madison, USA), or with phenol/chloroform purification followed by precipitation with sodium acetate and ethanol. To analyze the influence of the alternative cofactors each of them was incubated at three different concentrations (2

mM, 25 mM, 100 mM) with λ-DNA, followed by digestion with *EcoR1*.

For titration of pre-substrate, 40 U of the methyltransferase M.EcoRI were incubated with the dilutions 1:5, 1:10, 1:50, 1:100, 1:500, 1:1000, and 1:5000 of a 23 bp dsDNA fragment [100 µM] containing an *EcoRI* recognition site for 1 hour at 37 °C. The dsDNA molecule was prepared by annealing the synthetic oligonucleotides # 25 and its complement at equimolar concentrations at 79 °C (Tm + 5°C) for 10 minutes and subsequent cooling to room temperature over a period of one hour. Afterwards λ-DNA [16 nM] and SAM [1 mM] were added and further incubated for 1 hour at 37 °C, followed by heat inactivation at 65 °C for 15 minutes. As control reactions no SAM was added. Finally all reactions were digested with *EcoRI* for 2.5 hours at 37 °C, and analyzed by agarose gel electrophoresis. For analysis of cofactor dependence, the methyltransferase M.EcoRI was incubated with 2 µM (dilution 1:50) of the 23 bp fragment followed by incubation with λ-DNA [16 nM] and a methyl donor [25 mM]. Methylation reaction was followed by digestion with *EcoRI* for 2.5 hours at 37 °C and analyzed by agarose gel electrophoresis.

The action of cytosine-C5-methyltransferase M.HhaI (New England Biolabs, Ipswich, UK) was analyzed by incubation of 10 µM of a 23 bp ds DNA fragment containing a *HhaI* recognition site with 125 U M.HhaI, and a methyldonor (1 mM SAM, 1 M SMM, 250 mM Me3S, 250 mM Me3S=O, no donor). All reactions were performed in the supplied reaction buffer of NEB. The dsDNA molecule was prepared by annealing the synthetic oligonucleotides # 26 and its complement at equimolar concentrations at 45°C (Tm + 5 °C) for 10 minutes and subsequent cooling to room temperature over a period of one hour. As a control no enzyme was added in the presence of substrate and SAM. Reactions were incubated for 2 hours at 37 °C, followed by heat inactivation for 15 minutes at 65 °C. Afterwards DNA was digested to nucleosides by incubation with 2 U Nuclease P1 (Sigma-Aldrich, St. Louis, USA) for 2 hours at 60 °C and incubation with 30 U shrimp alkaline phosphatase (SAP), (Fermentas, St.Leon-Rot, Germany). Reactions were stopped by heating to 90 °C for 10 minutes. After centrifugation the supernatants were analyzed by HPLC-MS (Section 4.7.1).

5 References

[1] T. Purkarthofer, K. Gruber, M. Gruber-Khadjawi, K.Waich, W. Skranc, D.Mink, and H. Griengl. A biocatalytic henry reaction–the hydroxynitrile lyase from Hevea brasiliensis also catalyzes nitroaldol reactions. *Angew. Chem. Int. Ed.*., 45(21):3454-6, **2006**.

[2] M. Pohl and A. Liese. Industrial processes using lyases for C-C, C-N and C-O bond formation. in *Biocatalysis in the pharmaceutical and biotechnology industries*. Taylor & Francis, New York, pp.661-676, **2006**.

[3] C. Friedel and J. M. Crafts. A new general synthetic method of producinghydrocarbons, &c. *J. Chem. Soc.*, 32:725-791, **1877**.

[4] E Breitmaier and G Jung. *Organische Chemie*. Thieme, Stuttgart, **2001**.

[5] M. Rüping and B. J. Nachtsheim. A review of new developments in the Friedel-crafts alkylation - from green chemistry to asymmetric catalysis. *Beilstein J. Org. Chem.* 6:6, **2010**.

[6] F. H. Arnold. Combinatorial and computational challenges for biocatalyst design. *Nature*, 409(6817):253-7, **2001**.

[7] S. Lutz and U.T. Bornscheuer. *Protein engineering handbook*. Volume 1, Wiley-VCH Verlag, Weinheim,**2009**.

[8] K. Buchholz, V. Kasche, and U.T. Bornscheuer. *Biocatalysts and enzyme technology*.Wiley-VCH Verlag, Weinheim,**2005**.

[9] H. Jochens, M. Hesseler, K. Stiba, S.K. Padhi, R.J. Kazlauskas, and U.T. Bornscheuer. Protein engineering of α/β-hydrolase fold enzymes. *ChemBioChem*, 12(10):1508-1517, **2011**.

[10] R. K. P. Kuipers, H. Joosten, E.Verwiel, S. Paans, J. Akerboom, J. van der Oost, N. G. H. Leferink, W. J. H. van Berkel, G. Vriend, and Peter J Schaap. Correlated mutation analyses on super-family alignments reveal functionally important residues. **Proteins**, 76(3):608-16, **2009**.

[11] H. Jochens and U. T. Bornscheuer. Natural diversity to guide focused directed evolution. *ChemBioChem*, 11(13):1861-6, **2010**.

[12] J. Tao and J.H. Xu. Biocatalysis in development of green pharmaceutical processes. *Curr. Opin. Chem. Biol.*, 13(1):43-50, **2009**.

[13] C. Dalhoff, M. Hüben, T. Lenz, P. Poot, E.Nordhoff, H. Käster, and E. Weinhold. Synthesis of S-adenosyl-L-homocysteine capture compounds for selective photoinduced isolation of methyltransferases. *Chembiochem*, 11(2):256-65, **2010**.

[14] G. L. Cantoni. Biological methylation: selected aspects. *Ann.Rev. Biochem.*, 44:435-451, **1975**.

[15] X. Cheng and R. M. Blumenthal. *S-Adenosylmethionine-Dependent Methyltransferases: Structures and Functions.* World Scientific, Singapore, New Jersey, London, Hong Kong, **1999**.

[16] D. K. Ho, J. C. Wu, D. V. Santi, and H. G. Floss. Stereochemical studies of the C-methylation of deoxycytidine catalyzed by HhaI methylase and the N-methylation of deoxyadenosine catalyzed by EcorI methylase. *Arch. Biochem. Biophys.*, 284(2):264-269, **1991**.

[17] S. Klimašauskas and G. Lukinavičius. AdoMet-dependent methyltransferases, chemistry of. *Wiley Encycl. Chem. Biol* (Begley T. P. eds.), John Wiley & Sons, Inc. 1, 8-17, **2009**.

[18] M. G. Marinus. *Methylation of DNA. In Escherichia coli and Salmonella typhimurium.* 2nd ed., ed. by F. C. Neidhardt, ASM Press Washington DC, **1996**.

[19] X. Cheng, S. Kumar, J. Posfai, J. W. Pflugrath, and R. J .Roberts. Crystal structure of the HhaI DNA methyltransferase complexed with S-adenosyl-L-methionine. *Cell*, 74(2):299-307, **1993**.

[20] S. Klimašauskas, S. Kumar, R. J . Roberts, and X. Cheng. Hhai methyltransferase flips its target base out of the DNA helix. *Cell*, 76(2):357-69, **1994**.

[21] D. H. Kruger and T. A. Bickle. Bacteriophage survival: multiple mechanisms for avoiding the deoxyribonucleic acid restriction systems of their hosts. *Microbiol. Rev.*, 47(3):345-60, **1983**.

[22] C. Dalhoff, G. Lukinavičius, S. Klimašauskas, and E, Weinhold. Direct transfer of extended groups from synthetic cofactors by DNA methyltransferases. *Nat. Chem. Biol.*, 2(1):31-32, **2005**.

[23] Z. Liutkevičiute, G. Lukinavičius, V. Masevičius, D.Daujotyte, and S. Klimašauskas. Cytosine-5-methyltransferases add aldehydes to DNA. *Nat. Chem. Biol.*, 5(6):400-2, **2009**.

[24] V. E. Russo, R. A. Martienssen, and A. D. Riggs. *Epigenetic Mechanisms of Gene Regulation.* Cold Spring Harbor Press, New York, **1996**.

[25] J. A. Yoder, C. P. Walsh, and T. H. Bestor. Cytosine methylation and the ecology of intragenomic parasites. *Trends Genet.*, 13(8):335-40, **1997**.

[26] X. Cheng and R. M. Blumenthal. Mammalian DNA methyltransferases: a structural perspective. *Structure*, 16(3):341-50, **2008**.

[27] J. Flynn, J. F. Glickman, and N. O. Reich. Murine DNA cytosine C5 methyltransferase: pre-steady- and steady-state kinetic analysis with regulatory DNA sequences. *Biochemistry*, 35(23):7308-15, **1996**.

[28] Z. M. Svedruzic and N. O. Reich. DNA cytosine C5 methyltransferase Dnmt1: catalysis-dependent release of allosteric inhibition. *Biochemistry*, 44(27):9472-85, **2005**.

[29] S. C. Wu and Y. Zhang. Active DNA demethylation: many roads lead to Rome. Nat. Rev. Mol. Cell. Biol., 11(9):607-620, **2010**.

[30] M. Münzel, D. Globisch, and T. Carell. 5-hydroxymethylcytosine, the sixth base of the genome. *Angew. Chem. Int. Ed.*, 11;50(29):6460-8 **2011**.

[31] Z. Liutkevičiute, E. Kriukiene, I. Grigaityte, V. Masevičius, and S. Klimašauskas. Methyltransferase-directed derivatization of 5- hydroxymethylcytosine in DNA. *Angew. Chem. Int. Ed.*l, 50(9):2090-3, **2011**.

[32] A. K. Hopper and E. M. Phizicky. tRNA transfers to the limelight. *Genes Dev.*, 17(2):162-80, **2003**.

[33] T. G. Hagervall, T. M. Tuohy, J. F. Atkins, and G. R. Björk. Deficiency of 1- methylguanosine in tRNA from Salmonella typhimurium induces frameshifting by quadruplet translocation. *J. Mol. Biol.*, 232(3):756-65, **1993**.

[34] G. Das, D. K. Thotala, S.Kapoor, S.i Karunanithi, S. S. Thakur, N. S. Singh, and U. Varshney. Role of 16S ribosomal RNA methylations in translation initiation in Escherichia coli. *EMBO J.*, 27(6):840-51, **2008**.

[35] C. S. Chow, T. N. Lamichhane, and S. K. Mahto. Expanding the nucleotide repertoire of the ribosome with post-transcriptional modifications. *ACS Chem. Biol.*, 2(9):610-9, **2007**.

[36] R. Skinner, E. Cundliffe, and F. J. Schmidt. Site of action of a ribosomal RNA methylase responsible for resistance to erythromycin and other antibiotics. *J. Biol. Chem.*, 258(20):12702-6, **1983**.

[37] D. L. Gillian-Daniel, N. K. Gray, J. Aström, A Barkoff, and M. Wickens. Modifications of the 5' cap of mRNAs during Xenopus oocyte maturation: Independence from changes in poly(A) length and impact on translation. *Mo.l Cell. Biol.*, 18(10):6152-63, **1998**.

[38] J. A. Bokar, M. E. Shambaugh, D. Polayes, A. G. Matera, and F. M. Rottman. Purification and cDNA cloning of the AdoMet-binding subunit of the human mRNA (N6-adenosine)-methyltransferase. *RNA*, 3(11):1233-47, **1997**.

[39] C. D. Krause, Z. H. Yang, Y. S. Kim, J. H. Lee, J. R. Cook, and S. Pestka. Protein arginine methyltransferases: evolution and assessment of their pharmacological and therapeutic potential. *Pharmacol. Ther.*, 113(1):50-87, **2007**.

[40] T. Osborne, R. L. Roska, S. R. Rajski, and P. R. Thompson. In situ generation of a bisubstrate analogue for protein arginine methyltransferase 1. *J. Am. Chem. Soc.*, 130(14):4574-5, **2008**.

[41] E. J. Bennett, J. Bjerregaard, J. E. Knapp, D. A. Chavous, A. M. Friedman, W. E. Royer, and C. M. O'Connor. Catalytic implications from the Drosophila protein L-isoaspartyl methyltransferase structure and site-directed mutagenesis. *Biochemistry*, 42(44):12844-53, **2003**.

[42] J. Vidgren, L. A. Svensson, and A. Liljas. Crystal structure of Catechol O-methyltransferase. *Nature*, 368(6469):354-8, **1994**.

[43] C. L. Freel Meyers, M, Oberthür, H. Xu, L. Heide, D. Kahne, and C.T. Walsh. Characterization of NovP and NovN: completion of novobiocin biosynthesis by sequential tailoring of the noviosyl ring. *Angew. Chem. Int. Ed.*, 43(1):67-70, **2004**.

[44] A. Velasco, P. Acebo, A. Gomez, C. Schleissner, P. Rodriguez, T. Aparicio, S. Conde, R. Munoz, F. de la Calle, Jose L. Garcia, and J. M. Sanchez-Puelles. Molecular characterization of the safracin biosynthetic pathway from Pseudomonas uorescens A2-2: Designing new cytotoxic compounds. *Mol. Microbiol.*, 56(1):144-54, **2005**.

[45] L. Li, W. Deng, J. Song, W. Ding, Q. F. Zhao, C. Peng, W. W. Song, G. L. Tang, and W. Liu. Characterization of the saframycin A gene cluster from Streptomyces lavendulae NRRL 11002 revealing a nonribosomal peptide synthetase system for assembling the unusual tetrapeptidyl skeleton in an iterative manner. *J. Bacteriol.*, 190(1):251-63, **2008**.

[46] K. Goedecke, M. Pignot, R. S. Goody, A. J. Scheidig, and E. Weinhold. Structure of the N6-adenine DNA methyltransferase M.TaqI in complex with DNA and a cofactor analog. *Nat. Struct. Biol.*, 8(2):121-5, **2001**.

[47] A. Jeltsch. The cytosine N4-methyltransferase M.PvuII also modifies adenine residues. *Biol. Chem.*, 382(4):707-10, **2001**.

[48] W. Gong, M. O'Gara, R. M. Blumenthal, and X. Cheng. Structure of PvuII DNA-(cytosine N4) methyltransferase, an example of domain permutation and protein fold assignment. *Nucleic Acids Res.*, 25(14):2702-15, **1997**.

[49] Y. Huang, J. Komoto, K. Konishi, Y. Takata, H. Ogawa, T. Gomi, M. Fujioka, and F. Takusagawa. Mechanisms for auto-inhibition and forced product release in glycine N-methyltransferase: crystal structures of wild-type, mutant R175K and S-adenosylhomocysteine-bound R175K enzymes. *J. Mol. Biol.*, 298(1):149-62, **2000**.

[50] X. Zhang, L. Zhou, and X. Cheng. Crystal structure of the conserved core of protein arginine methyltransferase PRMT3. *EMBO J.*, 19(14):3509-19, **2000**.

[51] F. James, K. D. Nolte, and A. D. Hanson. Purification and properties of S-adenosyl-L-methionine:L-methionine S-methyltransferase from Wollastonia biflora leaves. *J. Biol. Chem.*, 270(38):22344-50, **1995**.

[52] J. Attieh, R. Djiana, P. Koonjul, C. Etienne, S. A. Sparace, and H. S. Saini. Cloning and functional expression of two plant thiol methyltransferases: a new class of enzymes involved in the biosynthesis of sulfur volatiles. *Plant Mol. Biol.*, 50(3):511-21, **2002**.

[53] H. Coiner, G. Schöder, E. Wehinger, C. J. Liu, J. P. Noel, W.Schwab, and J. Schröder. Methylation of sulfhydryl groups: a new function for a family of small molecule plant O-methyltransferases. *Plant J.*, 46(2):193-205, **2006**.

[54] W. D. Nes. Enzyme mechanisms for sterol C-methylations. *Phytochemistry*, 64(1):75-95, **2003**.

[55] W. A. M. Loenen. S-adenosylmethionine: jack of all trades and master of everything? *Biochem. Soc. Trans.*, 34(Pt 2):330-3, **2006**.

[56] P. Ranocha, F. Bourgis, M. J. Ziemak, D. Rhodes, D. A. Gage, and A. D. Hanson. Characterization and functional expression of cDNAs encoding methionine-sensitive and -insensitive homocysteine S-methyltransferases from Arabidopsis. *J. Biol. Chem.*, 275(21):15962-8, **2000**.

[57] J. X. Wang, E. R. Lee, D. R. Morales, J. Lim, and R. R. Breaker. Riboswitches that sense S-adenosylhomocysteine and activate genes involved in coenzyme recycling. *Mol. Cell*, 29(6):691-702, **2008**.

[58] S. Schauder, K. Shokat, M. G. Surette, and B. L. Bassler. The LuxS family of bacterial autoinducers: biosynthesis of a novel quorum-sensing signal molecule. *Mol. Microbiol.*, 41(2):463-76, **2001**.

[59] H. J. Sofia, G. Chen, B. G. Hetzler, J. F. Reyes-Spindola, and N. E. Miller. Radical SAM, a novel protein superfamily linking unresolved steps in familiar biosynthetic pathways with radical mechanisms: functional characterization using new analysis and information visualization methods. *Nucleic Acids Res.*, 29(5):1097-106, **2001**.

[60] F. Pojer, S. M. Li, and L. Heide. Molecular cloning and sequence analysis of the clorobiocin biosynthetic gene cluster: new insights into the biosynthesis of aminocoumarin antibiotics. *Microbiology*, 148(Pt 12):3901-11, **2002**.

[61] L. Westrich, L. Heide, and S. M. Li. CloN6, a novel methyltransferase catalysing the methylation of the pyrrole-2-carboxyl moiety of clorobiocin. *ChemBioChem*, 4(8):768-73, **2003**.

[62] W. L. Kelly, L. Pan, and C. Li. Thiostrepton biosynthesis: prototype for a new family of bacteriocins. *J. Am. Chem. Soc.*, 131(12):4327-34, **2009**.

[63] R. T. Borchardt. S-adenosyl-L-methionine-dependent macromolecule methyltransferases: potential targets for the design of chemotherapeutic agents. *J. Med. Chem.*, 23(4):347-57, **1980**.

[64] M. Pignot, G. Pljevaljčić, and E. Weinhold. Efficient synthesis of s-adenosyl-L-homocysteine natural product analogues and their use to elucidate the structural determinant for cofactor binding of the DNA methyltransferase M.HhaI. *Eur. J. Org. Chem.*, 2000(3):549-555, **2000**.

[65] L. D. Boeck, G. M. Clem, M. M. Wilson, and J. E. Westhead. A9145, a new adenine-containing antifungal antibiotic: fermentation. *Antimicrob. Agents Chemother.*, 3(1):49-56, **1973**.

[66] G. Schluckebier, M. Kozak, N. Bleimling, E. Weinhold, and W. Saenger. Differential binding of S-adenosylmethionine S-adenosylhomocysteine and Sinefungin to the adenine-specific DNA methyltransferase M.TaqI. *J. Mol. Biol.*, 265(1):56-67, **1997**.

[67] G. Pljevaljčić, F. Schmidt, and E. Weinhold. Sequence-specific methyltransferase-induced labeling of DNA (smiling DNA). *ChemBioChem*, 5(3):265-9, **2004**.

[68] R. L. Weller and S. R. Rajski. Design, synthesis, and preliminary biological evaluation of a DNA methyltransferase-directed alkylating agent. *ChemBioChem*, 7(2):243-5, **2006**. [69] C. Zhang, R. L. Weller, J. S. Thorson, and S. R. Rajski. Natural product diversification using a non-natural cofactor analogue of S-adenosyl-L-methionine. *J. Am. Chem. Soc.*, 128(9):2760-1, **2006**.

[70] C. Dalhoff, G. Lukinavičius, S. Klimašauskas, and E. Weinhold. Direct transfer of extended groups from synthetic cofactors by DNA methyltransferases. *Nat. Chem. Biol.*, 2(1):31-2, **2006**.

[71] G. Lukinavičius, V. Lapiene, Z. Stasevskij, C. Dalhoff, E. Weinhold, and S. Klimašauskas. Targeted labeling of DNA by methyltransferase-directed transfer of activated groups (mTAG). *J. Am. Chem. Soc.*, 129(10):2758-9, **2007**.

[72] P. Ranocha, S. D. McNeil, M. J. Ziemak, C. Li, M. C. Tarczynski, and A. D. Hanson. The S-methylmethionine cycle in angiosperms: ubiquity, antiquity and activity. *Plant. J.*, 25(5):575-84, **2001**.

[73] S. S. Szegedi, C. C. Castro, M. Koutmos, and T. A. Garrow. Betaine-homocysteine S-methyltransferase-2 is an S-methylmethionine-homocysteine methyltransferase. *J. Biol. Chem.*, 283(14):8939-45, **2008**.

[74] A. P. Breksa and T. A. Garrow. Recombinant human liver betaine-homocysteine S-methyltransferase: identifocation of three cysteine residues critical for zinc binding. *Biochemistry*, 38(42):13991-8, **1999**.

[75] T. A. Garrow. Purification, kinetic properties, and cDNA cloning of mammalian betaine-homocysteine methyltransferase. *J. Biol. Chem.*, 271(37):22831-8, **1996**.

[76] M. Jansen and T.A. Hansen. DMSP: tetrahydrofolate methyltransferase from the marine sulfate-reducing bacterium strain WN. *J. Sea Res.*, 43(3-4):225-231, **2000**.

[77] J. Seravalli, S. Zhao, and S. W. Ragsdale. Mechanism of transfer of the methyl group from (6S)-methyltetrahydrofolate to the corrinoid/iron-sulfur protein catalyzed by the methyltransferase from Clostridium thermoaceticum: a key step in the Wood-Ljungdahl pathway of acetyl-CoA synthesis. *Biochemistry*, 38(18):5728-35, **1999**.

[78] J. T. Jarrett, S. Huang, and R. G. Matthews. Methionine synthase exists in two distinct conformations that differ in reactivity toward methyltetrahydrofolate, adenosylmethionine, and flavodoxin. *Biochemistry*, 37(16):5372-82, **1998**.

[79] R. Banerjee. The Yin-Yang of cobalamin biochemistry. *Chem. Biol.*, 4(3):175-86, **1997**.

[80] R. Banerjee. B12 trafficking in mammals: A case for coenzyme escort service. *ACS Chem Biol.*, 1(3):149-159, **2006**.

[81] B. Kräutler. Vitamin B12: chemistry and biochemistry. *Biochem. Soc. Trans.*, 33(4):806-10, **2005**.

[82] G. A. Maw. Thetin-homocysteine transmethylase. the distribution of the enzyme, studied with the aid of trimethylsulphonium chloride as substrate. *Biochem. J.*, 72(4):602-8, **1959**.

[83] S. Slow, M. Lever, M. B. Lee, P. M. George, and S. T. Chambers. Betaine analogues alter homocysteine metabolism in rats. *Int. J. Biochem. Cell Biol.*, 36(5):870-80, **2004**.

[84] C. Wagner, S. M. Lusty, H. F. Kung, and N. L. Rogers. Preparation and properties of trimethylsulfonium-tetrahydrofolate methyltransferase. *J. Biol. Chem.*, 242(6):1287-93, **1967**.

[85] J. L. Martin and F. M. McMillan. SAM (dependent) I AM: the S-adenosylmethionine-dependent methyltransferase fold. *Curr. Opin. Struct. Biol.*, 12(6):783-793, **2002**.

[86] M. Gerstein. A structural census of genomes: comparing bacterial, eukaryotic, and archaeal genomes in terms of protein structure. *J. Mol. Biol.*, 274(4):562-76, **1997**.

[87] H. L. Schubert, R. M. Blumenthal, and X. Cheng. Many paths to methyltransfer: a chronicle of convergence. *Trends Biochem. Sci.*, 28(6):329-35, **2003**.

[88] Z. Fu, Y. Hu, K. Konishi, Y. Takata, H. Ogawa, T. Gomi, M. Fujioka, and F. Takusagawa. Crystal structure of glycine N-methyltransferase from rat liver. *Biochemistry*, 35(37):11985-93, **1996**.

[89] A. E. Hodel, P. D. Gershon, X. Shi, and F. A. Quiocho. The 1.85 Å structure of vaccinia protein VP39: a bifunctional enzyme that participates in the modification of both mRNA ends. *Cell*, 85(2):247-56, **1996**.

[90] M. M. Dixon, S. Huang, R. G. Matthews, and M. Ludwig. The structure of the C-terminal domain of methionine synthase: presenting S-adenosylmethionine for reductive methylation of B12. *Structure*, 4(11):1263-75, **1996**.

[91] H. L. Schubert, K. S. Wilson, E. Raux, S. C. Woodcock, and M. J. Warren. The X-ray structure of a cobalamin biosynthetic enzyme, cobalt-precorrin-4 methyltransferase. *Nat. Struct. Biol.*, 5(7):585-92, **1998**.

[92] G. Michel, V. Sauve, Robert Larocque, Yunge Li, Allan Matte, and Miroslaw Cygler. The structure of the RlmB 23S rRNA methyltransferase reveals a new methyltransferase fold with a unique knot. *Structure*, 10(10):1303-15, **2002**.

[93] V. Anantharaman, E. V. Koonin, and L. Aravind. SPOUT: a class of methyltransferases that includes spoU and trmD RNA methylase superfamilies, and novel superfamilies of predicted prokaryotic RNA methylases. *J. Mol. Microbiol. Biotechnol.*, 4(1):71-5, **2002**.

[94] A. B. Taylor, B. Meyer, B. Z. Leal, P. Kötter, V. Schirf, B. Demeler, P. J. Hart, K. D. Entian, and J. Wöhnert. The crystal structure of Nep1 reveals an extended SPOUT-class methyltransferase fold and a pre-organized SAM-binding site. *Nucleic Acids Res.*, 36(5):1542-54, **2008**.

[95] R. C. Trievel, E. M. Flynn, R. L. Houtz, and J. H. Hurley. Mechanism of multiple lysine methylation by the SET domain enzyme Rubisco LSMT. *Nat. Struct. Biol.*, 10(7):545-52, **2003**.

[96] A. Maxwell. DNA gyrase as a drug target. *Trends Microbiol.*, 5(3):102-109, **1997**.

[97] J. A. Ali, A. P. Jackson, A. J. Howells, and A. Maxwell. The 43-kilodalton N-terminal fragment of the DNA gyrase B protein hydrolyzes ATP and binds coumarin drugs. *Biochemistry*, 32(10):2717-24, **1993**.

[98] M. A. Montecalvo, H. Horowitz, G. P. Wormser, K. Seiter, and C. A. Carbonaro. Effect of novobiocin-containing antimicrobial regimens on infection and colonization with vancomycin-resistant Enterococcus faecium. *Antimicrob. Agents Chemother.*, 39(3):794, **1995**.

[99] I. I. Raad, R. Y. Hachem, D. Abi-Said, K. V. Rolston, E. Whimbey, A. C. Buzaid, and S. Legha. A prospective crossover randomized trial of novobiocin and rifampin prophylaxis for the prevention of intravascular catheter infections in cancer patients treated with interleukin-2. *Cancer*, 82(2):403-411, **1998**.

[100] D. B. Wigley, G. J. Davies, E. J. Dodson, A. Maxwell, and G. Dodson. Crystal structure of an N-terminal fragment of the DNA gyrase B protein. *Nature*, 351(6328):624-629, **1991**.

[101 R. J. Lewis, O. M. Singh, C. V. Smith, T. Skarzynski, A. Maxwell, A. J. Wonacott, and D. B. Wigley. The nature of inhibition of DNA gyrase by the coumarins and the cyclothialidines revealed by X-ray crystallography. *EMBO J.*, 15(6):1412-20, **1996**.

[102 Daniel. Lafitte, V. Lamour, P. O. Tsvetkov, A. A. Makarov, M. Klich, P. Deprez, D. Moras, C. Briand, and R. Gilli. DNA gyrase interaction with coumarin-based inhibitors: the role of the hydroxybenzoate isopentenyl moiety and the 5'-methyl group of the noviose. *Biochemistry*, 41(23):7217-23, **2002**.

[103] Z. X. Wang, S. M. Li, and L. Heide. Identification of the coumermycin A(1) biosynthetic gene cluster of Streptomyces rishiriensis DSM 40489. *Antimicrob. Agents Chemother.*, 44(11):3040-8, **2000**.

[104] M. Steffensky, A. Muehlenweg, Z. X. Wang, S. M. Li, and L. Heide. Identification of the novobiocin biosynthetic gene cluster of Streptomyces spheroides NCIB 11891. *Antimicrob. Agents Chemother.*, 44(5):1214-22, **2000**.

[105] M. Pacholec, J. Tao, and C. T. Walsh. CouO and NovO: C-methyltransferases for tailoring the aminocoumarin scaffold in coumermycin and novobiocin antibiotic biosynthesis. *Biochemistry*, 44(45):14969-76, **2005**.

[106] F. Pojer, E. Wemakor, B. Kammerer, H.i Chen, C. T. Walsh, S. M.Li, and L. Heide. CloQ, a prenyltransferase involved in clorobiocin biosynthesis. *Proc. Natl. Acad. Sci. U S A*, 100(5):2316-21, **2003**.

[107] H. T. Chiu, B. K. Hubbard, A. N. Shah, J. Eide, R. A. Fredenburg, C. T. Walsh, and C. Khosla. Molecular cloning and sequence analysis of the complestatin biosynthetic gene cluster. *Proc. Natl. Acad. Sci. U S A*, 98(15):8548-53, **2001**.

[108] C. L. Freel Meyers, M. Oberthür, L. Heide, D. Kahne, and C. T. Walsh. Assembly of dimeric variants of coumermycins by tandem action of the four biosynthetic enzymes CouL, CouM, CouP, and NovN. *Biochemistry*, 43(47):15022-36, **2004**.

[109] A.S. Eustáquio, B. Gust, U. Galm, S. M. Li, K. F. Chater, and L. Heide. Heterologous expression of novobiocin and clorobiocin biosynthetic gene clusters. *Appl. Environ. Microbiol.*, 71(5):2452-9, **2005**.

[110] M. Wolpert, L. Heide, B.Kammerer, and B. Gust. Assembly and heterologous expression of the coumermycin A1 gene cluster and production of new derivatives by genetic engineering. *ChemBioChem*, 9(4):603-12, **2008**.

[111] Y. Ikeda, H. Idemoto, F. Hirayama, K. Yamamoto, K. Iwao, T. Asao, and T. Munakata. Safracins, new antitumor antibiotics. I. Producing organism, fermentation and isolation. *J. Antibiot. (Tokyo)*, 36(10):127983, **1983**.

[112] T. Arai, K. Takahashi, K. Ishiguro, and Y. Mikami. Some chemotherapeutic properties of two new antitumor antibiotics, saframycins A and C. *Gann.*, 71(6):790-6, **1980**.

[113] G. Schwartsmann, A. Brondani da Rocha, R. G. Berlinck, and J. Jimeno. Marine organisms as a source of new anticancer agents. *Lancet. Oncol.*, 2(4):221-5, **2001**.

[114] M. Zewail-Foote, V. S. Li, H. Kohn, D. Bearss, M. Guzman, and L. H. Hurley. The inefficiency of incisions of ecteinascidin 743-DNA adducts by the UvrABC nuclease and the unique structural feature of the DNA adducts can be used to explain the repair-dependent toxicities of this antitumor agent. *Chem. Biol.*, 8(11):1033-49, **2001**.

[115] C. Xing, J. R. LaPorte, J. K. Barbay, and A. G. Myers. Identification of GAPDH as a protein target of the saframycin antiproliferative agents. *Proc. Natl. Acad. Sci. U S A*, 101(16):5862-6, **2004**.

[116] J. D. Scott and R. M. Williams. Chemistry and biology of the tetrahydroisoquinoline antitumor antibiotics. *Chem. Rev.*, 102(5):1669-730, **2002**.

[117] I. Crnovčić, R. Süssmuth, and U. Keller. Aromatic C-methyltransferases with antipodal stereoselectivity for structurally diverse phenolic amino acids catalyze the methylation step in the biosynthesis of the actinomycin chromophore. *Biochemistry*, 49(45):9698-705, **2010**.

[118] G. H. Jones. Combined purification of actinomycin synthetase I and 3- hydroxyanthranilic acid 4-methyltransferase from Streptomyces antibioticus. *J. Biol. Chem.*, 268(10):6831-4, **1993**.

[119] J. Meienhofer and E. Atherton. Structure-activity relationships in the actinomycins. *Adv. Appl. Microbiol.*, 16:203-300, **1973**.

[120] E. Frei. The clinical use of actinomycin. *Cancer Chemother. Rep.*, 58(1):49-54, **1974**.

[121] Y. Hu, V. Pelan, I. Ntai, C. M. Farnet, E. Zazopoulos, and B. O. Bachmann. Benzodiazepine biosynthesis in Streptomyces refuineus. *Chem. Biol.*, 14(6):691-701, **2007**.

[122] W. Li, A. Khullar, S. Chou, A. Sacramo, and B. Gerratana. Biosynthesis of sibiromycin, a potent antitumor antibiotic. *Appl. Environ. Microbiol.*, 75(9):2869-78, **2009**.

[123] M. L. Kopka, D. S. Goodsell, I. Baikalov, K. Grzeskowiak, D. Cascio, and R. E. Dickerson. Crystal structure of a covalent DNA-drug adduct: anthramycin bound to C-C-A-A-C-G-T-T-G-G and a molecular explanation of specificity. *Biochemistry*, 33(46):13593-610, **1994**.

[124] A. Kamal, M. V. Rao, N. Laxman, G. Ramesh, and G. S. K. Reddy. Recent developments in the design, synthesis and structure-activity relationship studies of pyrrolo[2,1-c][1,4]benzodiazepines as DNA-interactive antitumour antibiotics. *Curr. Med. Chem. Anticancer Agents*, 2(2):215-54, **2002**.

[125] B. T. Porse, I. Leviev, A. S. Mankin, and R. A. Garrett. The antibiotic thiostrepton inhibits a functional transition within protein L11 at the ribosomal GTPase centre. *J. Mol. Biol.*, 276(2):391-404, **1998**.

[126] G. Lentzen, R. Klinck, N. Matassova, F. Aboul-ela, and A. I. H. Murchie. Structural basis for contrasting activities of ribosome binding thiazole antibiotics. *Chem. Biol.*, 10(8):769-78, **2003**.

[127] R. Donovick, J. F. Pagano, H. A. Stout, and M. J. Weinstein. Thiostrepton, a new antibiotic. I. In vitro studies. *Antibiot. Annu.*, 3:554-9, **1955-1956**.

[128] W. P. Jambor, B. A. Steinberg, and L. O. Suydam. Thiostrepton, a new antibiotic. III. In vivo studies. *Antibiot. Annu.*, 3:562-5, **1955-1956**.

[129] J. D. Dutcher and J. Vandeputte. Thiostrepton, a new antibiotic. II. Isolation and chemical characterization. *Antibiot. Annu.*, 3:560-1, **1955-1956**.

[130] W. H. Trejo, L. D. Dean, J. Pluscec, E. Meyers, and W. E. Brown. Streptomyces laurentii, a new species producing thiostrepton. *J. Antibiot. (Tokyo)*, 30(8):639-43, **1977**.

[131] M. Bodanszky, J. D. Dutcher, and N. J. Williams. The establishment of the identity of thiostrepton with thiactin (bryamycin). *J. Antibiot. Ser. A* 16(2):76-9, **1963**.

[132] T. Frenzel, P. Zhou, and H. G. Floss. Formation of 2-methyltryptophan in the biosynthesis of thiostrepton: isolation of S-adenosylmethionine:tryptophan 2- methyltransferase. *Arch. Biochem. Biophys.*, 278(1):35-40, **1990**.

[133] R. Liao, L. Duan, C. Lei, H. Pan, Y. Ding, Q. Zhang, D. Chen, B. Shen, Y.Yu, and W. Liu. Thiopeptide biosynthesis featuring ribosomally synthesized precursor peptides and conserved posttranslational modifications. *Chem. Biol.*, 16(2):141-7, **2009**. [134] P. T. Lee, A. Y. Hsu, H. T. Ha, and C. F. Clarke. A C-methyltransferase involved in both ubiquinone and menaquinone biosynthesis: isolation and identification of the Escherichia coli ubiE gene. *J. Bacteriol.*, 179(5):1748-54, **1997**.

[135] M. Kawamukai. Biosynthesis, bioproduction and novel roles of ubiquinone. *J. Biosci. Bioeng.*, 94(6):511-7, **2002**.

[136] U. Wissenbach, D. Ternes, and G. Unden. An Escherichia coli mutant containing only demethylmenaquinone, but no menaquinone: effects on fumarate, dimethylsulfoxide, trimethylamine N-oxide and nitrate respiration. *Arch. Microbiol.*, 158(1):68-73, **1992**.

[137] R. J. Barkovich, A. Shtanko, J. A. Shepherd, P. T. Lee, D. C. Myles, A. Tzagoloff, and C. F. Clarke. Characterization of the coq5 gene from Saccharomyces cerevisiae. evidence for a C-methyltransferase in ubiquinone biosynthesis. *J. Biol. Chem.*, 272(14):9182-8, **1997**.

[138] L. Ernster and G. Dallner. Biochemical, physiological and medical aspects of ubiquinone function. *Biochim. Biophys. Acta.*, 1271(1):195-204, **1995**.

[139] M. Gruber-Khadjawi, T. Purkarthofer, W. Skranc, and H. Griengl. Hydroxynitrile lyase-catalyzed enzymatic nitroaldol (henry) reaction. *Adv.Synth. Catal.*, 349(8-9):1445-1450, **2007**.

[140] A.S. Demir, P. Ayhan, and S.B. Sopaci. Thiamine pyrophosphate dependent enzyme catalyzed reactions: Stereoselective C-C bond formations in water. *CLEAN: Soil, Air, Water*, 35(5):406-412, **2007**.

[141] J. Sukumaran and U. Hanefeld. Enantioselective C-C bond synthesis catalyzed by enzymes. *Chem. Soc. Rev.*, 34(6):530-542, **2005**.

[142] M. Pohl, B. Lingen, and M. Müller. Thiamin-diphosphate-dependent enzymes: New aspects of asymmetric C-C bond formation. *Chem. Eur. J.*, 8(23):5288-5295, **2002**.

[143] M. H. Fechter and H. Griengl. Hydroxynitrile lyases: biological sources and application as biocatalysts. in *Enzyme Catalysis in Organic Synthesis* (Eds.: K. Drauz, H. Waldmann), Wiley-VCH, Weinheim, pp.974-989, **2002**.

[144] A. D. M. Curtis. 1 carbon-carbon bond formation using enzymes. in *Biotechnology, Vol. 8b* (Ed.: D. R. Kelly), Wiley-VCH, Weinheim, pp.5-40, **2000**.

[145] G. Seoane. Enzymatic C-C bond-forming reactions in organic synthesis. *Curr. Org. Chem.*, 4(3):283-304, **2000**.

[146] W. D Fessner. Enzyme mediated C-C bond formation. *Curr. Opin. Chem. Biol.*, 2(1):85-97, **1998**.

[147] S. M. Roberts. Preparative biotransformations: the employment of enzymes and whole-cells in synthetic organic chemistry. *J. Chem. Soc. Perkin Trans. 1*, 157-169, **1998**.

[148] W. D. Fessner and C. Walter. Enzymatic C-C bond formation in asymmetric synthesis. *Top. Curr. Chem.*, 184:97-194, **1997**.

[149] M. Breuer and B. Hauer. Carbon-carbon coupling in biotransformation. *Curr. Op. Biotechnol.*, 14(6):570-576, **2003**.

[150] C. Wandrey, A. Liese, and D. Kihumbu. Industrial biocatalysis: Past, present, and future. *Org. Process Res. Dev.*, 4(4):286-290, **2000**.

[151] L. Wessjohann, B. Sontag, and M. A. Dessoy in *Bioorganic Chemistry: Highlights and New Aspects* (Ed.: U. Diederichsen), Wiley-VCH, Weinheim, pp. 79-88, **1999**. [152] L. Poppe and J. Retey. Friedel-crafts-type mechanism for the enzymatic elimination of ammonia from histidine and phenylalanine. *Angew. Chem. Int. Ed.*, 44(24):3668-88, **2005**.

[153] S. Klimašauskas and E. Weinhold. A new tool for biotechnology: AdoMet-dependent methyltransferases. *Trends Biotechnol.*, 25(3):99-104, **2007**.

[154] H. Kawaguschi, H. Tsukikura , M. Okanishi, T. Miyaki, T. Ohmori, K. Fujisawa, and H. Koshiyama. Studies on coumermycin, a new antibiotic. I. Production, isolation and characterization of coumermycin A1. *J. Antibiot. Ser. A*, 18:1-10, **1965**.

[155] E. A. Kaczka, F. J. Wolf, F. P. Rathe, and K. Folkers. Canthomysin. I. Isolation and characterization. *J. Am. Chem. Soc.*, 77:6404-6405, *1955*.

[156] H. Hoeksema, M. E. Bergy, W. G. Jackson, J. W. Shell, J. W. Hinman, A. E. Fonken, G. A. Boyack, E. L. Caron, J. H. Ford, W. H. DeVries, and G. F. Crum. Streptonivicin, a new antibiotic. II. Isolation and characterization. *Antibiot. Chemother.*, 6:143-148, *1956*.

[157] A. J. Birch, D. W. Cameron, P. W. Holloway, and R. W. Rickards. Further examples of biological C-methylation: novobiocin and actinomycin. *Tetrahedron Lett.*, 1(25):26-31, **1960**.

[158] L. Heide, B. Gust, C. Anderle, and S.-M. Li. Combinatorial biosynthesis, metabolic engineering and mutasynthesis for the generation of new aminocoumarin antibiotics. *Curr. Top. Med.Chem.*, 8(8):667-679, **2008**.

[159] S. M. Li, L. Westrich, J. Schmidt, C. Kuhnt, and L. Heide. Methyltransferase genes in Streptomyces rishiriensis: new coumermycin derivatives from gene-inactivation experiments. *Microbiology*, 148(10):3317-3326, **2002**.

[160] T. Kieser, M. J. Bibb, M. J. Buttner, K. F. Chater, and D. A. Hopwood. *Practical Streptomyces Genetics.* The John Innes Foundation, Norwich, **2000**.

[161] C.F. Lin, T.C. Chang, C.C. Chiang, H.J. Tsai, and L.Y. Hsu. Synthesis of selenium containing polyphenolic acid esters and evaluation of their effects on antioxidation and 5-lipoxygenase inhibition. *Chem. Pharm. Bull.*, 53(11):1402-1407, **2005**.

[162] M. Flipo, T. Beghyn, J. Charton, V.A. Leroux, B.P. Deprez, and R.F. Deprez-Poulain. A library of novel hydroxamic acids targeting the metallo-protease family: Design, parallel synthesis and screening. *Bioorg. Med. Chem.*, 15(1):63-76, **2007**.

[163] J. Tao, S. Hu, M. Pacholec, and C. T. Walsh. Synthesis of proposed oxidation-cyclization-methylation intermediates of the coumarin antibiotic biosynthetic pathway. *Org. Lett.*, 5(18):3233-3236, *2003*.

[164] E. J. Barreiro, A. E. Kummerle, and C. A. Fraga. The methylation effect in medicinal chemistry. *Chem. Rev.*,DOI:10.1021/cr200060g, **2011**.

[165] E. Purta, M. O'Connor, J. M. Bujnicki, and S. Douthwaite. YccW is the m5C methyltransferase specific for 23s rRNA nucleotide 1962. *J. Mol. Biol.*, 383(3):641-51, **2008**.

[166] K. Ishida, K. Fritzsche, and C. Hertweck. Geminal tandem C-methylation in the discoid resistomycin pathway. *J. Am. Chem. Soc.*, 129(42):12648-12649, **2007**.

[167] F. Fawaz and G. H. Jones. Actinomycin synthesis in Streptomyces antibioticus. Purification and properties of a 3-hydroxyanthranilate 4-methyltransferase. *J. Biol. Chem.*, 263(10):4602-4606, **1988**.

[168] H. Stecher, M. Tengg, B. J. Ueberbacher, P. Remler, H. Schwab, H. Griengl, and M. Gruber-Khadjawi. Biocatalytic Friedel-Crafts alkylation using non-natural cofactors. *Angew. Chem. Int. Ed.*, 48(50):9546-8, **2009**.

[169] J. Braman, C. Papworth, and A. Greener. Site-directed mutagenesis using double-stranded plasmid DNA templates. *Methods Mol. Biol.*, 57:31-44, **1996**.

[170] C. Fabrega, S. Hausmann, V. Shen, S. Shuman, and C. D. Lima. Structure and mechanism of mRNA cap (guanine-N7) methyltransferase. *Mol. Cell*, 13(1):77-89, **2004**.

[171] D. J. Miller, N. Ouellette, E. Evdokimova, A. Savchenko, A. Edwards, and W. F. Anderson. Crystal complexes of a predicted S-adenosylmethionine-dependent methyltransferase reveal a typical AdoMet binding domain and a substrate recognition domain. *Protein Sci.*, 12(7):1432-42, **2003**.

[172] C. Zubieta, X. Z. He, R. A. Dixon, and J. P. Noel. Structures of two natural product methyltransferases reveal the basis for substrate specificity in plant O-methyltransferases. *Nat. Struct. Biol.*, 8(3):271-279, **2001**.

[173] A. Jansson, J. Niemi, Y. Lindqvist, P. Mantsala, and G.Schneider. Crystal structure of aclacinomycin-10-hydroxylase, a S-adenosyl-L-methionine-dependent methyltransferase homolog involved in anthracycline biosynthesis in Streptomyces purpurascens. *J. Mol. Biol.*, 334(2):269-80, **2003**.

[174] A. Jansson, H. Koskiniemi, A. Erola, J. Wang, P. Mantsala, G. Schneider, and J. Niemi. Aclacinomycin 10-hydroxylase is a novel substrate-assisted hydroxylase requiring S-adenosyl-L-methionine as cofactor. *J. Biol. Chem.*, 280(5):3636-44, **2005**.

[175] W. D. Nes, P. Jayasimha, W. Zhou, R. Kanagasabai, C. Jin, T. T. Jaradat, R. W. Shaw, and J. M. Bujnicki. Sterol methyltransferase: functional analysis of highly conserved residues by site-directed mutagenesis. *Biochemistry*, 43(2):569-76, **2004**.

[176] X. Zhang, L. Zhou, and X. Cheng. Crystal structure of the conserved core of protein arginine methyltransferase PRMT3. *EMBO J.*, 19(14):3509-3519, **2000**.

[177] K. Wada, H. Yamaguchi, J. Harada, K. Niimi, S. Osumi, Y. Saga, H. Oh-Oka, H. Tamiaki, and K.Fukuyama. Crystal structures of BchU, a methyltransferase involved in bacteriochlorophyll c biosynthesis, and its complex with S-adenosylhomocysteine: implications for reaction mechanism. *J. Mol. Biol.*, 360(4):839-49, **2006**.

[178] G. H. Jones. Actinomycin synthesis in Streptomyces antibioticus: enzymatic conversion of 3-hydroxyanthranilic acid to 4-methyl-3-hydroxyanthranilic acid. *J. Bacteriol.*, 169(12):5575-8, **1987**.

[179] A. Haese and U. Keller. Genetics of actinomycin C production in Streptomyces chrysomallus. *J. Bacteriol.*, 170(3):1360-8, **1988**.

[180] F. Schauwecker, F. Pfennig, W. Schröder, and U. Keller. Molecular cloning of the actinomycin synthetase gene cluster from Streptomyces chrysomallus and functional heterologous expression of the gene encoding actinomycin synthetase II. *J. Bacteriol.*, 180(9):2468-74, **1998**.

[181] F. Pfennig, F. Schauwecker, and U. Keller. Molecular characterization of the genes of actinomycin synthetase I and of a 4-methyl-3-hydroxyanthranilic acid carrier protein involved in the assembly of the acylpeptide chain of actinomycin in Streptomyces. *J. Biol. Chem.*, 274(18):12508-16, **1999**.

[182] H. Stecher. Biocatalytic Friedel-Crafts alkylation. *PhD thesis*, TU Graz, **2011**.

[183] M. Shobayashi, N. Mukai, K. Iwashita, Y. Hiraga, and H. Iefuji. A new method for isolation of S-adenosylmethionine (SAM)-accumulating yeast. *Appl. Microbiol. Biotechnol.*, 69(6):704-710, **2006**.

[184] J. He, J. Deng, Y. Zheng, and J. Gu. A synergistic effect on the production of S-adenosyl-L-methionine in Pichia pastoris by knocking in of S-adenosyl-L-methionine synthase and knocking out of cystathionine-beta synthase. *J. Biotechnol.*, 126(4):519-527, **2006**.

[185] H. Chen, J. Chu, S. Zhang, Y. Zhuang, J. Qian, Y. Wang, and X. Hu. Intracellular expression of Vitreoscilla hemoglobin improves S-adenosylmethionine production in a recombinant Pichia pastoris. *Appl. Microbiol. Biotechnol.*, 74(6):1205-1212, **2007**.

[186] B. Holz, E. Weinhold, S. Klimašauskas, and S. Serva. 2-Aminopurine as a fluorescent probe for DNA base flipping by methyltransferases. *Nucleic acids Res.*, 26(4):1076-83, **1998**.

[187] D. Daujotyte, Z. Liutkevičiute, G. Tamulaitis, and S. Klimašauskas. Chemical mapping of cytosines enzymatically flipped out of the DNA helix. *Nucleic acids Res.*, 36(10):e57, **2008**.

[188] J. Sambrook and D.W. Russell. *Molecular cloning: a laboratory manual.* Cold spring harbor laboratory press, **2001**.

[189] F. M. Ausubel, R. Brent, R. E. Kingston, D. D. Moore, J. G. Seidman, J. A. Smith, and K. Struhl. *Curr. Protoc. Mol. Biol.*, John Wiley & Sons, **1987**.